PREDICTING THE ANCIENT OCCURRENCE OF COAL DEPOSITS USING PALEOCLIMATE MODELING

by

MANDI BECK

Presented to the Faculty of the Graduate School of
The University of Texas at Arlington in Partial Fulfillment
of the Requirements
for the Degree of

MASTER OF SCIENCE IN GEOLOGY

THE UNIVERSITY OF TEXAS AT ARLINGTON
DECEMBER 2012

ACKNOWLEDGEMENTS

I would like to thank Dr. Christopher Scotese for helping me put together my thesis topic, proposal, and work. He has been a great help throughout my research and was always willing to meet whenever I needed help. I would also like to thank Arghya Goswami for helping me with my climate envelopes, GIS support, and for answering any questions I had for him. I would like to thank Amiratu Yamusah for her previous work that was helpful in this process.

Huge thanks for my friends who have supported me and motivated me to finish. Last but not least, a thank you to my parents who have always been there for me and only wanted to see me succeed. This thesis would not have been possible without all of their support. Thank you.

November 13, 2012

ABSTRACT

PREDICTING THE ANCIENT OCCURRENCE

OF COAL DEPOSITS USING

PALEOCLIMATE

MODELING

Mandi Beck, M.S.

The University of Texas at Arlington, 2012

Supervising Professor: Christopher Scotese

Coals are accumulated and consolidated remains of plant material, which means that in order to form coals, a certain amount of annual precipitation is required. This study uses paleo-precipitation data obtained from Fast Ocean Atmosphere Model (FOAM) and predicts where paleo-coal deposits might occur. All predicted coal localities were plotted on paleogeographic reconstructions (obtained from the PALEOMAP Project) for thirteen time intervals from the Early Carboniferous to present. Once these predicted coal deposits were plotted, observed coals from the Boucot et al., 2012 database were then plotted on the same reconstructed basemaps. The predicted coal deposits were then compared with the observed coals to determine if a statistical correlation between the predicted and observed coal deposits could be made. The results show poor visual correlation between the predicted and the observed coals for the Cenozoic and the Mesozoic and works for most of the Paleozoic. There are many factors that could cause this thesis prediction to fail the hypothesis. First, it can be observed that any time interval that has predicted coals in higher latitudes is more likely to pass the null hypothesis. It can also be seen

that there is less predicted coal area for the older time intervals. With less prediction you have less opportunity to have hits. Finally, climate patterns may have been different during the older time intervals. We do not fully understand the climates during the older time intervals and prediction models use modern climate patterns to model past climates. With future exploration, this technique can possibly predict where other climate indicators formed to help better understand past climates and paleo-geology.

TABLE OF CONTENTS

LIST OF ILLUSTRATIONS

Figure Page

LIST OF TABLES

CHAPTER 1

INTRODUCTION

1.1 Presentation of the Data

The focus of this thesis is to map the location of coal deposits across geologic time and to test the hypothesis that coal deposits can be predicted using paleoclimate simulations. A statistical analysis was conducted to determine the predictability between the predicted coal deposits and known coal deposits occurrences. This chapter, the Introduction, describes the nature and formation of coal deposits.

This thesis is arranged into six chapters. Chapter 1 contains the introduction for this thesis. Chapter 2 contains information pertaining to the data, method used, and statistical procedures used to test whether the predicted distribution of coals passes the null hypothesis. Chapters 3, 4, and 5 outline the tectonic and climate settings of coal deposits for the Cenozoic, Mesozoic, and Paleozoic, and provides statistical results for each time period within each Era. Chapter 6, the final chapter, reviews the results for each Era and describes whether the prediction model is significant.

1.2 Formation of Coals

Coal is the family name for a group of accumulated and consolidated remains of plant material. A rock must contain more than 50% by weight and 70% by volume carbonaceous material to be considered a coal (Considine et al., 2008). The typical environments that produce coals are fresh water swamps or deltas, coastal plains, or in inland lake basins (Considine et al., 2008). When the parent plant material is physically or chemically altered by metamorphism or diagenesis, the processes is known as coalification (Considine et al., 2008). Through coalification, the swamp deposits progress through one or more stages and produce various grades of coals. Coal deposits are not uniform, and there are many different factors that can

cause various coal deposits to form. Different grades of coal are formed by differences in plant materials, degree of metamorphism, and the kinds of impurities (Considine et al., 2008).

The grades of coal include peat, lignite, sub-bituminous, bituminous, and anthracite. The most abundant grade of coal by volume is peat, since it is the first product of compaction. Peat forms from plant material in subaqueous environments with anaerobic conditions (Dietrich, 1979). The peat-to-anthracite theory of coal formation states that the process of coal formation is due to increasing metamorphism (Considine et al., 2008).

1.2.1 Formation of Coal Deposits Through Geologic Time

Coals are found worldwide (Figure 1.1). However, the modern distribution of coals does not reflect where coal deposits originally formed. In order to understand the formation of coals, it is necessary to plot coal deposits on paleogeographic reconstructions (Scotese, 2012).

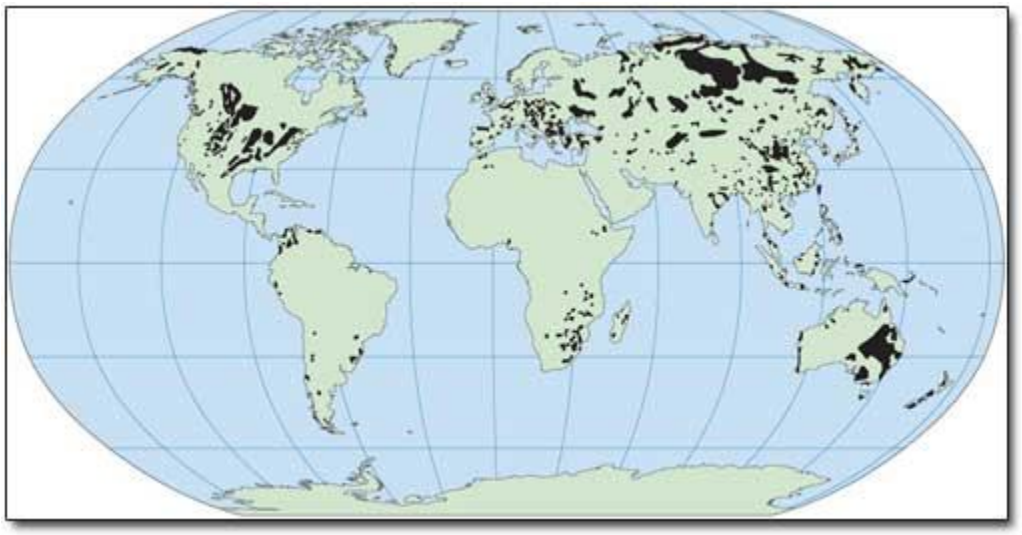

Figure 1.1 Map Showing the Earth's Coal Deposits Distribution in the Present Day

Looking back at the geologic record, numerous coal deposits formed during the Carboniferous, Cretaceous, Paleocene, and Eocene (Figure 1.2). The greatest volume of coal was deposited during the Pennsylvanian and the Permian. Most of the world's lignite is of Late Mesozoic or Cenozoic age; most peat is of Pleistocene or recent age (Dietrich, 1979).

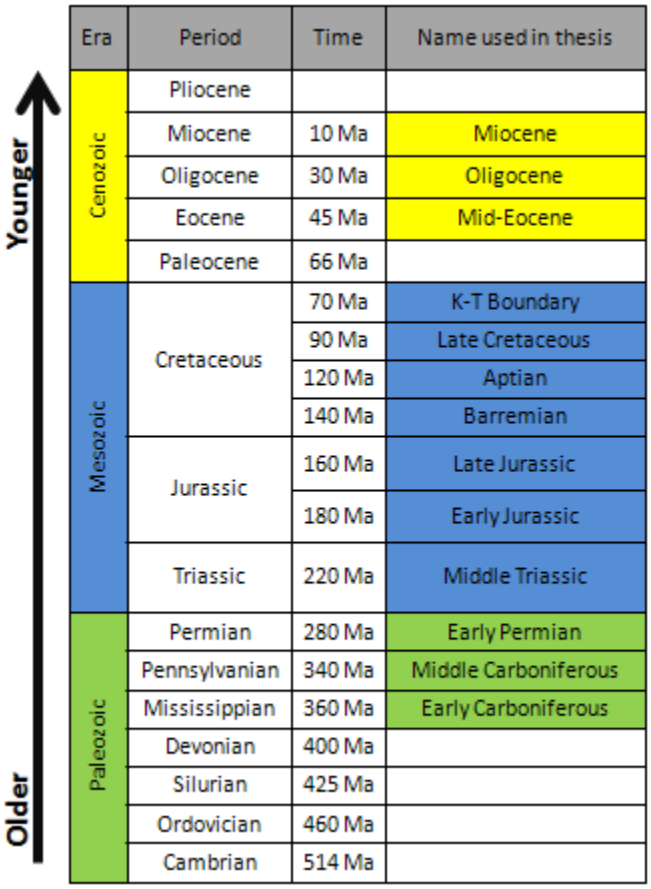

Era	Period	Time	Name used in thesis
Cenozoic	Pliocene		
	Miocene	10 Ma	Miocene
	Oligocene	30 Ma	Oligocene
	Eocene	45 Ma	Mid-Eocene
	Paleocene	66 Ma	
Mesozoic	Cretaceous	70 Ma	K-T Boundary
		90 Ma	Late Cretaceous
		120 Ma	Aptian
		140 Ma	Barremian
	Jurassic	160 Ma	Late Jurassic
		180 Ma	Early Jurassic
	Triassic	220 Ma	Middle Triassic
Paleozoic	Permian	280 Ma	Early Permian
	Pennsylvanian	340 Ma	Middle Carboniferous
	Mississippian	360 Ma	Early Carboniferous
	Devonian	400 Ma	
	Silurian	425 Ma	
	Ordovician	460 Ma	
	Cambrian	514 Ma	

Figure 1.2 Geologic Time Scale with Names used in this Thesis

Paleozoic coal deposits account for almost half of the coal reserves in the United States (Royer et al., 2004). During this major coal-forming period, the climate of North America was warm and humid. The coal-forming swamps were enormous, covering tens of thousands of square miles (about 30% of the total land), much like modern tropical rainforests. The Equator (where a majority of the coal deposits in Europe, North America and China during this time formed) was wet and hot. The calculated mean surface temperature for the Carboniferous was ~ 14^{o} Celsius (Royer et al., 2004). The cool temperate regions of Gondwana were located around 45^{o} North and South latitudes and most coal deposits in this region formed near the coast (Fig 1.3) (Scotese, 2001).

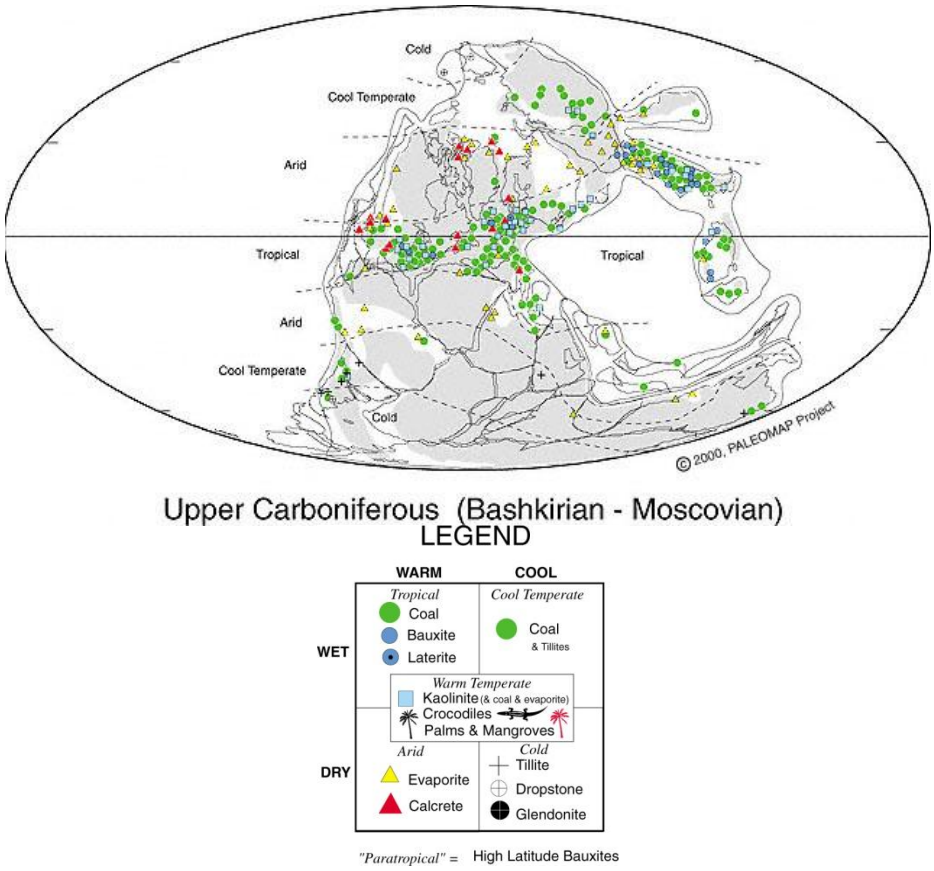

Figure 1.3 Earth during the Upper Carboniferous with the Distribution of Climate-Sensitive Sediments (Scotese, 2012)

1.3 Importance of Coal

This section will discuss the importance of coal in today's society. It will review coal usage during the past, the present, and potential coal usage in the future.

Coals have been studied extensively throughout time due to their importance as a natural resource and as a source of energy. Coals have been a vital part in the energy industry since the Industrial Revolution dated back to the 1800s. Coal is still important to the economy because approximately 40% of the world electricity is produced from coal (World Coal Institute, 2005).

Coal has many important uses worldwide which make it economical. The four main uses for coal are steel production, electricity generation, cement manufacturing, and in the form of liquid fuel (World Coal Institute, 2005).

Different types of coals have different economical uses. High ranking coals (coals that contain high carbon content and low moisture levels), such as bituminite and anthracite, are characterized by their harder texture and vitreous luster. These types of coals allows for more energy to be produced, so they are generally used in power generation and steel production (Considine et al., 2008).

Other industries that use coal, besides power generators and steel producers, are paper manufacturers, alumina refineries, and chemical and pharmaceutical industries. Coal by-products can be found in many everyday materials and common household items: aspirin, soap, dyes, and synthetic fabrics (Considine et al., 2008).

1.4 Coal Economy: Past, Present, and Future

Coal has been an important fuel resource. The next three sections will look at coal usage in the past, the present, and future.

1.4.1 Coal Economy: Past

One of the earliest known usages of coal, in the United States, dates back to the 1300s, when Native Americans, in what is now North America, used coal for cooking, heat, and making pottery. The first coal mine was opened in Virginia in the mid-1700s (American Coal Foundation, 2011).

Although coal usage began hundreds of years ago, coal began to be widely used during the Industrial Revolution (from 1750 to around 1850), when the demand for coal and energy sources rapidly increased. Soon after, steam-powered trains developed, which were fuelled by coal. These trains became a major form of transportation during the 19th century, especially in the United States. During this time, coal was also used during the American Civil War to fuel factories for the production of weapons (American Coal Foundation, 2011).

During the last 100 years, the United States coal used has peaked. Coal is used for: heating houses, providing heat for cooking, creating electricity, powering transportation vehicles, and fuelling factories. (American Coal Foundation, 2011).

1.4.2 Coal Economy: Present

Even though coal has been replaced by oil as the main source of energy today, it is still used heavily in some industries. About fifty-six percent of electricity used in the United States is coal-generated. Other uses for coal include the making of chemicals, cement, paper, ceramics, metal products, plastics, medicines, fertilizers, and tar (American Coal Foundation, 2011). The United States exports approximately nine percent of the total coal mined to about forty countries: mainly, Canada, Japan, and Western Europe (American Coal Foundation, 2011).

1.4.3 Coal Economy: Future

The demand for coal around the world is expected to increase due to the increase in electricity, manufacturing, and transportation needs of an increasing population. Although the demand for coal will increase in the United States, it is projected to greatly increase in areas such as China and India, where it will be used for electricity generation (American Coal Foundation, 2011).

1.5 Previous Work

This study uses many previous works pertaining to climate modelling. Climate is the long-term weather conditions within a certain region. Atmospheric properties that influence weather include temperature, precipitation, evaporation, air pressure, humidity, cloudiness, and winds. Regions with similar climatic conditions can be grouped into climatic zones (Walter, 1985).

Coal deposits are found in climatic zones where precipitation exceeds evaporation, and can form in either warm or cool temperature regions. Warm coal deposits are found near the equator in tropical biomes, also known as the tropical rainforests (Morley, 2000). Rainforest floras extend from the equator to beyond the Tropics to about 30^{o} north and south (Negrelle,

2002). Although typically the rainforest extends from the equator to 30°, geologic records show evidence for tropical rainforests extending up into the 50° range (Wolfe, 1985).

Tropical rainforests are the result of low-latitude atmospheric circulation called Hadley cells. Figure 1.4 shows an example of the Hadley circulation cells (Parrish, 1998). This same process happens near 60° north and south. Baroclinic waves bring warm moist air from the tropics and cause an increase in precipitation in these latitudes.

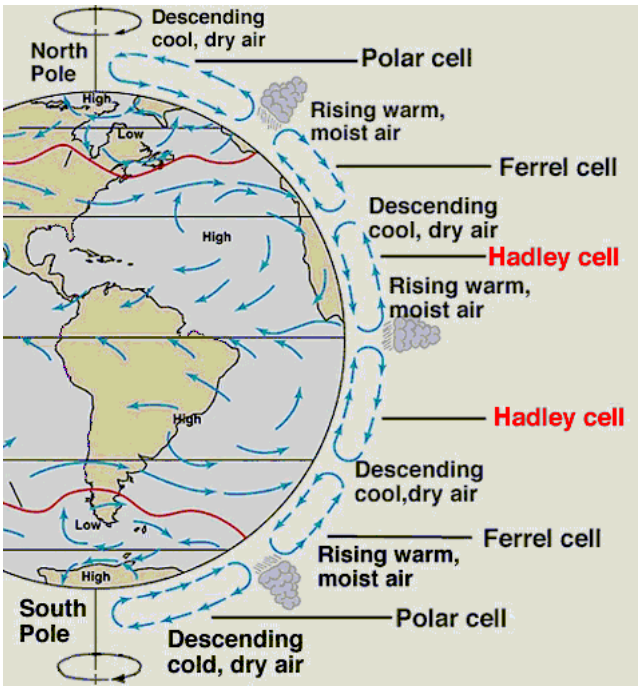

Figure 1.4 Global Image Showing the Different Atmospheric Circulation Patterns (Ruddiman, 2008)

Coal deposits are dependent on the hydrological cycle, particularly on pattern of precipitation and evaporation. Coals form in humid areas where precipitation exceeds evaporation. Figure 1.5 shows latitudinal occurrence of coal deposits from the Permian to Recent (Ziegler et al., 2003). Three clear peaks are visible: one around the Equator from 30° north to 30° south and two other peaks at 50° north and 65° south. These are the latitudinal zones where we should see coal being deposited. In this thesis, a hypothesis will be assessed, whether coals predominantly form in areas where precipitation exceeds evaporation.

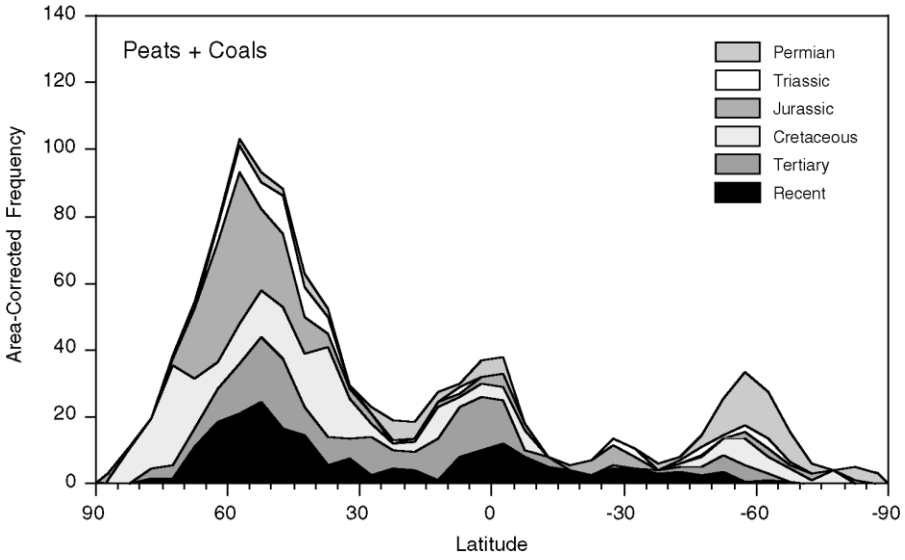

Figure 1.5 Graphical Distribution of Present Day Precipitation from Pole to Pole (Ziegler et al., 2003)

CHAPTER 2

METHODOLOGY

2.1 Method Introduction

Climate indicators, such as coals, evaporites, bauxites, etc., can be used to test the results of paleoclimate models. Coals are known to form in wet climates; however, coals form in two separate temperature climatic zones: the equatorial rainy belt or the temperate rainy belt. Since moisture is the main contributing factor, this study will only consider the relationship between precipitation and coal formation.

In this thesis, the data is organized into thirteen different time intervals and presented on paleogeographic reconstructions. These maps were produced by the PALEOMAP Project (Scotese, 2001). The process for creating these paleogeographic reconstructions will be discussed in this chapter. In this thesis, the hypothesis will test if coals form under specific climate conditions. The relationship between coals and climate is summarized in detail in the Introduction. To test this hypothesis, paleoclimate simulation results from the GANDOLPH Project (Scotese, 2005, 2006, 2007, 2011) will be compared with a database of Phanerozoic coal deposits compiled by Boucot et al., 2012. The coals were plotted on paleogeographic maps and gridded with a $5^{o}x5^{o}$ latitudinal/longitudinal grid. For each time interval, $5^{o}x5^{o}$ grid cells were also constructed that represented areas where paleo-precipitation exceeded paleo-evaporation. If a coal deposit occurred within a grid cell with sufficient precipitation ($P-E > 0$), then it was considered to be a “hit,” or a positive test that the formation of coals are controlled by precipitation. In this chapter, the hypothesis that coal formation is controlled by paleo-precipitation will be described in detail.

2.2 FOAM Paleoclimate Simulation Data

All paleoclimate maps were provided by the GANDOLPH Project (Scotese, 2007, 2008, 2009, 2011). The paleoclimate conditions for the thirteen different time intervals were simulated using the Fast Ocean and Atmosphere Model (Tobis et al., 1997). FOAM uses oceanic and atmospheric dynamic models along with sea-ice, land topography, and river models to simulate paleoclimates on a global scale. The thirteen time intervals used in this study were: Miocene (10 Ma), Oligocene (30 Ma), Mid-Eocene (45 Ma), K-T boundary (70 Ma), Late Cretaceous (90 Ma), Aptian (120 Ma), Barremian (140 Ma), Late Jurassic (160 Ma), Early Jurassic (180 Ma), Middle Triassic (220 Ma), Early Permian (280 Ma), Middle Carboniferous (340 Ma), and Early Carboniferous (360 Ma).

2.3 Data Processing

The modern precipitation values used in this thesis were from Legates and Wilmot Global Climate Database (Legates and Wilmot, 1990). Figure 2.1 is a modern map illustrating Annual Precipitation (Legates and Wilmot, 1990).

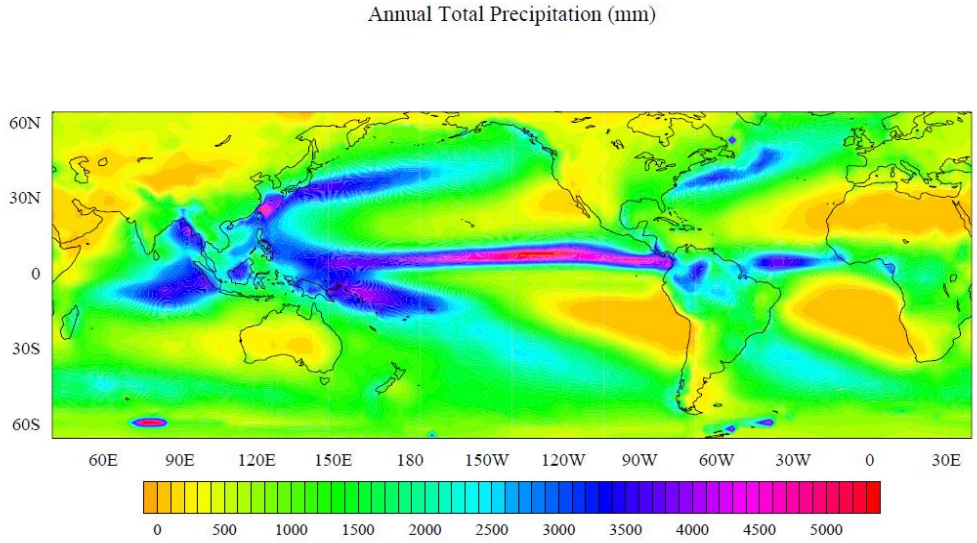

Figure 2.1 Map Showing Modern Precipitation Values from Legates and Wilmot Global Climate Database (Legates and Wilmot, 1990)

2.4 Data Analysis in ArcGIS: Preparation of Landmass, Coal, and Precipitation Area Maps

In order to test the central hypothesis of this thesis (namely that the occurrence of coal deposits is strongly associated with areas of high paleo-precipitation), it was necessary to estimate the area of ancient landmass, the area of coal occurrences, and the area of paleo-precipitation for each time interval. This section describes how these three different maps were constructed using ArcGIS.

Before discussing each type of map, the problem of equalizing area from equator to pole must be addressed. As mention in section 2.1, a $5^{o}x5^{o}$ grid was used to reduce the problem of uneven data clustering. Each $5^{o}x5^{o}$ grid cell is not the same amount of area from equator to the poles. Closer to the poles, the lines of longitude converge making each $5^{o}x5^{o}$ grid cell smaller progressively smaller as you approach the pole. To create an equal area grid, each latitudinal band was multiplied by an area factor. The number of grid cells in a latitudinal band multiplied by this scaling factor is the actual area is considered the "Area." To find the "Actual Area," the "Area" values were multiplied by the area one $5^{o}x5^{o}$ grid cell would be on Earth in square kilometers. Therefore, each "Area" value was multiplied by 308641.4 km^2 to find the "Actual Area". To simplify for this thesis all "Actual Area" values will be divided by one million.

2.5 Area of Ancient Landmasses

The distribution of land and its geographic distribution have changed through time. In this thesis, the paleogeographic maps of Scotese (Scotese, 2005, 2006, 2007, 2011) were used to create a $5^{o}x5^{o}$ grid that represented land areas through time. A $5^{o}x5^{o}$ grid was chosen to reduce the problem of uneven data cluster. For each map the amount of land was estimated by counting the number of 5^{o} grid cells in each latitudinal band. This count was then converted to an area estimate by taking into account how the relative area of a $5^{o}x5^{o}$ cell changes from pole to equator. Table 2.1 gives the area of each $5^{o}x5^{o}$ grid cell as a function of latitude. This table is an example using the land data for the Miocene.

Table 2.1 10 Ma Total Land Factored Table

Lat	Lat	Factor	RAW	Area	Actual Area in million sq km
85	90	22.9	0	0	0
80	85	7.654	23	3.004965	0.927456393
75	80	4.616	36	7.79896	2.407081648
70	75	3.322	60	18.06141	5.574497737
65	70	2.611	68	26.04366	8.038151032
60	65	2.164	66	30.49908	9.413276169
55	60	1.859	58	31.19957	9.62947755
50	55	1.641	53	32.29738	9.968307115
45	50	1.479	46	31.1021	9.59939315
40	45	1.355	46	33.94834	10.4778616
35	40	1.259	42	33.35981	10.29621687
30	35	1.185	39	32.91139	10.15781685
25	30	1.126	37	32.85968	10.14185635
20	25	1.081	36	33.3025	10.27852811
15	20	1.048	39	37.21374	11.48569939
10	15	1.023	35	34.2131	10.55957725
5	10	1.0008	31	30.97522	9.560233912
0	5	1	28	28	8.641958025
0	-5	1	26	26	8.024675309
-5	-10	1.0008	25	24.98002	7.709866058
-10	-15	1.023	24	23.46041	7.240852974
-15	-20	1.048	23	21.94656	6.77361759
-20	-25	1.081	21	19.42646	5.995808065
-25	-30	1.126	20	17.76199	5.482084512
-30	-35	1.185	19	16.03376	4.948680002
-35	-40	1.259	16	12.7085	3.922368331
-40	-45	1.355	15	11.07011	3.416694
-45	-50	1.479	9	6.085193	1.878142138
-50	-55	1.641	5	3.046923	0.940406332
-55	-60	1.859	2	1.075847	0.33205095
-60	-65	2.164	3	1.386322	0.427876189
-65	-70	2.611	36	13.78782	4.255491723
-70	-75	3.322	50	15.05117	4.645414781
-75	-80	4.616	65	14.08146	4.346119643
-80	-85	7.654	68	8.884244	2.742044989
-85	-90	22.9	72	3.144105	0.970400776
			1242	716.7218	221.2099835

Latitude was plotted along the x-axis from -90^{o} to 90^{o}. The scaled land value was plotted along the y-axis. Figure 2.2 shows an example of a land histogram with the area of land in each 5^{o} latitudinal zone for the Miocene.

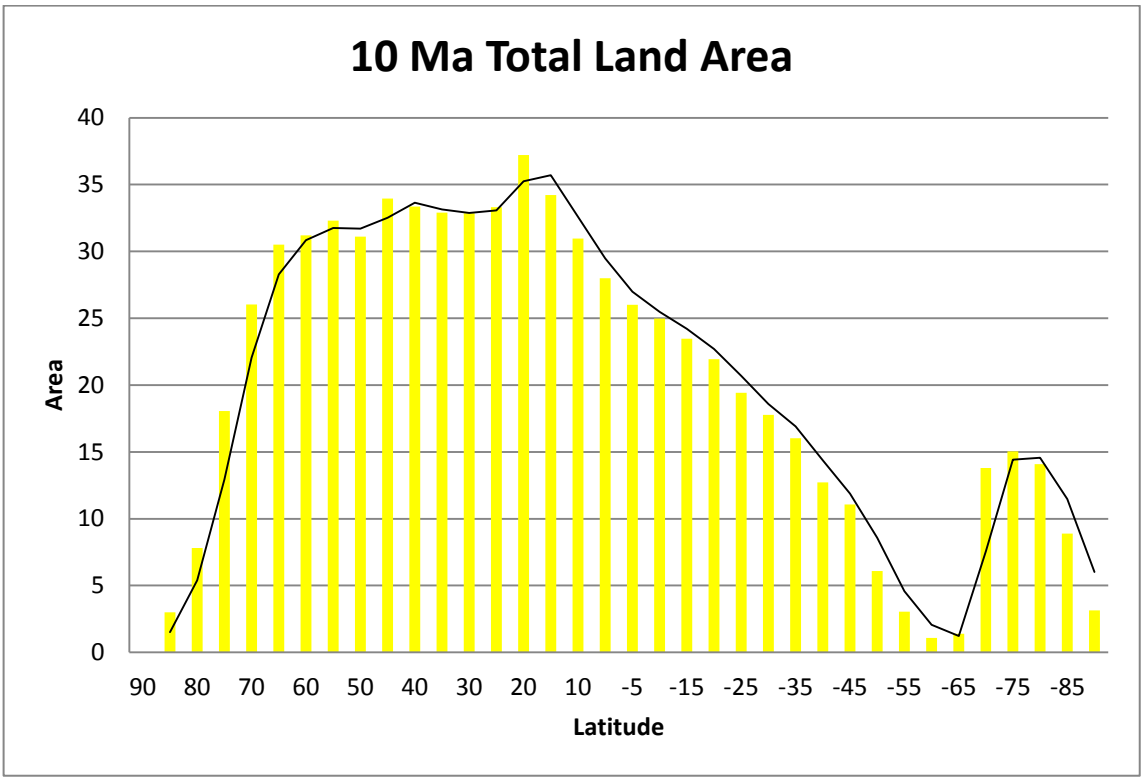

Figure 2.2 Histogram of 10 Ma Total Landmass Area Latitude

2.6 Area of Observed Coal Deposits

The same method used on total landmass was used to calculate the area of observed coal deposits. The known distribution of coal deposits were placed in their respective time interval layer on the paleogeographic maps. $5^{o}x5^{o}$ cells were selected if they contained at least one coal deposit locality.

The area of coal deposits was calculated in a manner identical to the technique used to estimate the area of ancient landmasses. The number of $5^{o}x5^{o}$ grid cells was summed for each 5^{o} latitudinal belt. This total represented the "raw" value for the number of coal localities. This "raw" value was then scaled as a function of latitude using the area parameter in Table 2.2 to obtain the true area represented by the grid cells. Table 2.2 is an example of the area of observed coal locations from the Late Miocene.

Table 2.2 10 Ma Observed Coals Factored Table

Lat	Lat	Factor	RAW	Area	Actual Area in million sq km
85	90	22.9	0	0	0
80	85	7.654	1	0.130651	0.040324191
75	80	4.616	0	0	0
70	75	3.322	1	0.301023	0.092908296
65	70	2.611	2	0.76599	0.236416207
60	65	2.164	8	3.696858	1.141003172
55	60	1.859	7	3.765465	1.162178325
50	55	1.641	12	7.312614	2.256975196
45	50	1.479	14	9.465855	2.921554437
40	45	1.355	17	12.54613	3.8722532
35	40	1.259	16	12.7085	3.922368331
30	35	1.185	6	5.063291	1.562741053
25	30	1.126	9	7.992895	2.46693803
20	25	1.081	8	7.400555	2.284117358
15	20	1.048	10	9.541985	2.945051126
10	15	1.023	9	8.797654	2.715319865
5	10	1.0008	11	10.99121	3.392341065
0	5	1	7	7	2.160489506
0	-5	1	7	7	2.160489506
-5	-10	1.0008	4	3.996803	1.233578569
-10	-15	1.023	3	2.932551	0.905106622
-15	-20	1.048	1	0.954198	0.294505113
-20	-25	1.081	2	1.850139	0.57102934
-25	-30	1.126	2	1.776199	0.548208451
-30	-35	1.185	2	1.687764	0.520913684
-35	-40	1.259	1	0.794281	0.245148021
-40	-45	1.355	3	2.214022	0.6833388
-45	-50	1.479	2	1.352265	0.41736492
-50	-55	1.641	1	0.609385	0.188081266
-55	-60	1.859	0	0	0
-60	-65	2.164	0	0	0
-65	-70	2.611	0	0	0
-70	-75	3.322	0	0	0
-75	-80	4.616	0	0	0
-80	-85	7.654	0	0	0
-85	-90	22.9	0	0	0
			166	132.6483	40.94074365

Figure 2.3 shows an example of a coal intersection histogram. This histogram shows the distribution of known coals in each 5^{o} latitudinal zone for the Miocene.

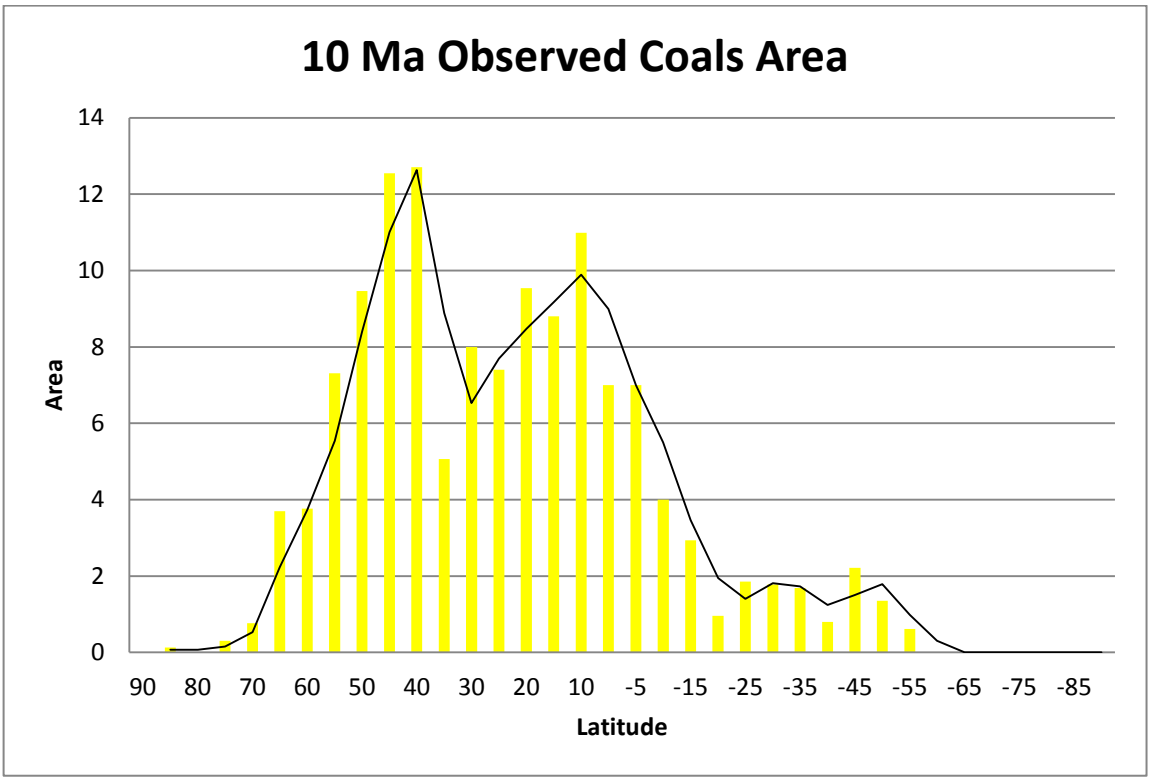

Figure 2.3 Histogram of 10 Ma Observed Coal Deposit Area Latitude

2.7 Area of High Precipitation/ Area of Predicted Coal Deposits

This thesis is proposing that the amount of rain/runoff needed to form coal must be greater than the amount of evaporation. Certain biomes have more precipitation than evaporation. Figure 2.4 shows a graph of each modern day biome and how much temperature and precipitation is necessary to maintain each biome (Peppe et al., 2011). Tropical rainforest, temperate rainforest, temperate forests, boreal forests, tropical seasonal forests, and grassland are all biomes that coals can form in. Figure 2.5 shows a map of the modern Earth with all the biomes (Peppe et al., 2011). All FOAM paleo-runoff points that fell within the ice, tundra, and deserts were removed from the dataset. The remaining data points all fell within a minimum precipitation of 250 mm/year. Figure 2.6 shows the 10 million year 250 mm/year or greater precipitation map.

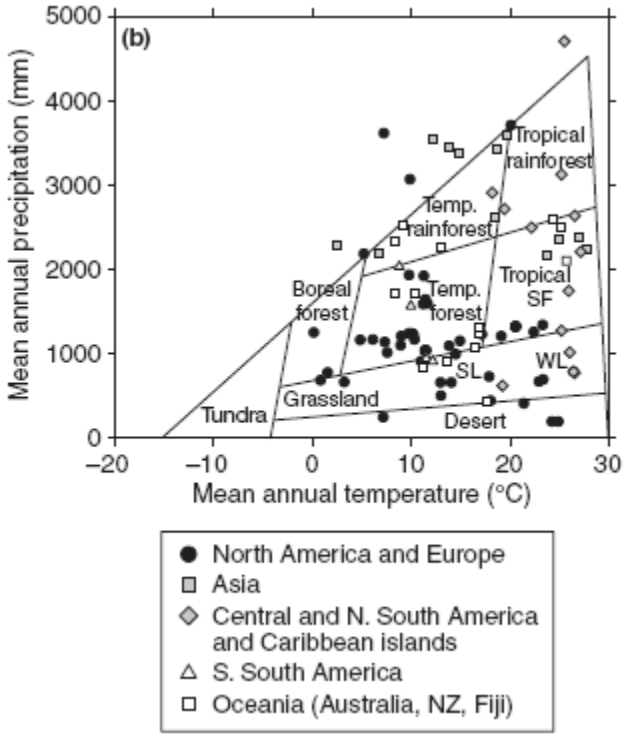

Figure 2.4 Graphical Display of Biomes Based on Mean Annual Temperature and Precipitation

(Peppe et al., 2011)

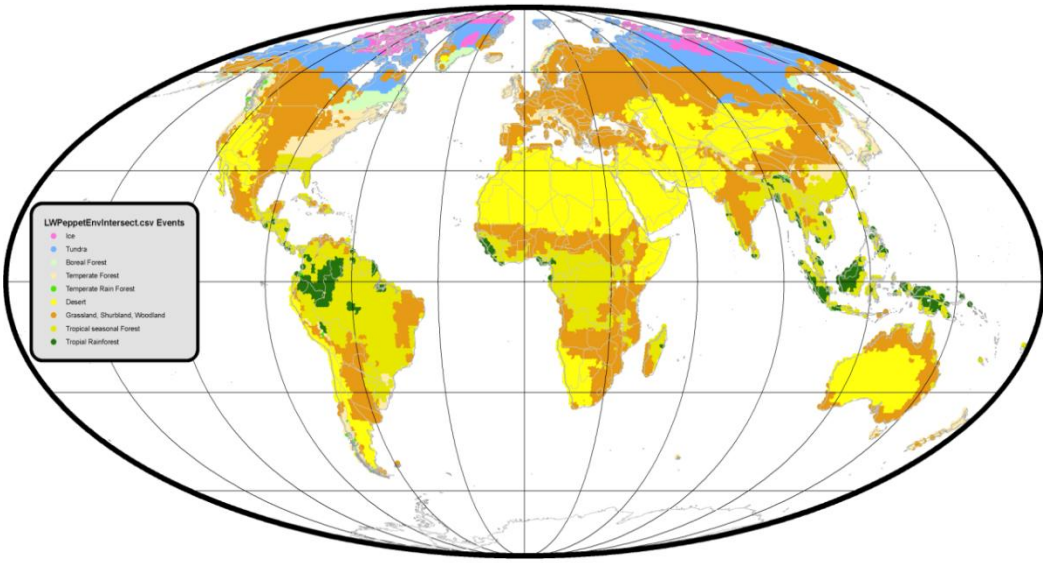

Figure 2.5 Map of Biomes for the Modern Day (Peppe et al., 2011)

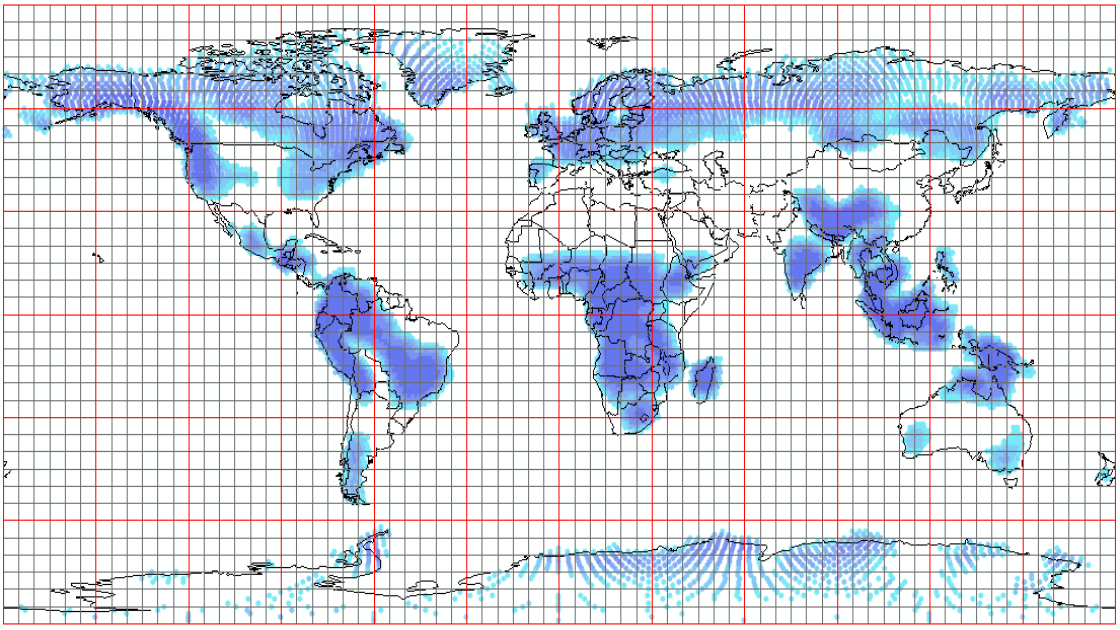

Figure 2.6 Map of 10 Ma Annual Runoff Simulated with FOAM for 10 Ma

A predicted coal deposit area shapefile was created for grid cells where simulated precipitation exceeded 250 mm/year.. Figure 2.7 shows the coal prediction grid for the Miocene (10 Ma).

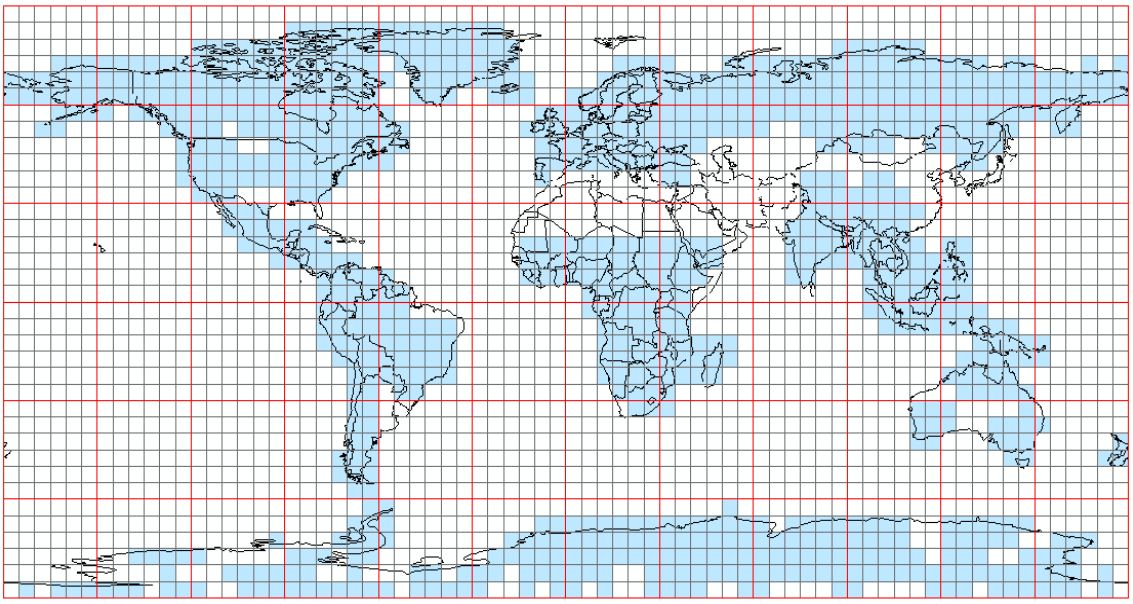

Figure 2.7 10 Ma Predicted Coal Deposit Area on 10 Ma Paleogeographic Map

The area where paleo-precipitation was sufficient to produce coal deposits was calculated in a manner identical to the techniques described in the two previous sections. Coal deposits were computed for each latitude, and adjusted to true area using the parameters in Table 2.3. As an example, the late Miocene was used.

Table 2.3 10 Ma Predicted Coals Factored Table

Lat	Lat	Factor	RAW	Area	Actual Area in million sq km
85	90	22.9		0	0
80	85	7.654	14	1.829109	0.564538674
75	80	4.616	27	5.84922	1.805311236
70	75	3.322	54	16.25527	5.017047963
65	70	2.611	67	25.66067	7.919942929
60	65	2.164	66	30.49908	9.413276169
55	60	1.859	56	30.12372	9.2974266
50	55	1.641	49	29.85984	9.215982049
45	50	1.479	34	22.98851	7.095203633
40	45	1.355	26	19.18819	5.9222696
35	40	1.259	19	15.09134	4.657812393
30	35	1.185	13	10.97046	3.385938949
25	30	1.126	11	9.769094	3.015146482
20	25	1.081	14	12.95097	3.997205377
15	20	1.048	30	28.62595	8.835153379
10	15	1.023	31	30.30303	9.352768425
5	10	1.0008	26	25.97922	8.0182607
0	5	1	20	20	6.172827161
0	-5	1	21	21	6.481468519
-5	-10	1.0008	24	23.98082	7.401471415
-10	-15	1.023	23	22.48289	6.939150767
-15	-20	1.048	23	21.94656	6.77361759
-20	-25	1.081	20	18.50139	5.710293395
-25	-30	1.126	13	11.54529	3.563354933
-30	-35	1.185	9	7.594937	2.34411158
-35	-40	1.259	9	7.148531	2.206332186
-40	-45	1.355	8	5.904059	1.8222368
-45	-50	1.479	7	4.732928	1.460777219
-50	-55	1.641	3	1.828154	0.564243799
-55	-60	1.859	2	1.075847	0.33205095
-60	-65	2.164	3	1.386322	0.427876189
-65	-70	2.611	32	12.25584	3.782659309
-70	-75	3.322	39	11.73992	3.623423529
-75	-80	4.616	45	9.7487	3.00885206
-80	-85	7.654	48	6.271231	1.935561169
-85	-90	22.9	47	2.052402	0.633456062
			933	527.1395	162.6970492

Figure 2.8 shows an example of a predicted coal deposit area histogram. This histogram shows the area of the predicted coals in each 5^{o} latitudinal zone for the Miocene.

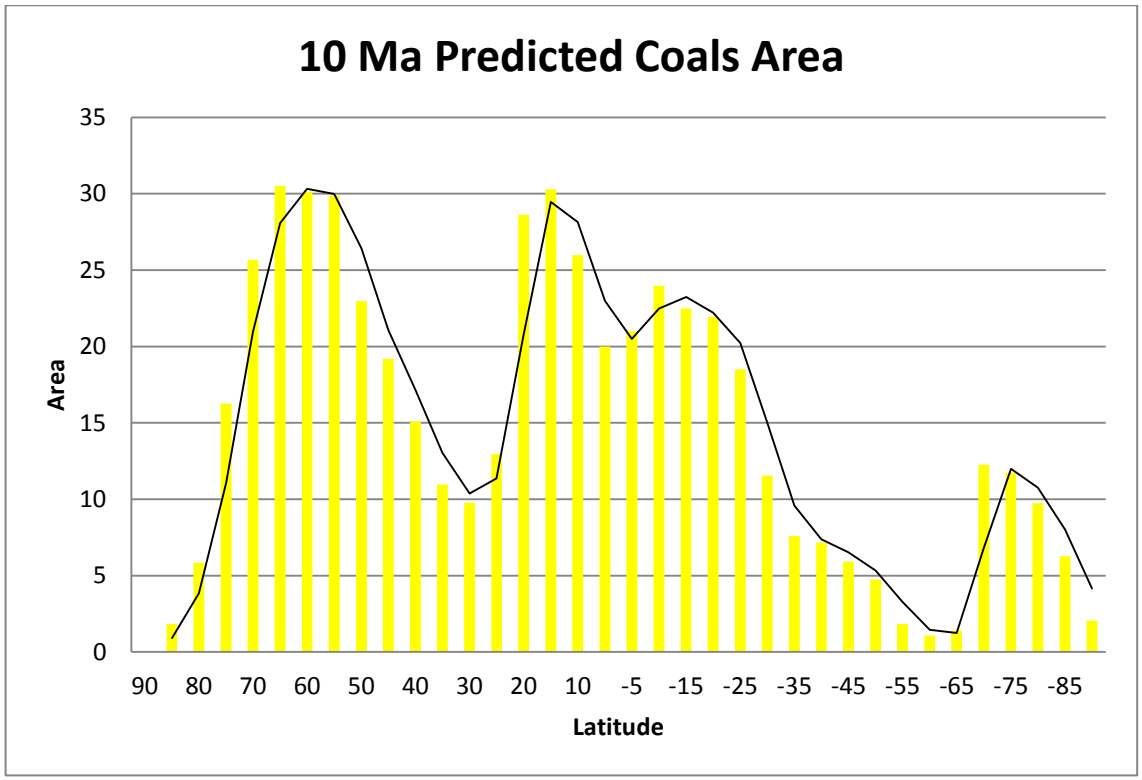

Figure 2.8 10 Map Predicted Coal Deposit Area Histogram Plotted Along Latitude

The predicted coals areas are found in three major latitudes. The warm and wet coals are found near the equator and span from around -20^{o} to 20^{o}. The cool and wet coals are found in two localities. In the southern hemisphere, the predicted coals span from -85^{o} to -60^{o}, and in the northern hemisphere, the predicted coals span from 40^{o} to 75^{o}. Figure 2.9 is a histogram that shows the total predicted coal areas and their latitudinal coordinate along the x-axis and number of predicted coals along the y-axis for all time intervals in this thesis.

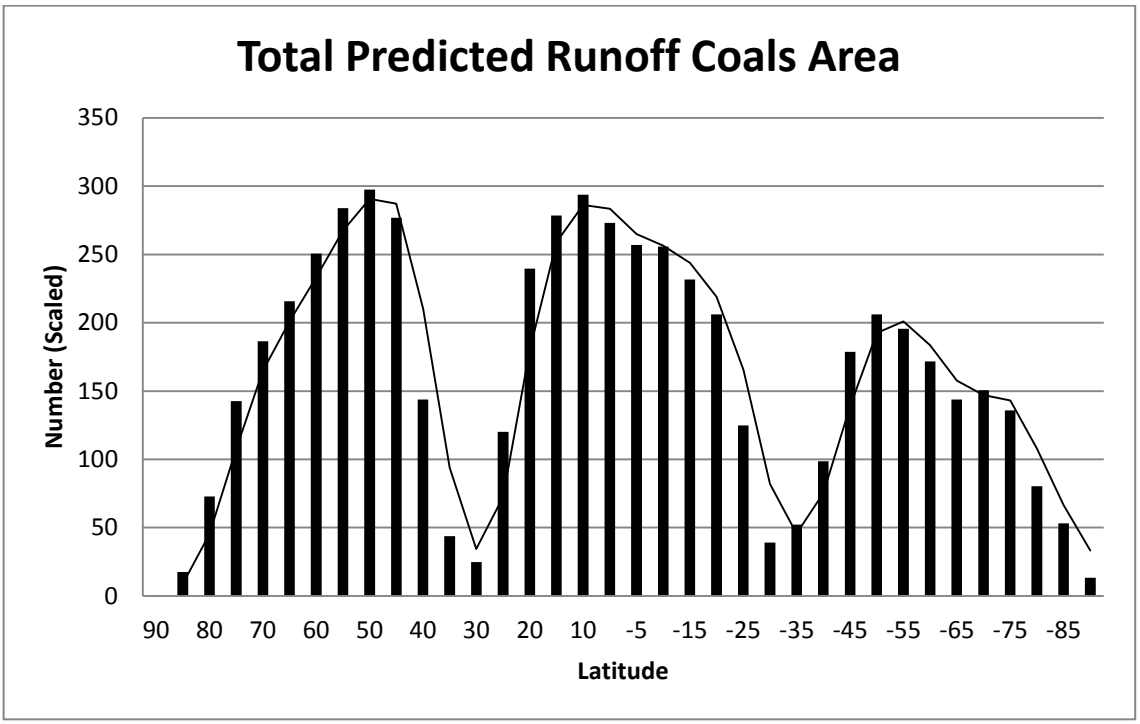

Figure 2.9 Histogram of Total Predicted Coal Deposit Area Latitude

2.8 Hits vs. Misses

When an observed coal $5^{o}x5^{o}$ grid cell coincides with a predicted coal $5^{o}x5^{o}$ grid cell, it is considered to be a "hit". ArcToolbox was used to select the $5^{o}x5^{o}$ grid cells that contained both an observed coal deposit and a predicted coal deposit grid cell. Figure 2.10 shows the observed coals intersected with the predicted coals for the Miocene (10 Ma). The pink boxes are the grid cells that contain both predicted and observed coal deposits within the Miocene.

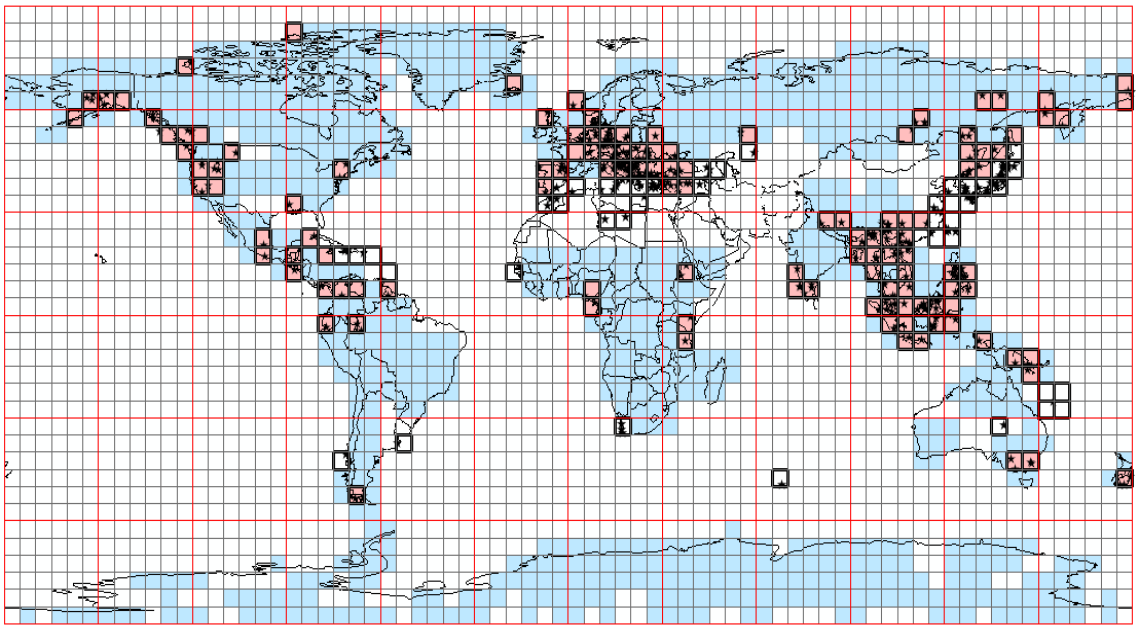

Figure 2.10 10 Ma Hits vs. Misses Coal Deposit Area Plotted on 10 Ma Paleogeographic Map

As you can see from Figure 2.10, there are more “hits” than “misses.” This is largely due to the fact that there are more grid cells where coals are predicted than where coals are not predicted. The total area of “hits” (i.e. matches) between the predicted coal localities and the observed coal localities was calculated in a manner identical to the procedures used to calculate the area of land, coal, and predicted coal localities. The number of 5^{o}x5^{o} grid cells was summed for each 5^{o} latitudinal belt. This “raw” total was then converted to true area using the parameters in Table 2.4. As an example the Miocene was used.

Table 2.4 10 Ma Hits Factored Table

Lat	Lat	Factor	RAW	Area	Actual Area in million sq km
85	90	22.9	0	0	0
80	85	7.654	1	0.130651	0.040324191
75	80	4.616	0	0	0
70	75	3.322	1	0.301023	0.092908296
65	70	2.611	2	0.76599	0.236416207
60	65	2.164	8	3.696858	1.141003172
55	60	1.859	7	3.765465	1.162178325
50	55	1.641	12	7.312614	2.256975196
45	50	1.479	12	8.11359	2.504189517
40	45	1.355	13	9.594096	2.9611348
35	40	1.259	5	3.971406	1.225740103
30	35	1.185	1	0.843882	0.260456842
25	30	1.126	5	4.440497	1.370521128
20	25	1.081	6	5.550416	1.713088019
15	20	1.048	7	6.679389	2.061535788
10	15	1.023	7	6.84262	2.111915451
5	10	1.0008	11	10.99121	3.392341065
0	5	1	7	7	2.160489506
0	-5	1	7	7	2.160489506
-5	-10	1.0008	4	3.996803	1.233578569
-10	-15	1.023	2	1.955034	0.603404414
-15	-20	1.048	1	0.954198	0.294505113
-20	-25	1.081	0	0	0
-25	-30	1.126	0	0	0
-30	-35	1.185	0	0	0
-35	-40	1.259	0	0	0
-40	-45	1.355	2	1.476015	0.4555592
-45	-50	1.479	1	0.676133	0.20868246
-50	-55	1.641	1	0.609385	0.188081266
-55	-60	1.859	0	0	0
-60	-65	2.164	0	0	0
-65	-70	2.611	0	0	0
-70	-75	3.322	0	0	0
-75	-80	4.616	0	0	0
-80	-85	7.654	0	0	0
-85	-90	22.9	0	0	0
			123	96.66727	29.83551813

Figure 2.11 shows an example of a "hits" histogram. This histogram shows the distribution of the "hits" in each 5^{o} latitudinal zone for the Miocene. The next section will discuss the statistical procedure used to determine if the number of hits were statistically significant.

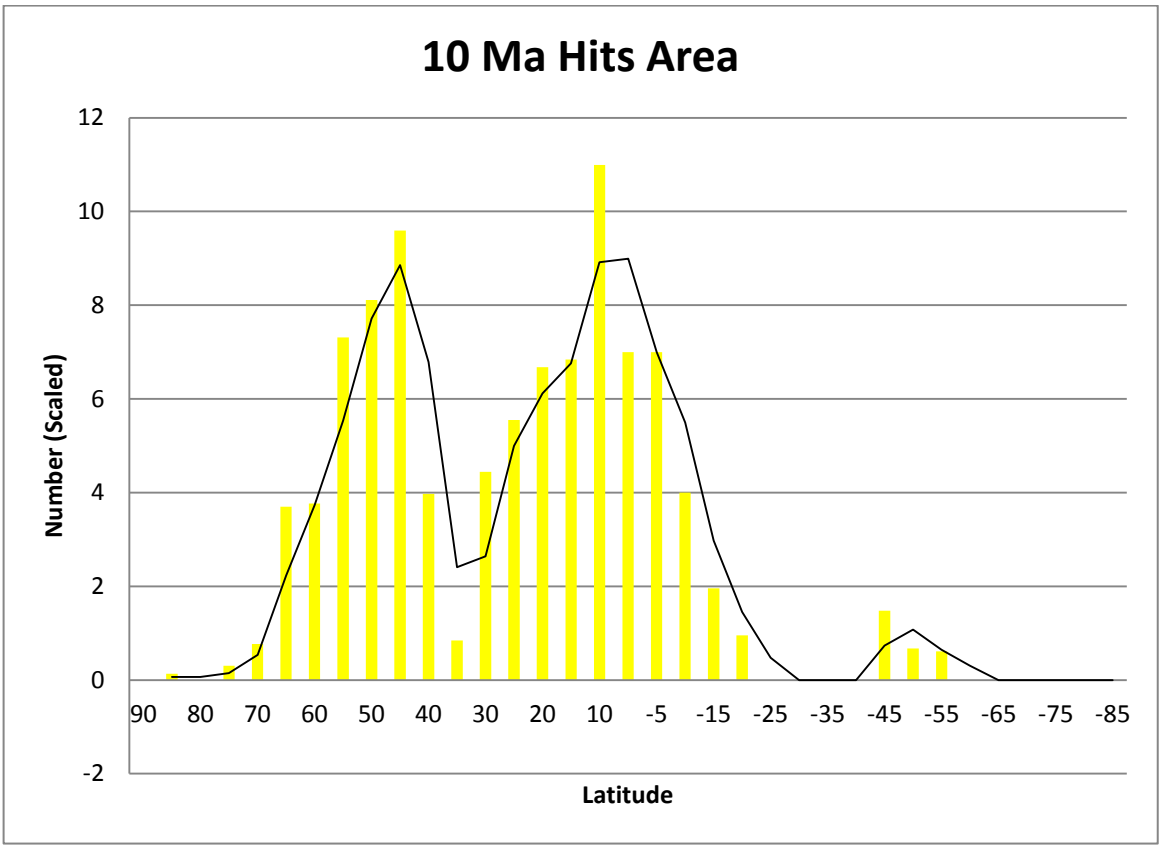

Figure 2.11 Histogram of Hits with Latitude for 10 Ma

2.9 Are the Number of Hits Statistically Significant?

A statistical procedure was used in order to check how well the observed coals $5^{o}x5^{o}$ grid cells matched with the predicted coals $5^{o}x5^{o}$ grid cells. A review of the statistical analysis used in this thesis will be shown using the late Miocene (10 Ma) as an example. In the following chapters, I will discuss in detail the statistical procedures and results for each geologic Era.

Table 2.5 is an example calculation for the Miocene period. The table lists: 1) total land area, 2) predicted coal area, 3) percentage of land occupied by predicted coal area, 4) observed

coals area, 5) predicted number of hits area, 6) actual hits area, 7) area of misses, and probability of randomness.

After determining the areas of the four principle variables: land area, area of predicted coals, area of observed coals, and area of hits; a simple statistical test was made to determine if the number of "hits" were statistically significant. The null hypothesis states that the observed distribution of known coals is random and does not significantly match the pattern of predicted coal localities based on paleo-precipitation. This thesis will try to prove that this null hypothesis is false and assess to what degree the distribution of coal is non-random.

Our expectations regarding the null hypothesis are as follows. The percentage of land area that is predicted to have coal deposits can be estimated by dividing the area of predicted coals (A_{pc}) by the total land area (A_{land}). In the case of the Miocene, the total land area is 221 x 10^6 km^2, and the area of predicted coals is 163 x 10^6 km^2. The ratio of predicted coals to total land area is $\frac{163}{221}$ x 10^6 km^2 or 73%. This means if we were to place 100 coal localities randomly on the map 73% should fall in the area where coal is predicted to occur. If 73 x 10^6 km^2 or some number close to 73 x 10^6 km^2 were to occur then the null hypothesis would pass suggesting the observed distribution of coals is random.

In the case of the Miocene the area of known coals is 41 x 10^6 km^2. According to prediction, 73% of this area should fall within the area of predicted coal deposits. These would be the predicted hits. In this case 73% of 41 x 10^6 km^2 is 30 x 10^6 km^2. The actual area of observed hits is 30 x 10^6 km^2. The actual number of hits is the same number as the predicted number of hits calculated (30/30=1). Since the actual hits area and the predicted hits area are the same, the null hypothesis stands suggesting that the distribution of observed coals is most likely random.

Table 2.5 10 Ma Total Results used during the Statistical Analysis

Total Land	Area of Predicted Coals	% Total Land Occupied by Predicted coals	Area of observed coals	Predicted number of hits	hits	Misses	% of Observing the Number of Predicted Hits
221	163	73	41	30	30	11	0.07

2.10 Probability that Observed Hits are Random

As described previously, the null hypothesis states that the expected number of hits should be proportional to the percentage of predicted coal grid cells. This leads to the question of whether or not the observed number of hits are random or not. Using Poisson distribution (Downing and Clark, 1989), the probability that the observed number of hits is due to randomness can be estimated.

The Poisson distribution is defined as: the probability of the frequency of a particular event P(x) can be estimated if the expected frequency of the event (λ) and the observed frequency of the event (K) are known (Downing and Clark, 1989). Below is the equation for the Poisson distribution:

$$P(x) = (e^{-\lambda}) (\lambda^{K})/ K! \quad (1)$$

Where,

P(x) = the probability of obtaining a particular number of hits

K= observed frequency of an event (number of observed occurrences)

λ= expected frequency of an event (number of predicted occurrences)

In this thesis, the predicted number of actual coal hits is λ. And the number of actual coal hits is K. For the Late Miocene as an example; λ is equal to 30 predicted hits area. The number of hits area, K, is 30. Using equation (1), we can solve for the probability P(x) for hits that are random. In this example,

$$P(x) = (e^{-30}) (30^{30})/ 30!, \text{ or } 0.07.$$

A comparison of the expected number of hits to the observed number of hits shows that the observed number of hits is the same as the expected number of hits. This suggests that the observed hits are random and thus the null hypothesis stands. Figure 2.12 shows the Poisson distribution for 10 Ma. The red line represents the actual number of hits observed and the dashed black line represents the predicted number of hits for the Miocene. The red box represents areas of randomness while the green boxes represent areas of significant departure from randomness. Any point that falls within the green is significant to a degree. During the Miocene, the number of predicted hits area equals the number of actual hits area. This means it is random and not significant. In the following 3 chapters, the statistical analysis results for the Cenozoic, Mesozoic, and Paleozoic Eras will be discussed.

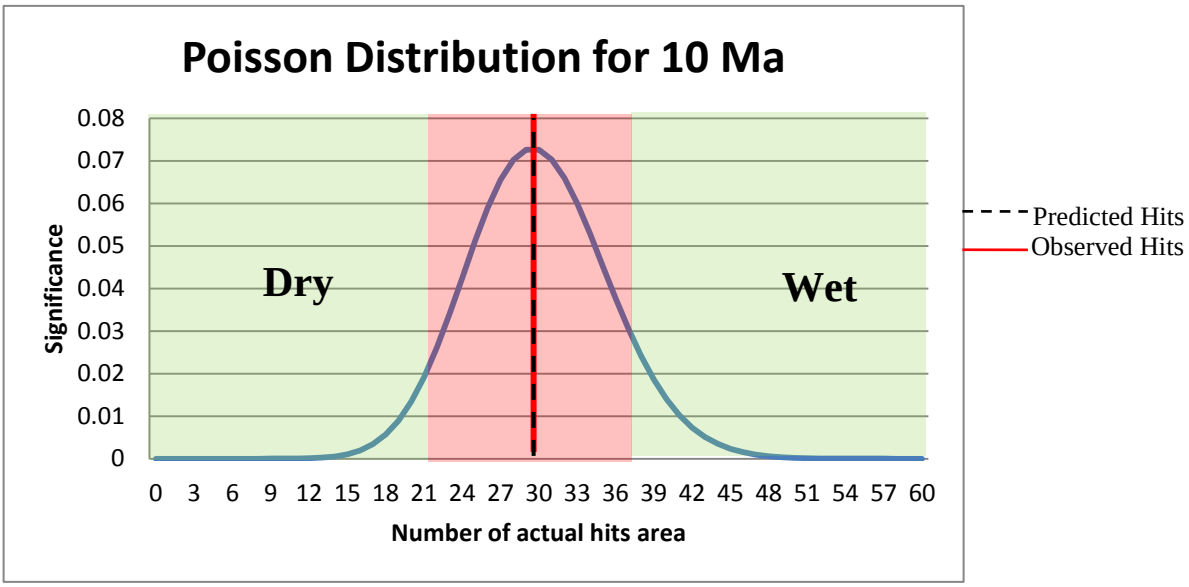

Figure 2.12 Poisson Distribution for 10 M

CHAPTER 3

CENOZOIC COALS

3.1 Introduction

This chapter and the following two chapters will discuss in detail the results of the Cenozoic, Mesozoic, and Paleozoic results, respectively. In each chapter, the observed coal deposit localities will be compared with the predicted coal deposit localities for each time interval and the statistical procedures described in Chapter 2 will be used to test if the coals pass or fail the null hypothesis.

The Cenozoic Era is broken up into six different time periods: Paleocene (66 Ma), Eocene (45 Ma), Oligocene (30 Ma), Miocene (10 Ma), Pliocene (5 Ma), and Quaternary (recent). This chapter will discuss the results for the Miocene (10 Ma), Oligocene (30 Ma), and Middle Eocene (45 Ma).

3.2 The Cenozoic Era

The Cenozoic Era is known for its fluctuation between hot house and ice house climates (Zachos et al., 2008). During the Eocene, the climate was warm and humid. Evidence of alligators and palm trees were found near the poles showing swamps were in these regions (Scotese, 2001). The Oligocene was slightly cooler than the Eocene, with ice covering the South Pole (Zachos et al., 2008). The Oligocene had warm temperate forests that covered northern Eurasia and North America (Scotese, 2001). The Miocene's climate is similar to today's climate but with slightly higher temperatures (Zachos et al., 2008). Australia was less arid than today and swamps could be found in northern Europe (Scotese, 2001).

There are many factors that have influenced the climate during the Cenozoic Era: Solar input, orbital variations (eccentricity and tilt), galactic mechanisms, atmospheric composition

(such as greenhouse gas concentration due to decreased spreading rate), changes in the Earth's surface (like weathering processes), and continental distribution (Raymo et al., 1992).

Scientists have wondered what climatic mechanisms forced dramatic climate changes during the Cenozoic. One popular idea is that the movement of the continents over the poles which could potentially cause a cooling effect (Raymo et al., 1992). Another mechanism is the development of the circum

Antarctic current (Raymo et al., 1992). Before the development of the circum-Antarctic current, a meridional heat transport caused higher sea surface temperatures around Antarctica which prevented continental ice sheets to form (Raymo et al., 1992). This in turn could have helped develop the circum-Antarctic current which caused cooling of Antarctica (Raymo et al., 1992). Scientists have also questioned the relationship between the Isthmus of Panama formation and the Northern Hemisphere glaciations (Raymo et al., 1992). One of the most interesting ideas is the uplift of the Tibetan plateau (Raymo et al., 1992). During the middle Eocene, the Indo-Australian plate collided with Asian plate causes an uplift of 5 km (Raymo et al., 1992). It is believed that the Tibetan plateau not only caused regional monsoon circulation but could also affect hemispheric atmospheric circulation (Raymo et al., 1992). These changes in circulation resulted in drier climates in certain regions around Asia (Raymo et al., 1992). Another factor causing changes in climate during the Cenozoic are known as Milankovich cycles (Raymo et al., 1992). Milankovich cycles take into consideration the precession (change in orientation of the rotational axis of the Earth), obliquity (Earth's tilt), and eccentricity (Earth's eccentric orbit) which cause different degrees of heat from the sun (Raymo et al., 1992).

The following sections discuss the results of the Cenozic time periods used for this thesis. The area of land, area of predicted coal deposits, area of observed coal deposits, and area of hit localities will be presented in each period.

3.3 Miocene (~10 Ma)

The Miocene period was approximately 10 million years ago. Climate at the time was cooler than other Cenozoic periods but warmer and more humid than present day climate (Schneck et al., 2012). The Northern Hemisphere was almost free of ice, although glaciations did start before the Miocene (Schneck et al., 2012). Vast forests and fewer deserts covered the Miocene compared to today's Earth (Schneck et al., 2012). Areas such as the modern Sahara had seasonal forest or savannah vegetation (Schneck et al., 2012). The boreal forests of today in the northern latitudes were more abundant and covered present day areas of tundra and ice (Schneck et al., 2012).

Miocene climate could have been affected by many geological and atmospheric processes. Orogenic effects causing CO_2 decline, plate tectonics, and land-sea distribution are considered major mechanisms for Miocene climate (Ramstein et al., 1997 and Fluteau et al., 1999, and Ruddiman et al., 1997, and Kutzbach et al., 2004). High abundance of vegetation during the early Miocene could also increase the temperatures during the Miocene (Micheels et al., 2007). The following section will discuss the Miocene observed coal area, predicted coal area, and results of this study for the Miocene.

3.3.1 Miocene Coal Deposits

A paleogeographic map was provided by the PALEOMAP project (Scotese, 2001). The land area during the Miocene was approximately 221 x 10^6 km^2 (Table 3.1). Since coals are formed from plant material, it can be inferred that all coals must form on land. Therefore, the amount of land during the Miocene is important because the areas where there is not land must be taken out of consideration for prediction.

Predicted coal deposit areas for the Miocene were based on a minimum precipitation value of 250 mm/year (Figure 3.1: by the blue squares). A total of 163 x 10^6 km^2 fell within the 250 mm/year annual runoff range. The predicted coals are found in North America, northern South

America, Central America, Europe, southern Africa, northern and western Asia, Antarctica and the Pacific West coast islands (Figure 3.1).

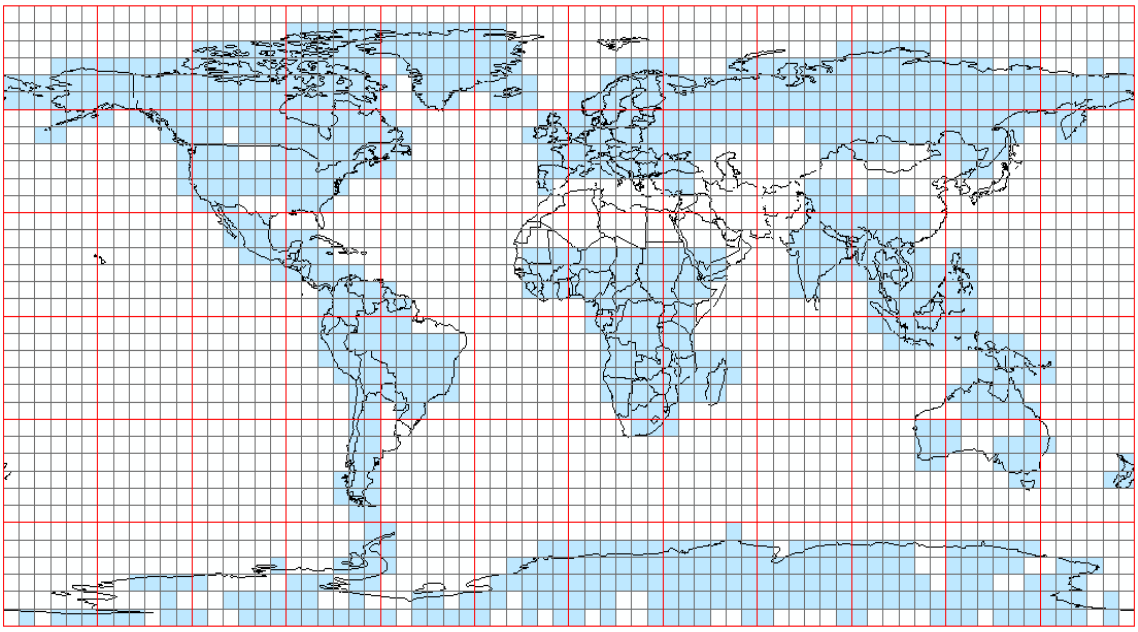

Figure 3.1 Predicted Coal Deposits Area Plotted on 10 Ma Paleogeographic Map

The distribution of observed coal localities was based on the compilation of Boucot et al. (Boucot et al., 2012). Observed coals from Boucot were found in north-western North America, Central America, northern South America, Europe, western Asia and the Pacific west coast islands. A total of 41 x 10^6 km^2 of observed coal deposit area is plotted in Figure 3.2.

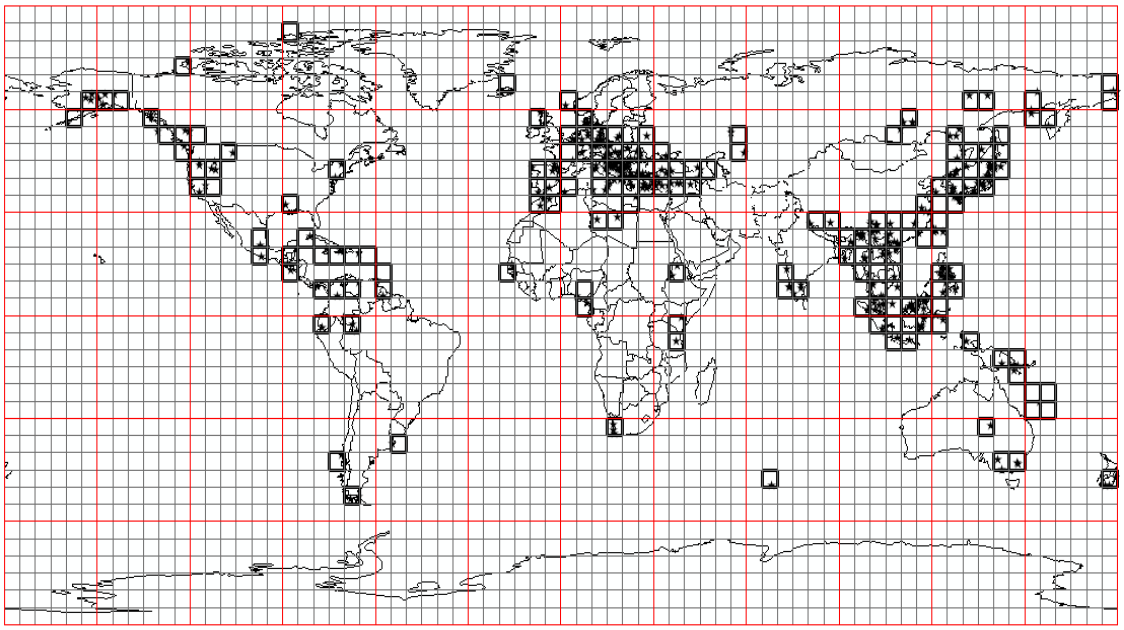

Figure 3.2 Observed Coal Deposits Area Plotted on 10 Ma Paleogeographic Map

Figure 3.3 shows Miocene “hits” (areas of intersection between observed and predicted coals). All $5^{o}x5^{o}$ grid cells highlighted pink represent areas of “hits.” During the Miocene 30 x 10^{6} km^{2} of “hits” were observed. “Hits” can been seen in north-western North America, Central America, Europe, northern Asia, southern Asia, and Pacific west coast islands. “Misses” are any observed coal $5^{o}x5^{o}$ grid cell that did not intersect with predicted coal $5^{o}x5^{o}$ grid cell. “Misses” can be seen in the Caribbean, southern Europe and west-central Asia.

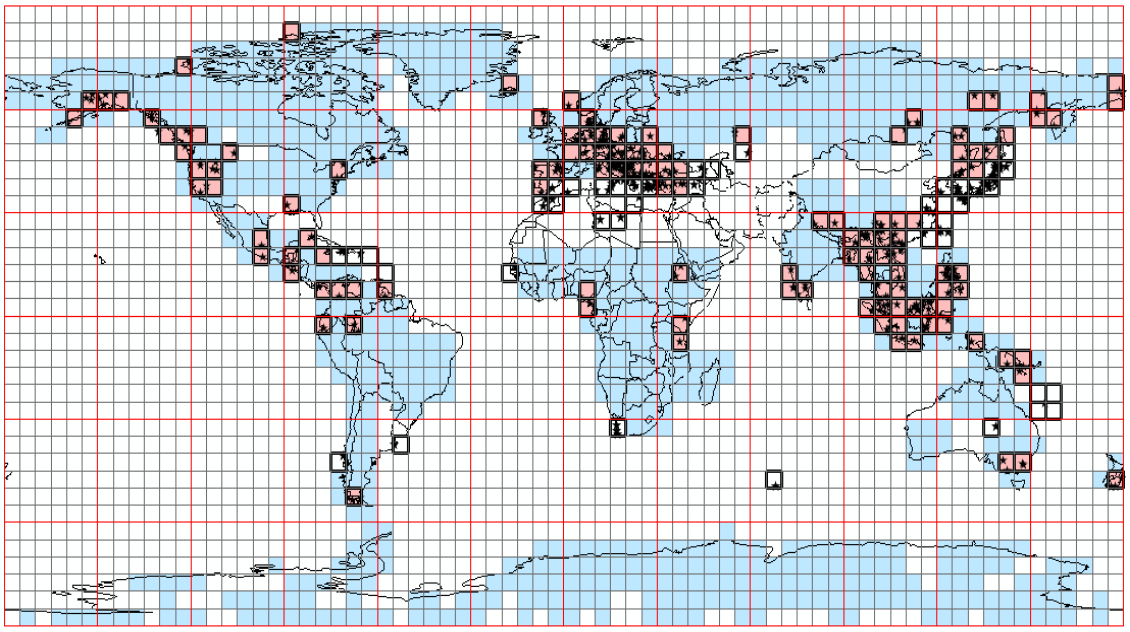

Figure 3.3 Hits Area Plotted on 10 Ma Paleogeographic Map

3.3.1.1 Statistical Analyzes for the Miocene

For the Miocene, there were 221 x 10^6 km^2 of land observed. Of these 221 x 10^6 km^2 land cells, 163 x 10^6 km^2 contained a predicted coal 5^ox5^o cell. This means that 73% of total land area intersects with a predicted coal area. 41 x 10^6 km^2 contained observed coal area. Finally, 30 x 10^6 km^2 containing both observed and predicted coals ("hits") were observed. The results for the entire Miocene can be seen in Table 3.1. Using the statistical analysis outlined in Chapter 2, the expected number of hits was 30 x 10^6 km^2 and the observed number of hits was 30 x 10^6 km^2. This makes the probability of hits due to random process 0.07 which suggests that the observed hits are likely to be insignificant and the null hypothesis stands. Figure 3.4 shows the Poisson distribution for 10 Ma. The red line represents the actual number of hits observed and the dashed black line represents predicted "hits" during the Miocene. The red box represents area of randomness while the green boxes represent areas of significance. Any point that falls within the green is significant to a degree. During the Miocene, the number of predicted hits area equals the number of actual hits area. This means it is insignificant and random.

Table 3.1 10 Ma Total Results used during the Statistical Analysis

Total Land	Number of Predicted Coals	% Total Land Occupied by Predicted coals	Number of observed coals	Predicted number of hits	hits	Misses	Probability that Hits are Random
221	163	73	41	30	30	11	0.07

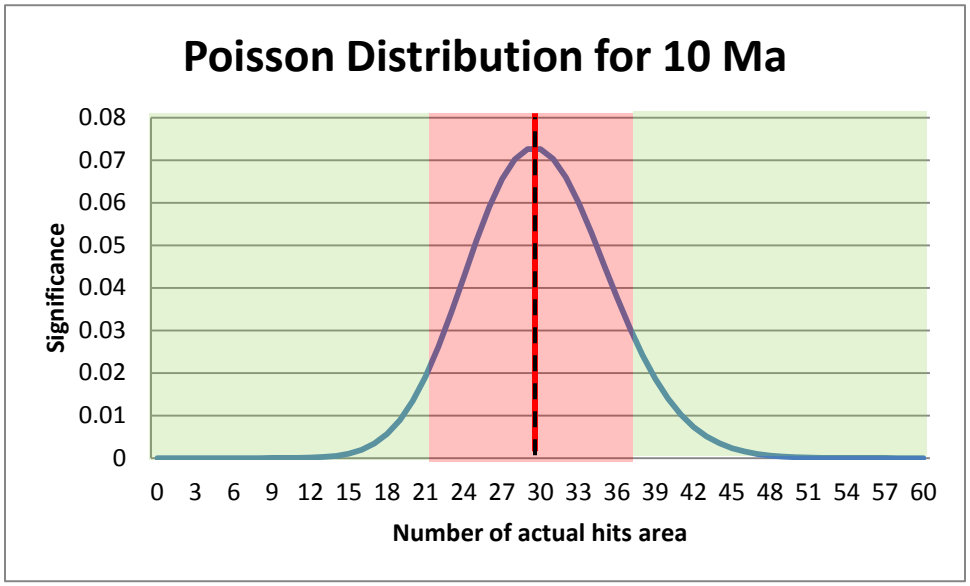

Figure 3.4 Poisson Distribution for 10 Ma

3.4 Oligocene (~30 Ma)

The Oligocene period was approximately 30 million years ago. A large scale global cooling event occurred at the beginning of the Oligocene. During this time period, major tectonic activity began when the Indo-Australian plate began to drift north. This increased spreading rate; increasing CO_2 levels (Katz et al., 2008). The increase in CO_2 levels increased temperatures, rain, and vegetation, which in turn increased chemical weathering, contributing to the decrease in CO_2 removal and caused global cooling (Ruddiman, 2008). At the same time, when Australia began to move northward, the Southern Ocean Seaway opened creating the Antarctic Circumpolar Current (Zanazzi et al., 2007). This current circled Antarctica and created a barricade preventing warm currents to reach Antarctica creating ice caps at the South Pole

(Zanazzi et al., 2007). The following section will discuss the Oligocene observed coal area, predicted coal area, and results of this study for the Oligocene.

3.4.1 Oligocene Coal Deposits

A paleogeographic map was provided by the PALEOMAP project (Scotese, 2001). The land area during the Oligocene was approximately 225 x 10^6 km^2 (Table 3.2). Predicted coals for the Oligocene were based on a minimum precipitation value of 250 mm/year. All 5^ox5^o grid cells containing a 250 mm/year or greater were plotted (Figure 3.5: by the blue squares). A total of 164 x 10^6 km^2 fell within the 250 mm/year annual runoff range. The predicted coals are found in North America, northern South America, Central America, Europe, southern Africa, northern Asia, Australia, Antarctica and the Pacific West coast islands (Figure 3.5).

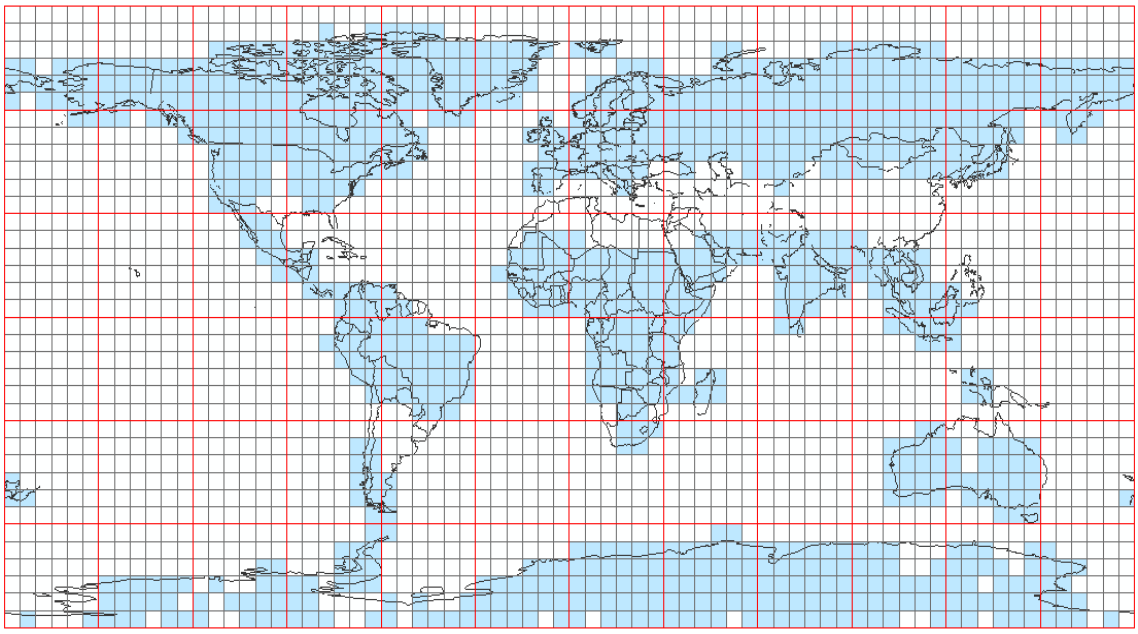

Figure 3.5 Predicted Coal Deposits Area Plotted on 30 Ma Paleogeographic Map

The distribution of observed coal localities was based on the compilation of Boucot et al. (Boucot et al., 2012). Observed coals from Boucot et al. were found in north western North America, northern South America, Europe, western Asia and the Pacific west coast islands. A total of 28 x 10^6 km^2 of observed coal area is plotted (Figure 3.6).

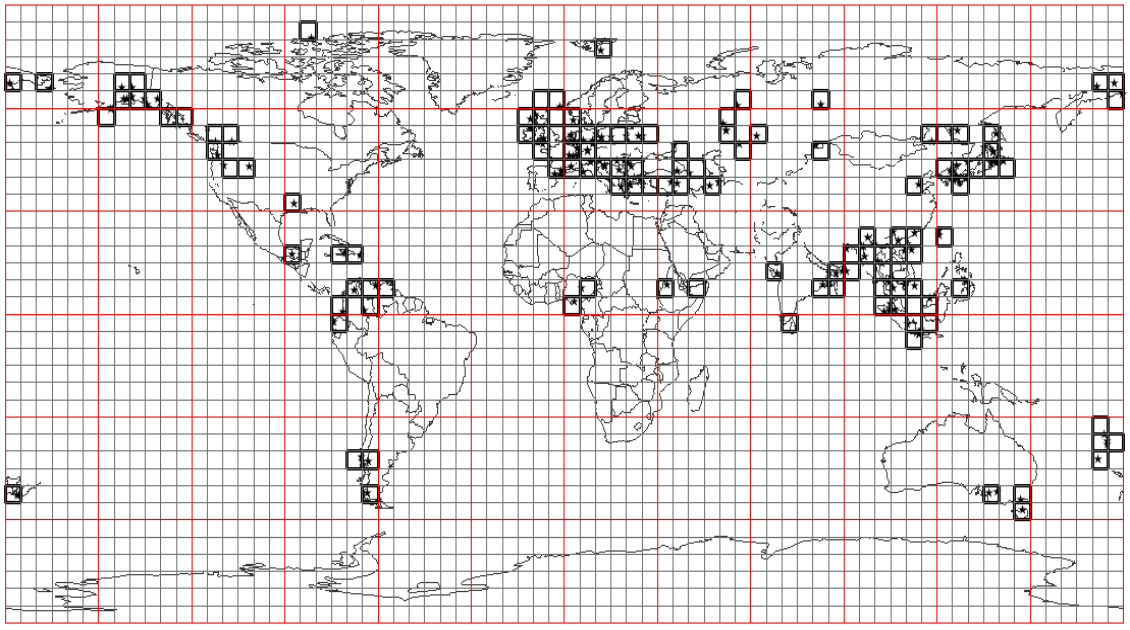

Figure 3.6 Observed Coal Deposits Area Plotted on 30 Ma Paleogeographic Map

Figure 3.7 shows Oligocene hits (areas of intersection between observed and predicted coals). All $5^{o}x5^{o}$ grid cells highlighted pink represent areas of "hits." During the Oligocene, 21 x 10^{6} km^{2} of "hits" were observed. "Hits" can been seen in north-western North America, northern South America, Europe, northern Asia, and Pacific west coast islands. "Misses" are any observed coal $5^{o}x5^{o}$ grid cells that did not intersect with predicted coal $5^{o}x5^{o}$ grid cells. "Misses" can be seen in the southern Europe and central Asia.

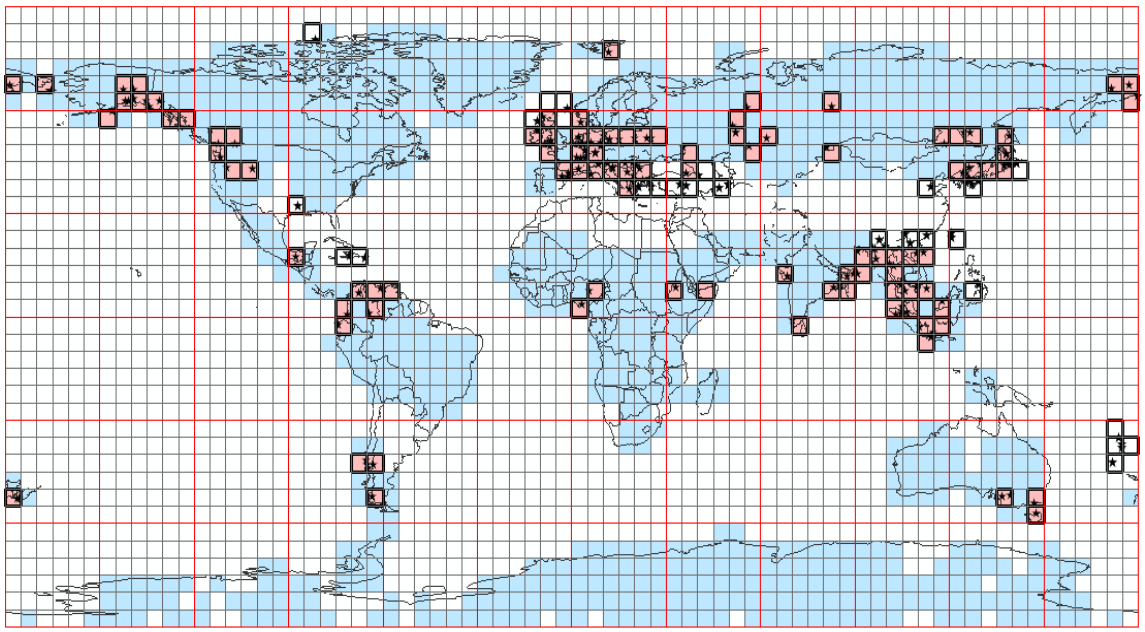

Figure 3.7 Hits Area Plotted on 30 Ma Paleogeographic Map

3.4.1.1 Statistical Analyzes for the Oligocene

For the Oligocene, there were 225 x 10^6 km^2 of land observed. Of these 225 x 10^6 km^2 of land area, 164 x 10^6 km^2 contained a predicted coal area. This means that 73% of total land area intersects with a predicted coal 5^ox5^o cell. 28 x 10^6 km^2 contained observed coals. Finally, 21 x 10^6 km^2 containing both observed and predicted coals ("hits") were observed. The results for the entire Oligocene can be seen in Table 3.2. Using the statistical analysis outlined in Chapter 2, the expected number of hits was 20 x 10^6 km^2 and the observed number of hits was 21 x 10^6 km^2. This makes the probability of hits due to random process 0.08 which suggests that the observed hits are likely to be insignificant and the null hypothesis stands. Figure 3.8 shows the Poisson distribution for 30 Ma. The red line represents the actual number of hits observed and the dashed black line represents the predicted number of hits during the Oligocene. The red box represents area of randomness while the green boxes represent areas of significance. Any point that falls within the green is significant to a degree. During the Oligocene, the number of predicted hits area is very close to the actual hits area. This means it is insignificant and random.

Table 3.2 30 Ma Total Results used during the Statistical Analysis

Total Land	Number of Predicted Coals	% Total Land Occupied by Predicted coals	Number of observed coals	Predicted number of hits	hits	Misses	Probability that Hits are Random
225	164	73	28	20	21	7	0.08

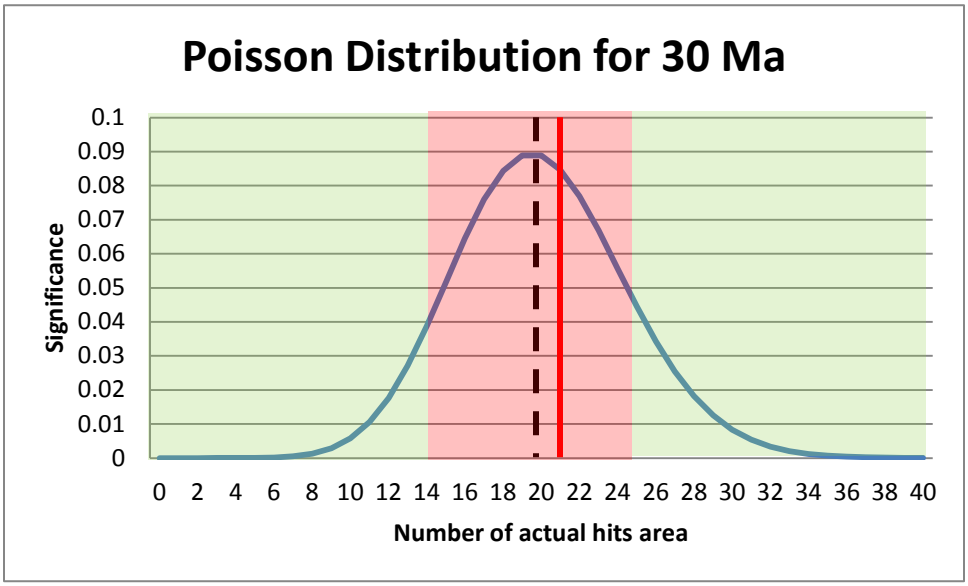

Figure 3.8 Poisson Distribution for 30 Ma

3.5 Middle Eocene (~45 Ma)

The middle Eocene was approximately 45 million years ago. The Eocene is known to have higher temperatures and higher amounts of precipitation comparable to other Cenozoic times (Scotese, 2001). The middle Eocene had an abundance of tropical rainforests and the temperature gradient between the poles and equator was low (Keating-Bitonti, 2011). Tectonic activity of the Indo-Australian plate began as India drifted north towards the Eurasian tectonic plate (Keating-Bitonti, 2011). This tectonic activity began the closing of the Tethys Ocean and started the creation of the Antarctic Circumpolar Current; when Australia began to pull away from Antarctica (Zanazzi et al., 2007). The following section will discuss the Middle Eocene observed coal area, predicted coal area, and results of this study for the Middle Eocene.

3.5.1 Middle Eocene Coal Deposits

A paleogeographic map was provided by the PALEOMAP project (Scotese, 2001). The land area during the Middle Eocene was approximately 215 x 10^6 km^2 (Table 3.3). Predicted coals for the Middle Eocene were based on a minimum precipitation value of 250 mm/year. All 5^ox5^o grid cells that contained a 250 mm/year or greater were plotted (Figure 3.9: by the blue squares). A total of 162 x 10^6 km^2 fell within the 250 mm/year annual runoff range. The predicted coals are found in North America, northern South America, Central America, Europe, Africa, northern Asia, Australia, Antarctica, India, and the Pacific west coast islands (Figure 3.9).

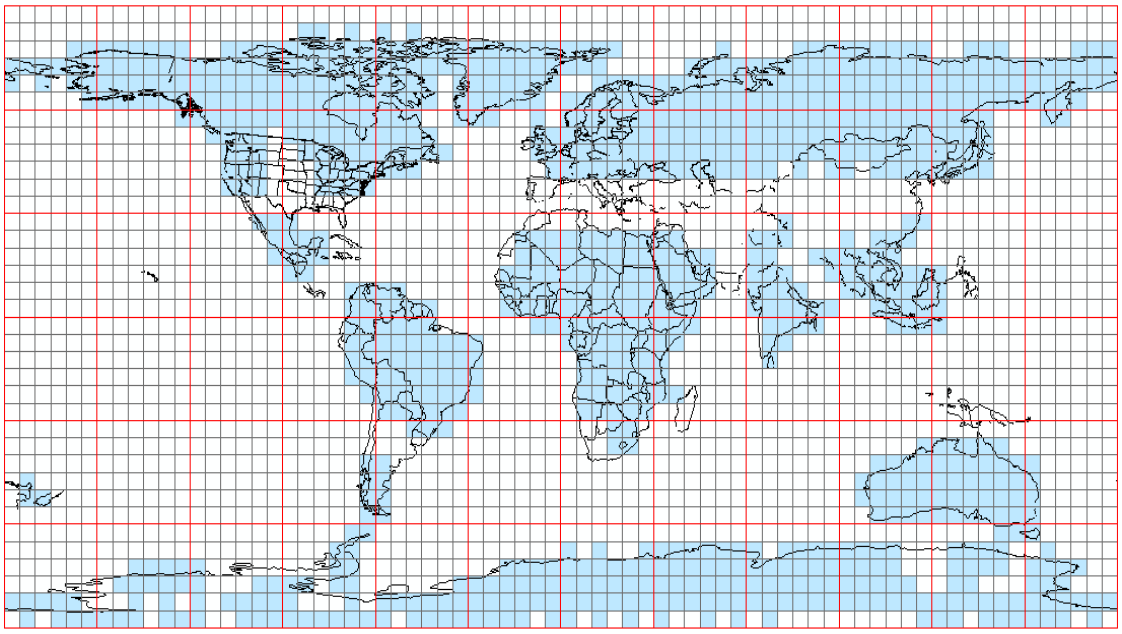

Figure 3.9 Predicted Coal Deposits Area Plotted on 45 Ma Paleogeographic Map

The distribution of observed coal localities was based on the compilation of Boucot et al. (Boucot et al., 2012). Observed coals from Boucot were found in north-western North America, Europe, north Asia, southern Australia, and the Pacific west coast islands. A total of 15 x 10^6 km^2 of observed coal area is plotted (Figure 3.10).

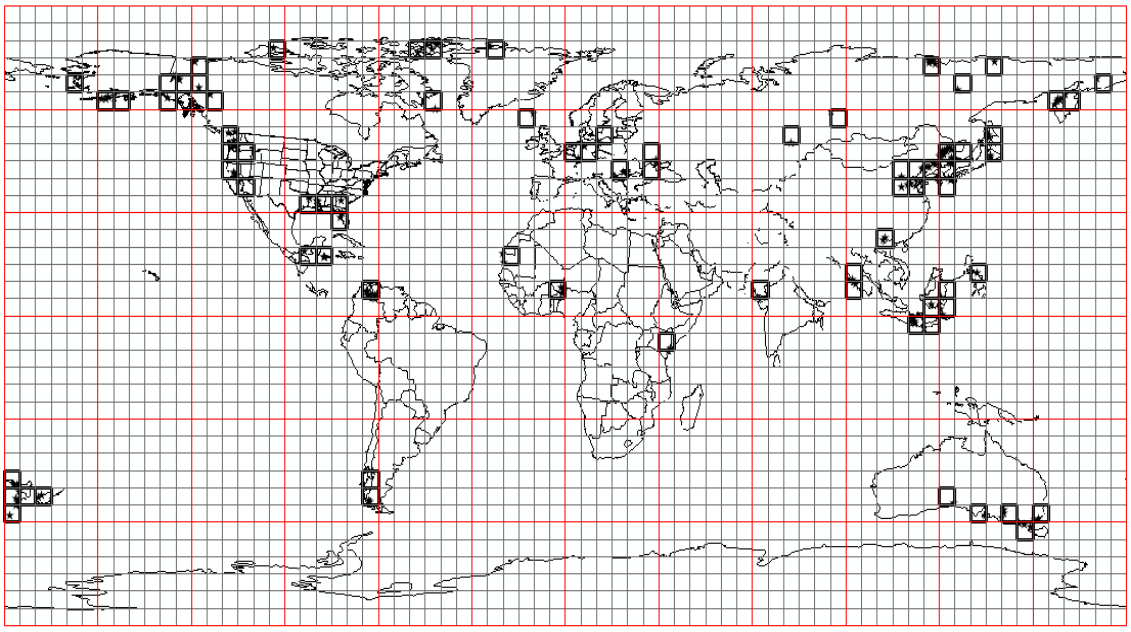

Figure 3.10 Observed Coal Deposits Area Plotted on 45 Ma Paleogeographic Map

Figure 3.11 shows Middle Eocene hits (areas of intersection between observed and predicted coals). All $5^{o}x5^{o}$ grid cells highlighted pink represent areas of "hits." During the Middle Eocene 13 x 10^{6} km^{2} of "hits" were observed. "Hits" can been seen in north-western North America, Europe, northern Asia, Australia, and Pacific west coast islands. "Misses" are any observed coal $5^{o}x5^{o}$ grid cells that did not intersect with predicted coal $5^{o}x5^{o}$ grid cells. "Misses" can be seen in the southern North America and central Asia.

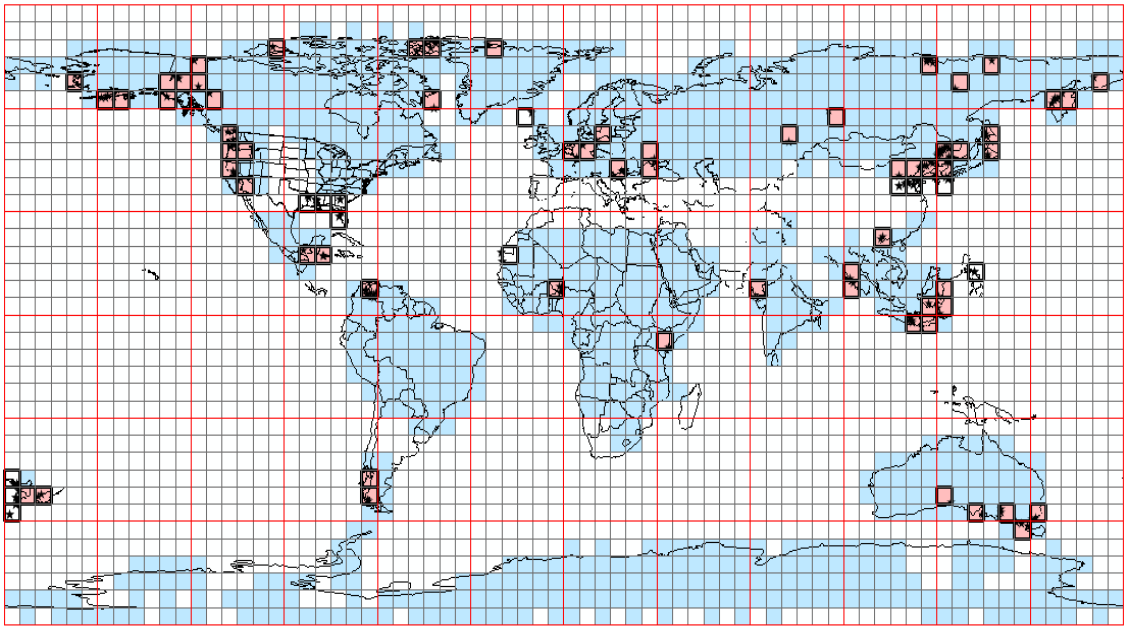

Figure 3.11 Hits Area Plotted on 45 Ma Paleogeographic Map

3.5.1.1 Statistical Analyzes for the Middle Eocene

For the Middle Eocene, there were 215 x 10^6 km^2 of land observed. Of these 215 x 10^6 km^2 of land area, 162 x 10^6 km^2 contained a predicted coal area. This means that 75% of total land area intersects with a predicted coal 5^ox5^o cell. 15 million km^2 contained observed coals. Finally, 13 x 10^6 km^2 containing both observed and predicted coals ("hits") were observed. The results for the entire Middle Eocene can be seen in Table 3.3. Using the statistical analysis outlined in Chapter 2, the expected number of hits was 11 x 10^6 km^2 and the observed number of hits was 13 x 10^6 km^2. This makes the probability of hits due to random process 0.09 which suggests that the observed hits are likely to be insignificant and the null hypothesis stands. Figure 3.12 shows the Poisson distribution for 45 Ma. The red line represents the actual number of hits observed and the dashed black line represents the predicted number of hits during the Middle Eocene. The red box represents area of randomness while the green boxes represent areas of significance. Any point that falls within the green is significant to a degree. During the Middle Eocene, the number of predicted hits area is very close to the actual hits area. This means it is insignificant and random.

Table 3.3 45 Ma Total Results used during the Statistical Analysis

Total Land	Number of Predicted Coals	% Total Land Occupied by Predicted coals	Number of observed coals	Predicted number of hits	hits	Misses	Probability that Hits are Random
215	162	75	15	11	13	2	0.09

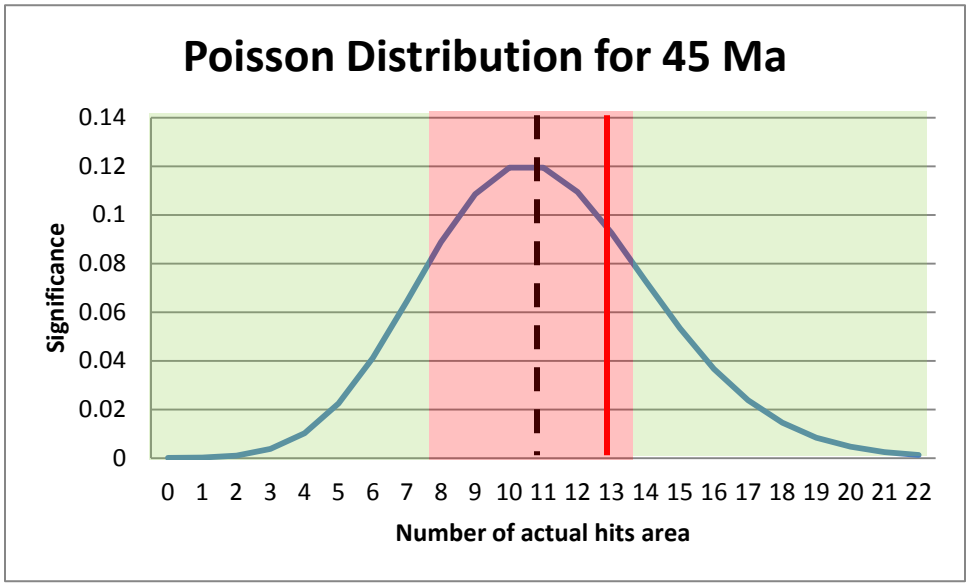

Figure 3.12 Poisson Distribution for 45 Ma

CHAPTER 4

MESOZOIC COALS

4.1 Introduction

The Mesozoic Era is broken up into three different time periods: Jurassic (70 Ma-160 Ma), Triassic (160 Ma-220 Ma), and Cretaceous (220 Ma-280 Ma). This chapter will discuss the results for the Cretaceous/Tertiary boundary (70 Ma), Late Cretaceous- Cenomanian/Turonian (90 Ma), Late Early Cretaceous- Aptian (120 Ma), Early Cretaceous- Berriasian (140 Ma), Late Jurassic (160 Ma), Early Jurassic (180 Ma), and Middle Triassic (220 Ma). The following sections will review the observed coal area, predicted coal area, and statistical procedures described in Chapter 2 for each of the time periods listed above.

4.2 The Mesozoic Era

The Mesozoic Era is thought by most scientists to be much warmer than present-day climates. The tropics extended into the mid-latitudes and temperate climates were experienced in the polar regions (Hallam, 1985). The Triassic and Jurassic faunal data suggests temperate conditions into the 60^{o} latitudes. During the Cretaceous, faunal data indicates temperate climates in present-day polar latitudes (Hallam, 1985).

There are many factors that could have influenced the climate during this Era: Solar input, orbital variations (eccentricity and tilt), atmospheric composition (such as greenhouse gas concentrations and dust), etc. (Ruddiman, 2008). However, a major factor during the Mesozoic was tectonic-induced changes of the climate by variations in the greenhouse gas concentrations (Ruddiman, 2008).

During the Mesozoic a global wide equable climate was present. One of the major factors for this was the tectonic activity during the Era (Hallam, 1985). Tectonically speaking, the Mesozoic was the Era when the super-continent Pangea reached it maximum and then

began to break apart (Hallam, 1985). The Mesozoic Era witnessed the closing of the Paleo-Tethys Ocean and the opening of the Tethys Ocean as well as the opening of the Pacific Ocean (Hallam, 1985). With major rifting of the continents and the opening of the new oceans, major seafloor spreading and volcanism occurred during the Mesozoic Era (Hallam, 1985). Increased volcanism pumped more CO_2 into the atmosphere causing a greenhouse effect to occur and increased the global temperature (Ocampo, 2006).

The shape and position of Pangea also played a large role in the global climate. Pangea spanned from pole to pole which made oceanic circulation impossible from equator to pole (Hallam, 1985). This made warm water transport to the poles and cooler water transport to the equator nearly impossible (Hallam, 1985). Thus, the global oceanic temperatures were rather equable. Since Pangea was large in width, this also brought problems for water transport in the atmosphere (Hallam, 1985). Mega-monsoons were in effect during most of the Mesozoic because as moisture filled winds from the Panthalassic Ocean reached the eastern coast of Pangea, the continent would act as a barrier, causing atmospheric winds to drop all precipitation on the eastern coast (Chandler, 1992). At the same time, these winds would continue across the continent without moisture, causing the interior of Pangea to be arid and hot (Chandler, 1992).

Another major factor determining the Mesozoic climate was the oceanic anoxic events that occur. This process is when high levels on CO_2 in the atmosphere cause a hot house climate (Schlanger, 1976). This increase in CO_2 causes an increase in marine organic productivity (Schlanger, 1976). The increase in marine organic productivity caused an expansion and intensified the oxygen minimum zone, which in turn added to the organic carbon, which was then buried in the ocean and causes a depletion of oxygen intensifying the hot house climate (Schlanger, 1976).

The following sections discuss the results of the Mesozoic time periods used for this study. The amount of land cell area, number of predicted coal area, observed coal area, and hit localities area will be presented in each period.

4.3 Cretaceous/Tertiary Boundary (~70 Ma)

The Cretaceous/Tertiary boundary, also known as the K-T boundary, was approximately 70 million years ago. This time marked the end of the Mesozoic and is one of the five mass extinctions. During this time, extinction of the non-avian dinosaurs occurred as well as many terrestrial plants (Ocampo, 2006). With the extinction of the dinosaurs, biological niches opened and mammalian creatures who survived the mass extinction began to evolve and thrive (Ocampo, 2006). Many hypotheses have surfaced to explain the causes of the mass extinction. The first possible cause is an asteroid impact around Yucatan, Mexico (Ocampo, 2006). The asteroid is approximately 110 miles wide. With the size of the asteroid, major destruction occurred (Ocampo, 2006). Many events such as mega tsunamis, large dust clouds, and influx of CO_2 into the atmosphere could all cause mass extinctions on the Earth. Another possible cause of the mass extinction is the Deccan traps (Ocampo, 2006). The Deccan traps are flood basalts that began to flow around 68 Ma (Ocampo, 2006). These basalt flows could have caused an increase in CO_2 emissions that increased aerosols in the atmosphere and thus increasing the greenhouse effect (Ocampo, 2006).

The K-T boundary climate was affected by many geological and atmospheric processes. There was a major drop in sea-level and a large increase in greenhouse gases which would cause the Earth to be dry and hot. The following section will discuss the K-T boundary observed coal area, predicted coal area, and results of this study for the K-T boundary.

4.3.1 K-T Boundary Coal Deposits

A paleogeographic map was provided the PALEOMAP project (Scotese, 2001). The land area during the K-T boundary was approximately 214 x 10^6 km^2 (Table 4.1). Predicted

coals for the K-T boundary were based on a minimum precipitation value of 250 mm/year. All $5^{o}x5^{o}$ grid cells that contained a 250 mm/year or greater were plotted (Figure 4.1: by the blue squares). A total of 152 x 10^{6} km^{2} fell within the 250 mm/year annual runoff range. The predicted coals are found in North America, northern South America, Central America, Europe, northern Africa, northern and western Asia, Antarctica, Australia, and the Pacific west coast islands (Figure 4.1).

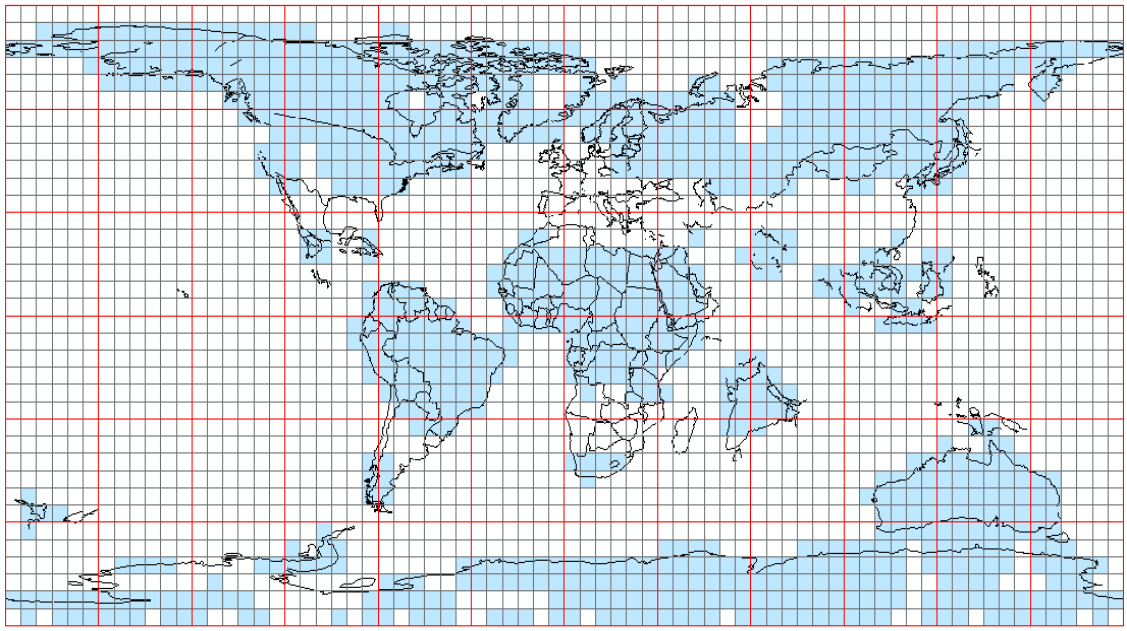

Figure 4.1 Predicted Coal Deposits Area Plotted on 70 Ma Paleogeographic Map

The distribution of observed coal localities was based on the compilation of Boucot et al. (Boucot et al., 2012). Observed coal area from Boucot was found in North America, Central America, Europe, north-western Asia, central Africa, and Australia. A total of 24 x 10^{6} km^{2} of observed coal area is plotted (Figure 4.2).

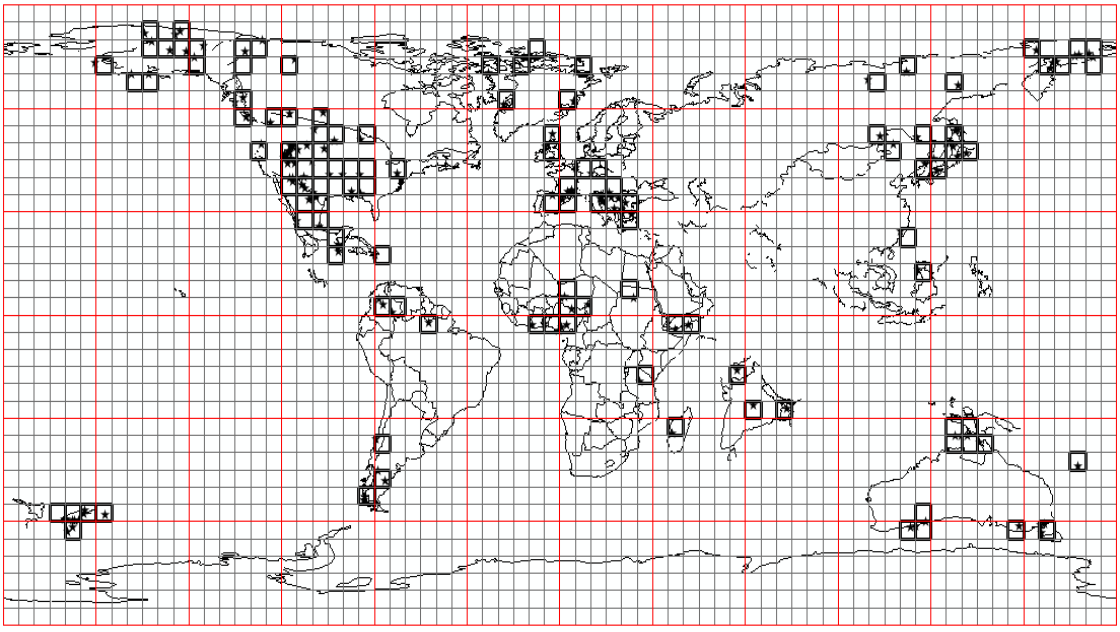

Figure 4.2 Observed Coal Deposits Area Plotted on 70 Ma Paleogeographic Map

Figure 4.3 shows K-T boundary hits (areas of intersection between observed and predicted coals). All $5^{o}x5^{o}$ grid cells highlighted pink represent areas of "hits." During the K-T boundary 15 x 10^{6} km^{2} of "hits" were observed. "Hits" can be seen in North America, central Africa, northern and western Asia, and Australia. "Misses" are any observed coal $5^{o}x5^{o}$ grid cells that did not intersect with predicted coal $5^{o}x5^{o}$ grid cells. "Misses" can be seen in the Europe, central North America and Australia.

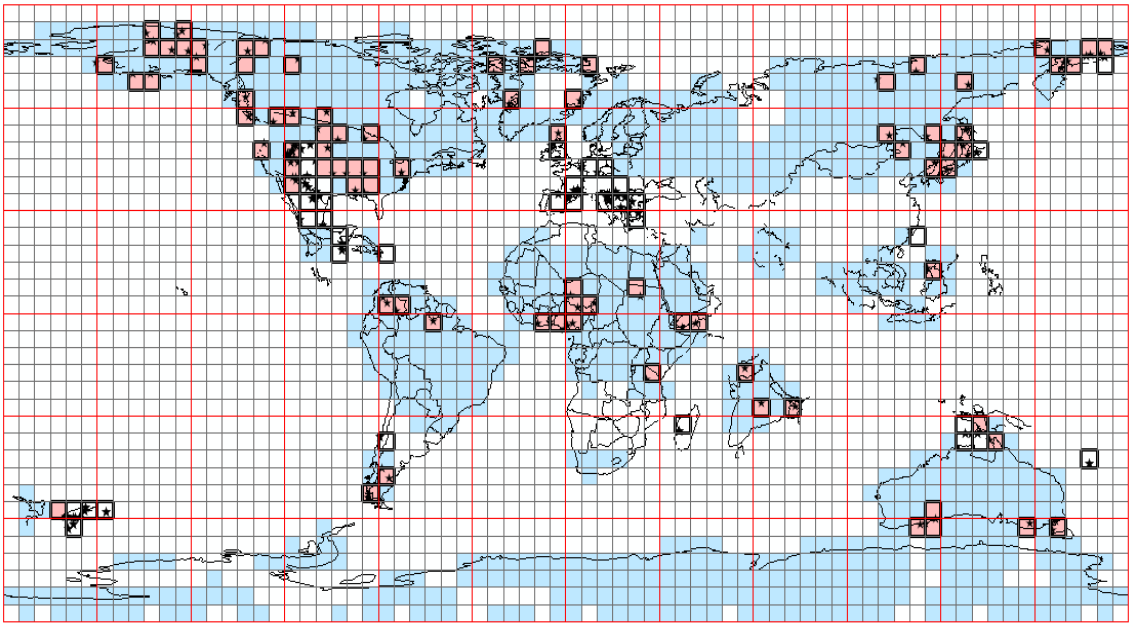

Figure 4.3 Hits Area Plotted on 70 Ma Paleogeographic Map

4.3.1.1 Statistical Analyzes for the K-T Boundary

For the K-T boundary, there were 214 x 10^6 km^2 of land observed. Of these 214 x 10^6 km^2 of land area, 152 x 10^6 km^2 contained a predicted coal area. This means that 71% of total land area intersects with a predicted coal 5^ox5^o cell. 24 x 10^6 km^2 contained observed coals. Finally, 15 x 10^6 km^2 containing both observed and predicted coals ("hits") were observed. The results for the entire K-T boundary can be seen in Table 4.1. Using the statistical analysis outlined in Chapter 2, the expected number of hits was 17 x 10^6 km^2 and the observed number of hits was 15 x 10^6 km^2. This makes the probability of hits due to random process 0.09 which suggests that the observed hits are likely to be insignificant and the null hypothesis stands. Figure 4.4 shows the Poisson distribution for 70 Ma. The red line represents the actual number of hits observed and the dashed black line represents the predicted number of hits during the K-T boundary. The red box represents area of randomness while the green boxes represent areas of significance. Any point that falls within the green is significant to a degree. During the K-T boundary, the number of predicted hits area is very close to the actual hits area. This means it is insignificant and random.

Table 4.1 70 Ma Total Results used during the Statistical Analysis

Total Land	Number of Predicted Coals	% Total Land Occupied by Predicted coals	Number of observed coals	Predicted number of hits	hits	Misses	Probability that Hits are Random
214	152	71	24	17	15	2	0.09

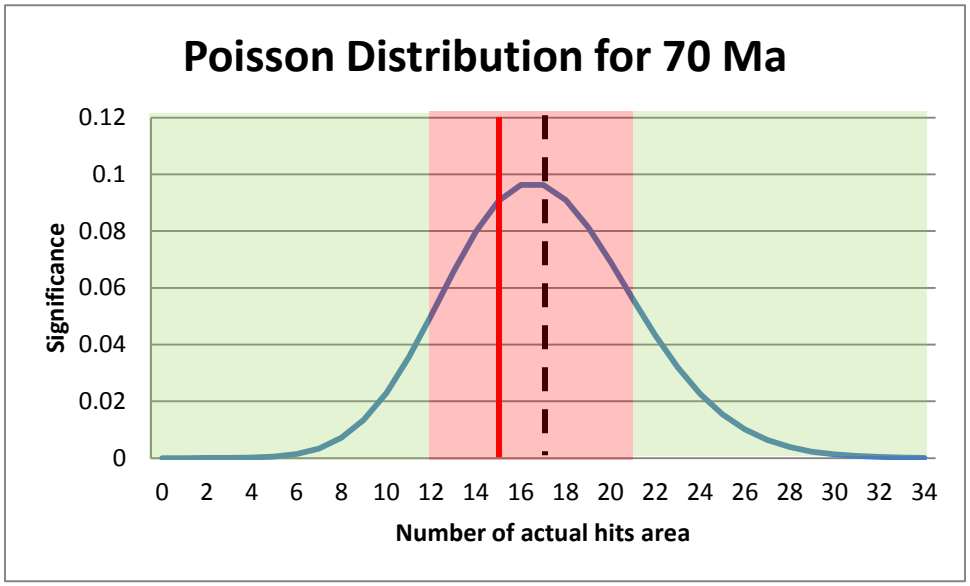

Figure 4.4 Poisson Distribution for 70 Ma

4.4 Late Cretaceous- Cenomanian/Turonian (~90 Ma)

The Late Cretaceous was approximately 90 million years ago. During the Late Cretaceous, Pangea was almost completely broken up. Eastern Gondwana split into India/Australia and Antarctica and Laurasia divides into North America and Eurasia. At this time, the Pacific Ocean continued to open. It is defined as a warm house climate with little to no evidence of sea ice at the polar regions (Schlanger, 1976). There were high sea levels which gave rise to epicontiental and shallow shelf seas (Schlanger, 1976). There are three main proposed ideas for warming during the Late Cretaceous. First, high sea levels gave rise to interior seaways and caused an increase in ocean heat transport to the poles (Schlanger, 1976). At the same time, the Tethys Ocean began to close which caused an oceanic anoxic

event to occur near present-day Asia (Otto-Bliesner, 1997, 2003, 2004 and Polsen et al., 2007). This gave rise to the second factor, green house gases which cause tropical heating (Otto-Bliesner, 1997, 2003 and Polsen et al., 2007). A third factor, is high-latitude forest vegetation which creates many climatic changes in albedo, wind circulation, atmospheric CO_2 concentration, etc. (Otto-Bliesner, 1997). The following section will discuss the Late Cretaceous period observed coal area, predicted coal area, and results of this study for the Late Cretaceous.

4.4.1 Late Cretaceous Coal Deposits

A paleogeographic map was provided by the PALEOMAP project (Scotese, 2001). The land area during the Late Cretaceous was approximately 213 x 10^6 km^2 (Table 4.2). Predicted coals for the Late Cretaceous were based on a minimum precipitation value of 250 mm/year. All 5^ox5^o grid cells that contained a 250 mm/year or greater were plotted (Figure 4.5: by the blue squares). A total of 150 x 10^6 km^2 fell within the 250 mm/year annual runoff range. The predicted coals are found in North America, northern South America, Central America, Europe, northern Africa, northern Asia, Antarctica, Australia, and the Pacific west coast islands (Figure 4.5).

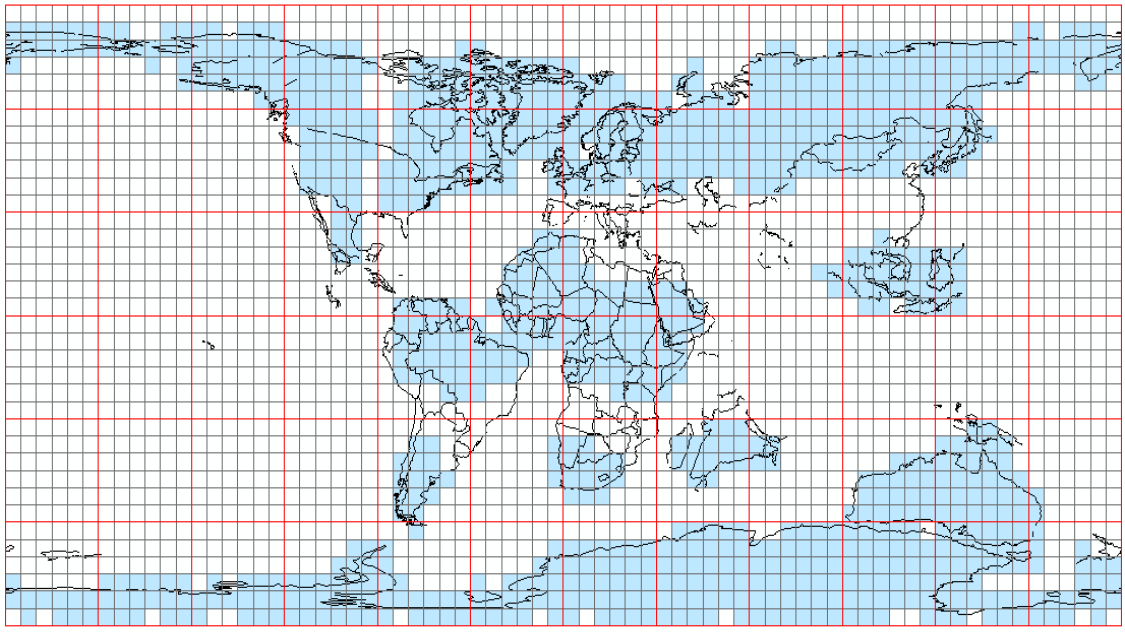

Figure 4.5 Predicted Coal Deposits Area Plotted on 90 Ma Paleogeographic Map

The distribution of observed coal localities was based on the compilation of Boucot et al. (Boucot et al., 2012). Observed coals from Boucot were found in North America, Central America, Europe, northern Asia, central Africa, and Australia/Antarctica. A total of 26 x 10^6 km^2 of observed coal area is plotted (Figure 4.6).

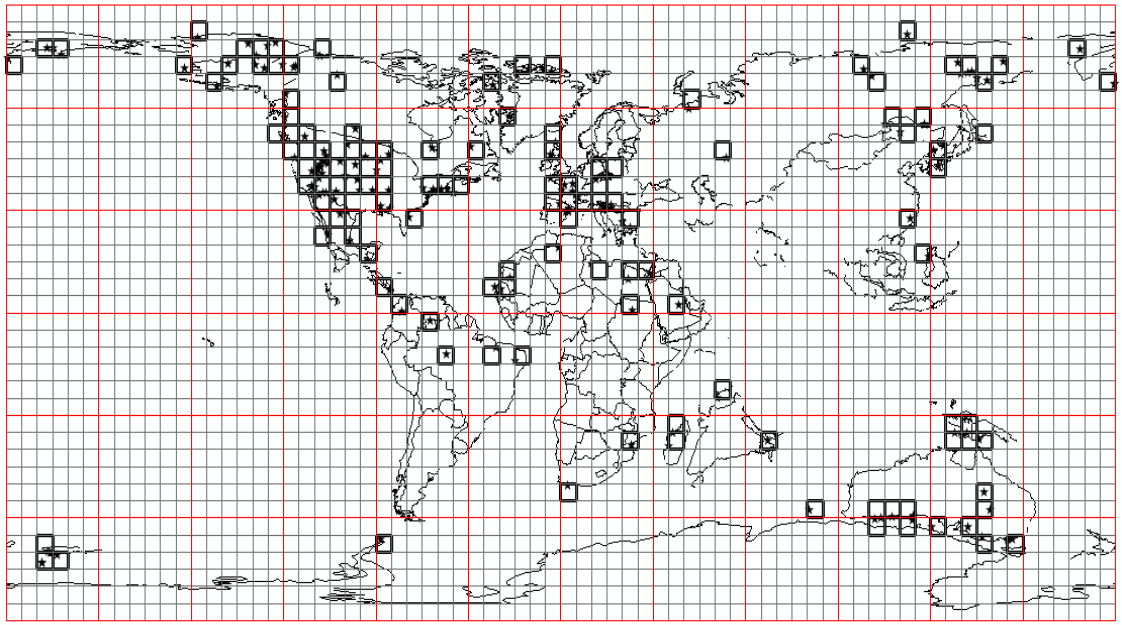

Figure 4.6 Observed Coal Deposits Area Plotted on 90 Ma Paleogeographic Map

Figure 4.7 shows Late Cretaceous hits (areas of intersection between observed and predicted coals). All $5^{o}x5^{o}$ grid cells highlighted pink represent areas of "hits." During the Late Cretaceous 18 x 10^{6} km^{2} of "hits" were observed. "Hits" can be seen in North America, central Africa, northern Asia and, Australia/Antarctica. "Misses" are any observed coal $5^{o}x5^{o}$ grid cells that did not intersect with predicted coal $5^{o}x5^{o}$ grid cells. "Misses" can be seen in the southern Europe.

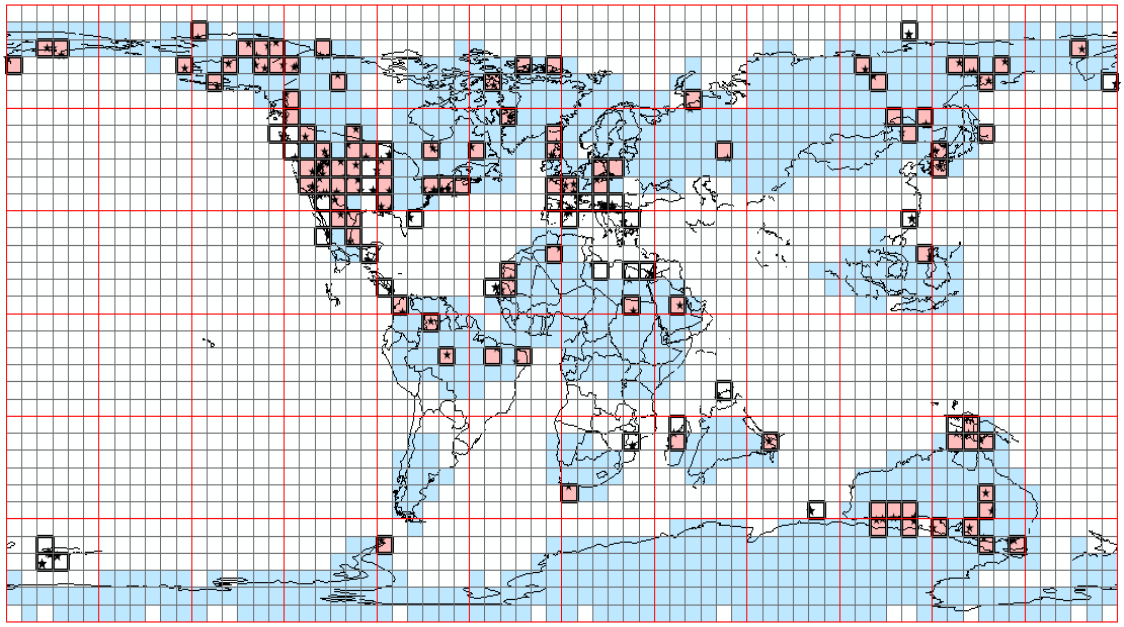

Figure 4.7 Hits Area Plotted on 90 Ma Paleogeographic Map

4.4.1.1 Statistical Analyzes for the Late Cretaceous

For the Late Cretaceous, there were 213 x 10^6 km^2 of land observed. Of these 213 x 10^6 km^2 of land area, 150 x 10^6 km^2 contained a predicted coal area. This means that 70% of total land area intersects with a predicted coal 5^ox5^o cell. 26 x 10^6 km^2 contained observed coals. Finally, 18 x 10^6 km^2 containing both observed and predicted coals ("hits") were observed. The results for the entire Late Cretaceous can be seen in Table 4.2. Using the statistical analysis outlined in Chapter 2, the expected number of hits was 18 x 10^6 km^2 and the observed number of hits was 18 x 10^6 km^2. This makes the probability of hits due to random process 0.09 which suggests that the observed hits are likely to be insignificant and the null hypothesis stands. Figure 4.8 shows the Poisson distribution for 90 Ma. The red line represents the actual number of hits observed and the dashed black line represents predicted number of hits during the Late Cretaceous. The red box represents area of randomness while the green boxes represent areas of significance. Any point that falls within the green is significant to a degree. During the Late Cretaceous, the number of predicted hits area the exact same as the actual hits area. This means it is insignificant and random.

Table 4.2 90 Ma Total Results used during the Statistical Analysis

Total Land	Number of Predicted Coals	% Total Land Occupied by Predicted coals	Number of observed coals	Predicted number of hits	hits	Misses	Probability that Hits are Random
213	150	70	26	18	18	8	0.09

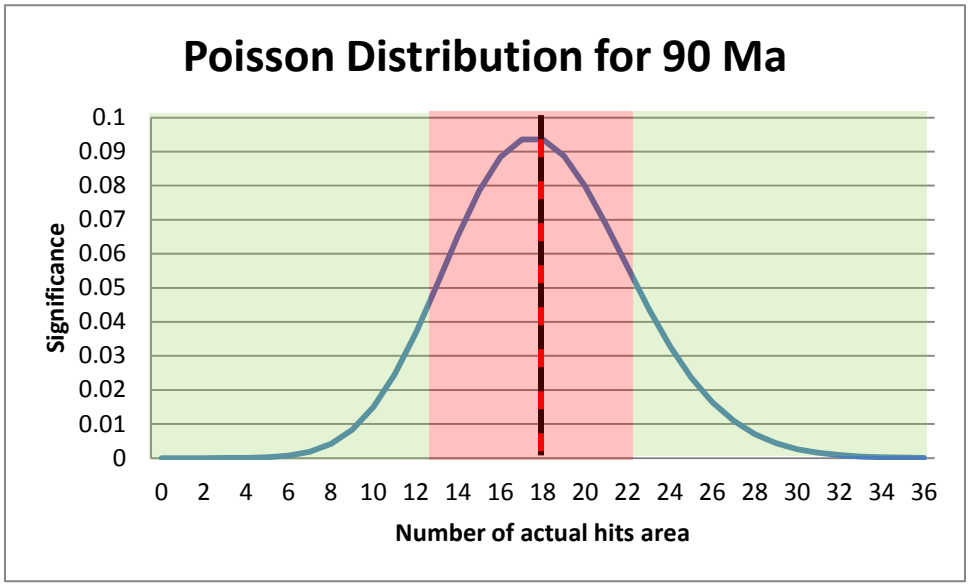

Figure 4.8 Poisson Distribution for 90 Ma

4.5 Late-Early Cretaceous- Aptian (~120 Ma)

The Aptian age of the Early Cretaceous was approximately 120 x 10^6 years ago. During this age, the breakup of Pangea was occurring. Western (South America and Africa) and Eastern Gondwana (India, Antarctica, and Australia) were separating and rapid sea-floor spreading and thus high emissions of greenhouse gases occurred (Otto-Bliesner, 1997, 2003 and Polsen et al., 2007). At this time, the Pacific Ocean continues to open between South America and Africa. It is defined as a warm house climate with little to no evidence of sea ice at the polar regions (Schlanger, 1976). The Earth's climate was mild and equable, and near the poles, temperate and subtropical flora was abundant. There were high sea levels which gave rise to epi-contiental and shallow shelf seas (Schlanger, 1976). An increase in volcanism and

sea-floor spreading is the proposed trigger for the climate warming during the Early Cretaceous (Keller, 2011). This in turn changed ocean circulation patterns and increased marine productivity. With an increase in marine productivity (especially within the lower to mid-latitudes within the Tethys Ocean), and Oceanic Anoxic Event occurred (Keller, 2011). Evidence for this are higher levels of black shale deposits during this time interval (Keller, 2011).The following section will discuss the Aptian age observed coal area, predicted coal area, and results of this study for the Late-Early Cretaceous.

4.5.1 Late-Early Cretaceous- Aptian Coal Deposits

A paleogeographic map was provided the PALEOMAP project (Scotese, 2001). The land area during the Late-Early Cretaceous was approximately 207 x 10^6 km^2 (Table 4.3). Predicted coals for the Late-Early Cretaceous were based on a minimum precipitation value of 250 mm/year. All 5^ox5^o grid cells that contained a 250 mm/year or greater were plotted (Figure 4.9: by the blue squares). A total of 145 x 10^6 km^2 fell within the 250 mm/year annual runoff range. The predicted coals are found in North America, northern South America, Central America, Europe, northern Africa, northern Asia, Antarctica, Australia, and the Pacific west coast islands (Figure 4.9).

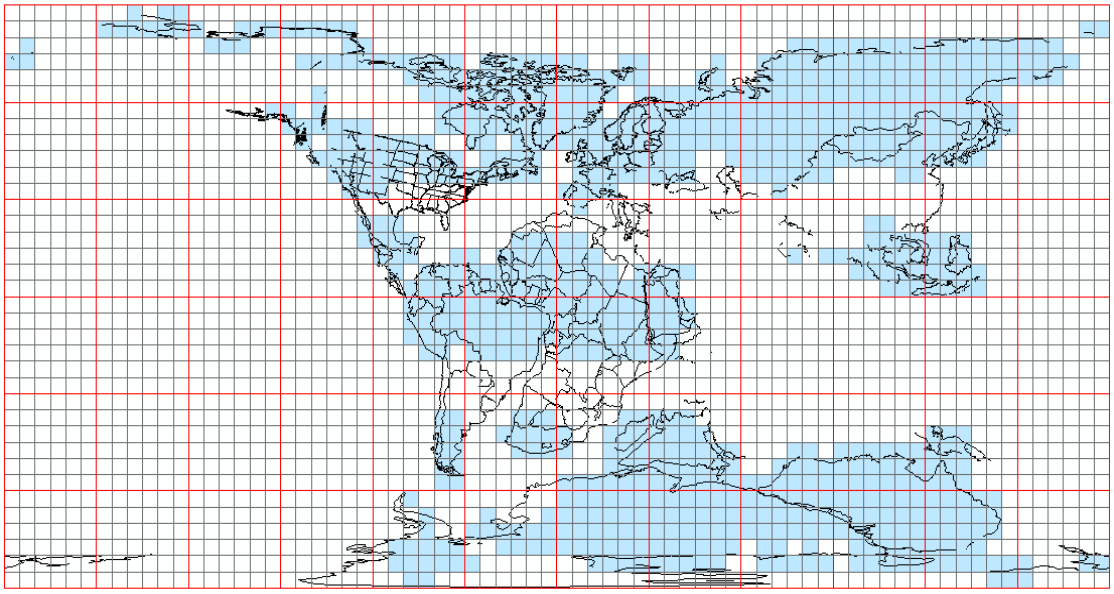

Figure 4.9 Predicted Coal Deposits Area Plotted on 120 Ma Paleogeographic Map

The distribution of observed coal localities was based on the compilation of Boucot et al. (Boucot et al., 2012). Observed coals from Boucot were found in North America, Europe, northern Asia, central Africa, and Australia/Antarctica. A total of 27 x 10^6 km^2 of observed coal area is plotted (Figure 4.10).

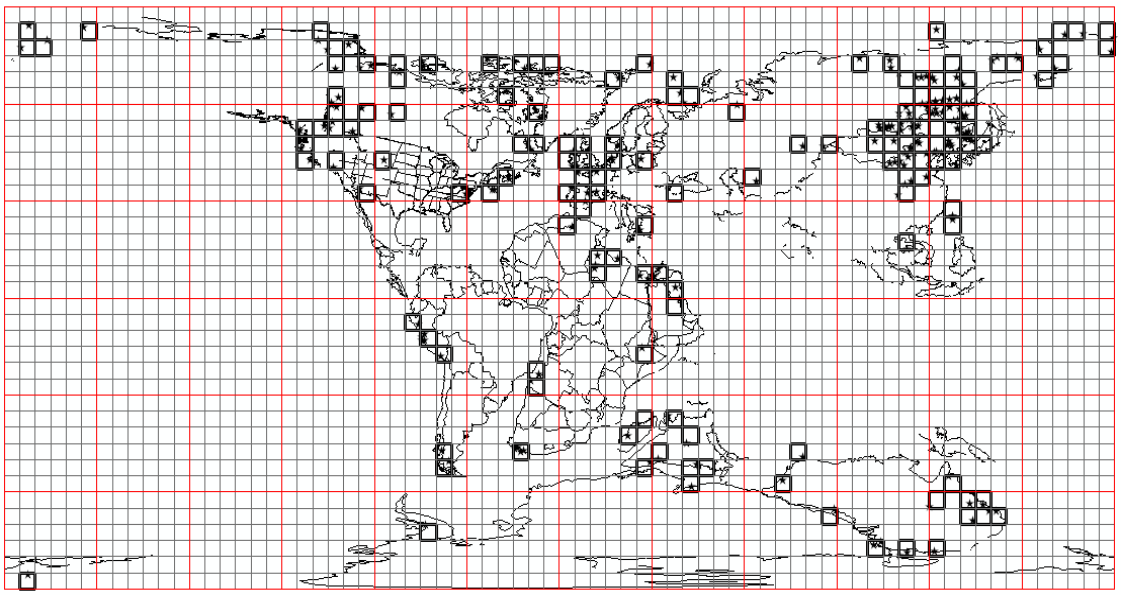

Figure 4.10 Observed Coal Deposits Area Plotted on 120 Ma Paleogeographic Map

Figure 4.11 shows Late-Early Cretaceous hits (areas of intersection between observed and predicted coals). All $5^{o}x5^{o}$ grid cells highlighted pink represent areas of "hits." During the Late-Early Cretaceous 23 x 10^{6} km^{2} of "hits" were observed. "Hits" can be seen in North America, Europe, central Africa, northern Asia and, Australia/Antarctica. "Misses" are any observed coal $5^{o}x5^{o}$ grid cells that did not intersect with predicted coal $5^{o}x5^{o}$ grid cells. "Misses" can be seen in the North America and central Africa.

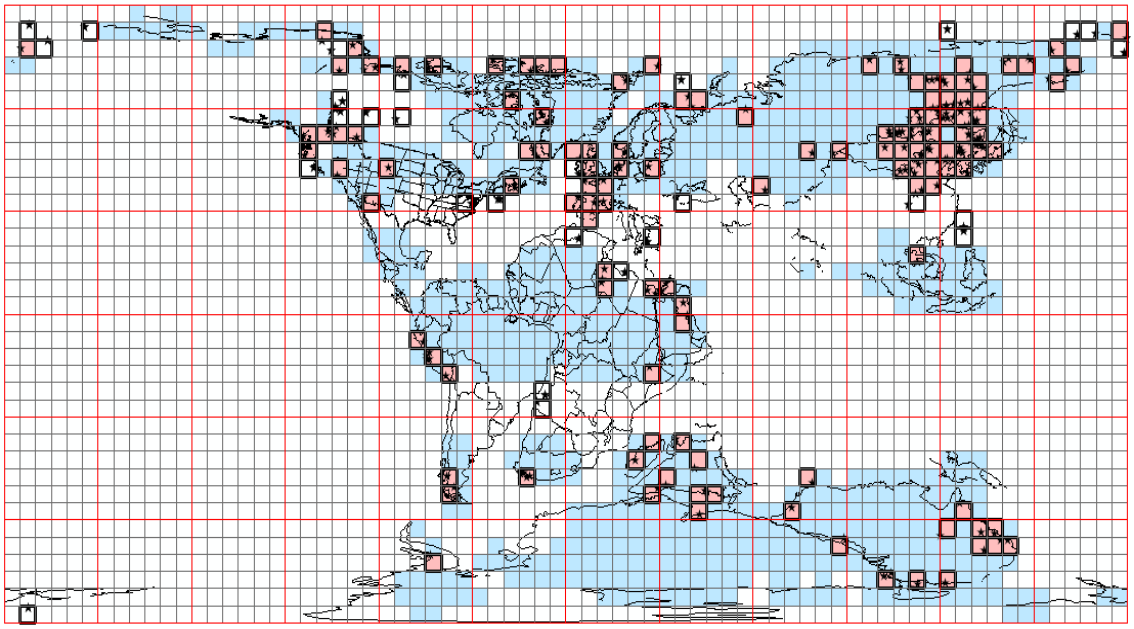

Figure 4.11 Hits Area Plotted on 120 Ma Paleogeographic Map

4.5.1.1 Statistical Analyzes for the Late-Early Cretaceous

For the Late-Early Cretaceous, there were 207 x 10^{6} km^{2} of land observed. Of these 207 x 10^{6} km^{2} of land area, 145 x 10^{6} km^{2} contained a predicted coal area. This means that 70% of total land area intersects with a predicted coal $5^{o}x5^{o}$ cell. 28 x 10^{6} km^{2} contained observed coals. Finally, 23 x 10^{6} km^{2} containing both observed and predicted coals ("hits") were observed. The results for the entire Late-Early Cretaceous can be seen in Table 4.3. Using the statistical analysis outlined in Chapter 2, the expected number of hits was 20 x 10^{6} km^{2} and the observed number of hits was 23 x 10^{6} km^{2}. This makes the probability of hits due to random process 0.07 which suggests that the observed hits are likely to be insignificant and the null

hypothesis stands. Figure 4.12 shows the Poisson distribution for 120 Ma. The red line represents the actual number of hits observed and the dashed black line represents the predicted number of hits during the Late-Early Cretaceous. The red box represents area of randomness while the green boxes represent areas of significance. Any point that falls within the green is significant to a degree. During the Late-Early Cretaceous, the number of predicted hits area is very close to the actual hits area. This means it is insignificant and random.

Table 4.3 120 Ma Total Results used during the Statistical Analysis

Total Land	Number of Predicted Coals	% Total Land Occupied by Predicted coals	Number of observed coals	Predicted number of hits	hits	Misses	Probability that Hits are Random
207	145	70	28	20	23	5	0.07

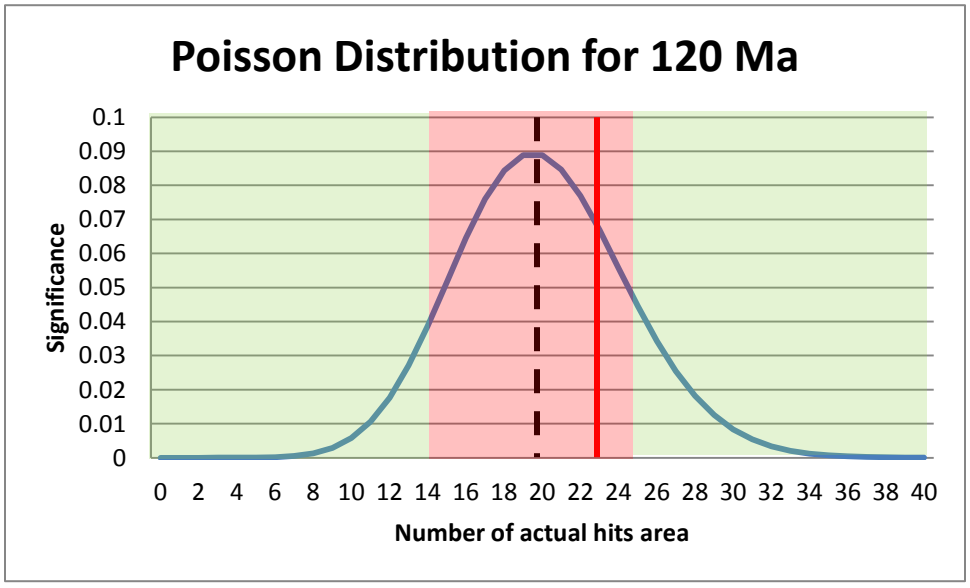

Figure 4.12 Poisson Distribution for 120 Ma

4.6 Early Cretaceous- Berriasian (~140 Ma)

The Berriasian age of the Early Cretaceous was approximately 140 million years ago. During this age, the breakup of Pangea was occurring. Western (South America and Africa) and Eastern Gondwana (India, Antarctica, and Australia) were separating and rapid sea-floor

spreading was occurring while the Pacific Ocean continued to open (Schlanger, 1976). It is defined as a warm house climate with little to no evidence of sea ice at the polar regions (Schlanger, 1976). The Berriasian was a time of arid climate globally (Föllmi, 2012). The aridity is believed to be caused by the super continent Pangea. With a super-continent centered on the equator, rainfall has a much harder time penetrating to the interior of the continent (Föllmi, 2012). This cause widespread aridness and cause the formation of such lithologies like evaporites (Föllmi, 2012). An increase in volcanism and sea-floor spreading is the proposed trigger for the climate warming during the Early Cretaceous (Keller, 2011). This then changed ocean circulation paths and increased marine productivity. With an increase in marine productivity (especially within the lower to mid-latitudes within the Tethys Ocean) an Oceanic Anoxic Event occurred (Keller, 2011). Evidence for this is an increase in marine black shales during this time interval (Keller, 2011). The following section will discuss the Berriasian age observed coal area, predicted coal area, and results of this study for the Early Cretaceous.

4.6.1 Early Cretaceous- Berriasian Coal Deposits

A paleogeographic map was provided by the PALEOMAP project (Scotese, 2001). The land area during the Early Cretaceous was approximately 213 x 10^6 km^2 (Table 4.4). Predicted coals for the Early Cretaceous were based on a minimum precipitation value of 250 mm/year. All 5^ox5^o grid cells that contained a 250 mm/year or greater were plotted (Figure 4.13: by the blue squares). A total of 146 x 10^6 km^2 fell within the 250 mm/year annual runoff range. The predicted coals are found in North America, northern South America, Central America, Europe, northern Africa, northern Asia, Antarctica, Australia, and the Pacific west coast islands (Figure 4.13).

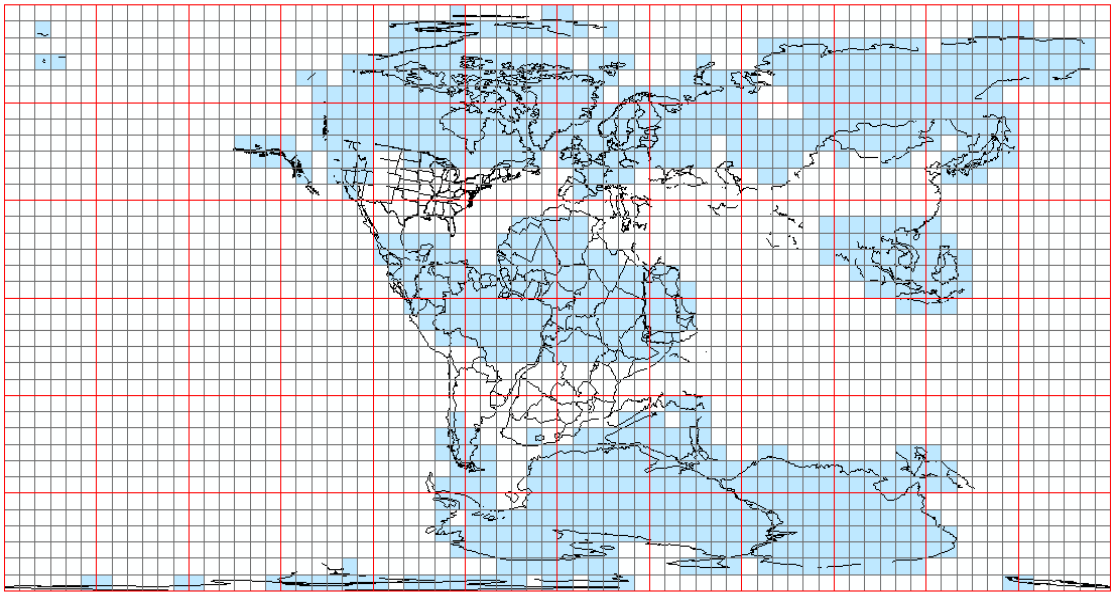

Figure 4.13 Predicted Coal Deposits Area Plotted on 140 Ma Paleogeographic Map

The distribution of observed coal localities was based on the compilation of Boucot et al (Boucot et al., 2012). Observed coals from Boucot were found in North America, Europe, northern Asia, central Africa, Australia/Antarctica, and western South America. A total of 28 x 10^6 km^2 of observed coal area is plotted (Figure 4.14).

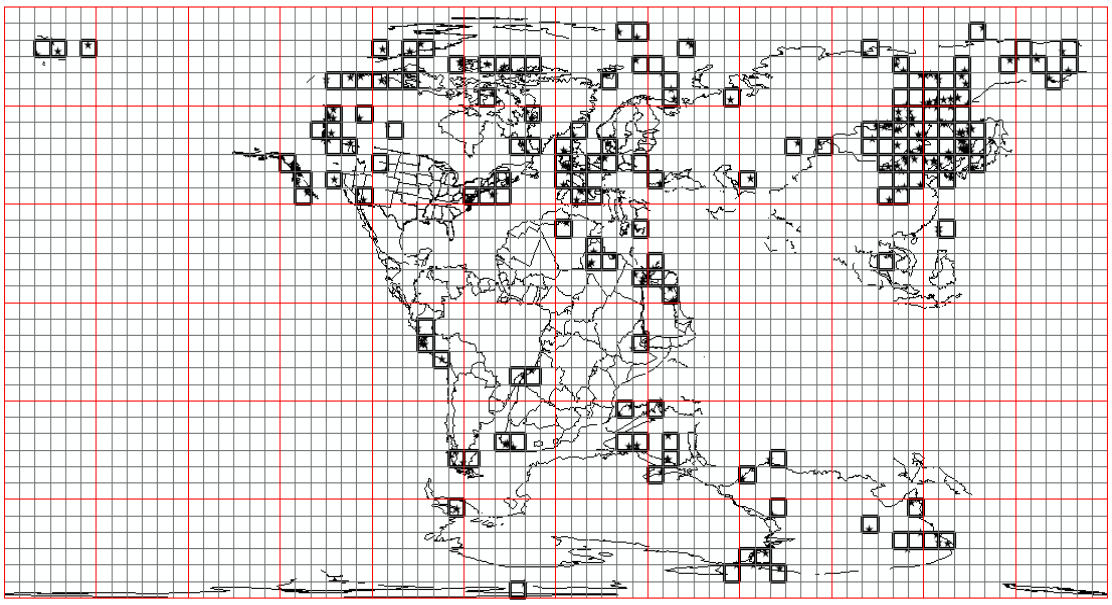

Figure 4.14 Observed Coal Deposits Area Plotted on 140 Ma Paleogeographic Map

Figure 4.15 shows Early Cretaceous hits (areas of intersection between observed and predicted coals). All $5^{o}x5^{o}$ grid cells highlighted pink represent areas of "hits." During the Early Cretaceous 19 x 10^{6} km^{2} of "hits" were observed. "Hits" can be seen in North America, Europe, central Africa, South America, Asia, and Australia/Antarctica. "Misses" are any observed coal $5^{o}x5^{o}$ grid cells that did not intersect with predicted coal $5^{o}x5^{o}$ grid cells. "Misses" can be seen in the North America, Asia, and southern Africa.

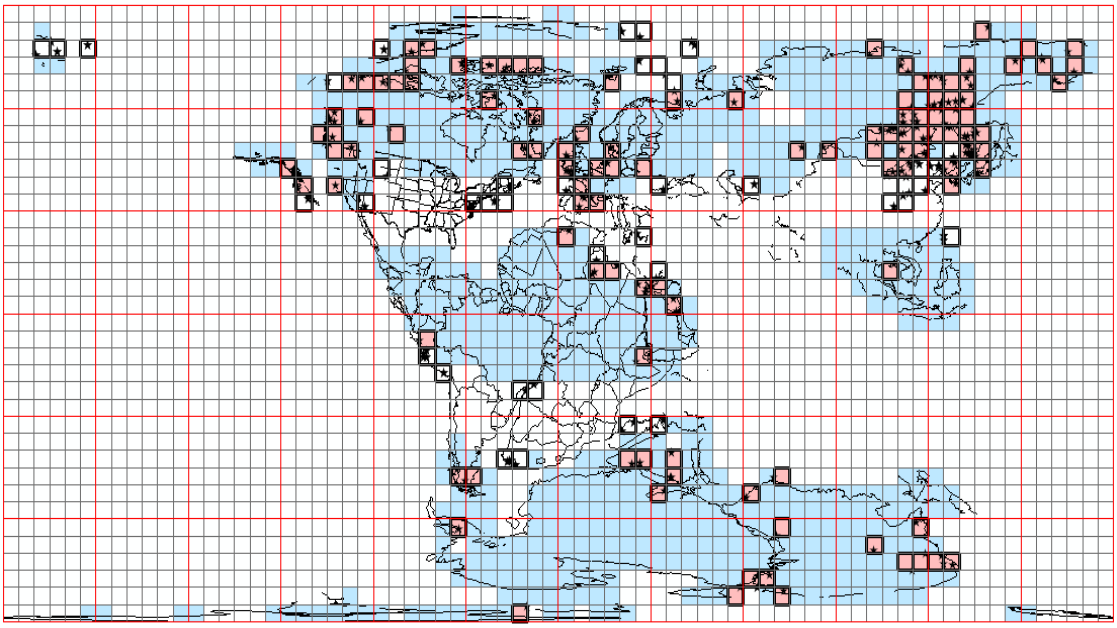

Figure 4.15 Hits Area Plotted on 140 Ma Paleogeographic Map

4.6.1.1 Statistical Analyzes for the Early Cretaceous

For the Early Cretaceous, there were 207 x 10^{6} km^{2} of land observed. Of these 207 x 10^{6} km^{2} of land area, 146 x 10^{6} km^{2} contained a predicted coal area. This means that 69% of total land area intersects with a predicted coal $5^{o}x5^{o}$ cell. 28 x 10^{6} km^{2} contained observed coals. Finally, 19 x 10^{6} km^{2} containing both observed and predicted coals ("hits") were observed. The results for the entire Early Cretaceous can be seen in Table 4.4. Using the statistical analysis outlined in Chapter 2, the expected number of hits was 19 x 10^{6} km^{2} and the observed number of hits was 19 x 10^{6} km^{2}. This makes the probability of hits due to random process 0.09 which suggests that the observed hits are likely to be insignificant and the null

hypothesis stands. Figure 4.16 shows the Poisson distribution for 140 Ma. The red line represents the actual number of hits observed and the dashed black line represents the predicted number of hits during the Early Cretaceous. The red box represents area of randomness while the green boxes represent areas of significance. Any point that falls within the green is significant to a degree. During the Early Cretaceous, the number of predicted hits area is the exact same as the actual hits area. This means it is insignificant and random.

Table 4.4 140 Ma Total Results used during the Statistical Analysis

Total Land	Number of Predicted Coals	% Total Land Occupied by Predicted coals	Number of observed coals	Predicted number of hits	hits	Misses	Probability that Hits are Random
213	146	69	28	19	19	9	0.09

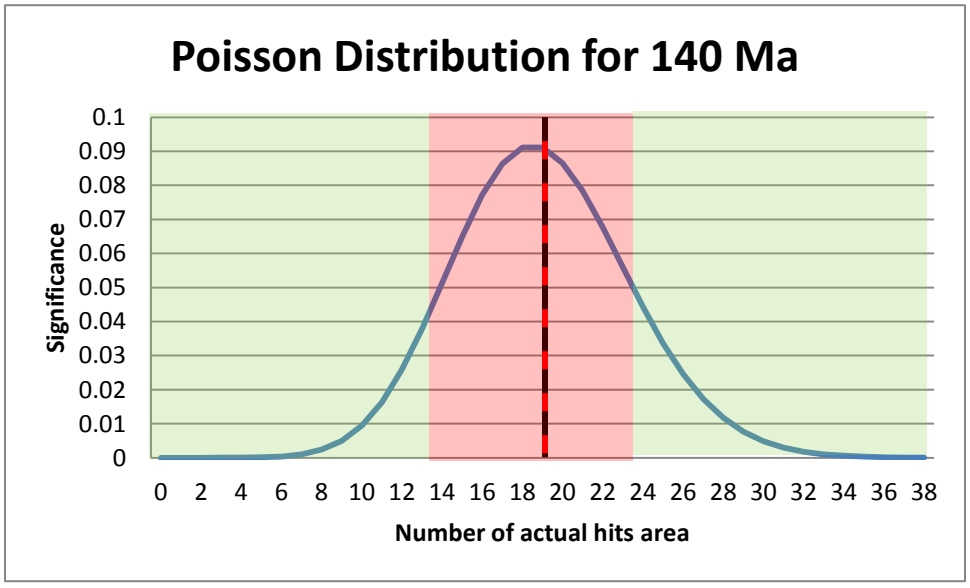

Figure 4.16 Poisson Distribution for 140 Ma

4.7 Late Jurassic (~160 Ma)

The Late Jurassic epoch of the Jurassic period was approximately 160 million years ago. It is defined as a green house climate with little to no evidence of sea ice at the polar regions (Schlanger, 1976). During the Late Jurassic, Pangea continued to breakup causing an

increase in sea-floor spreading and volcanism which increased the CO_2 levels in the atmosphere (Weissert and Mohr, 1996). With more CO_2 in the atmosphere, an increase in marine carbonate production occurred (Budyko et al., 1987). This increase in production caused an increase in organic carbon burial and reef growth (Weissert and Mohr, 1996). These processes are commonly linked with an increase in greenhouse gases which caused an increase in temperature during the Late Jurassic (Budyko et al., 1987). The increased burial was also triggered by monsoonal rainfall patterns in Asia created by the breakup of the supercontinent Pangea (Weissert and Mohr, 1996). The following section will discuss the Late Jurassic observed coal area, predicted coal area, and results of this study for the Late Jurassic.

4.7.1 Late Jurassic Coal Deposits

A paleogeographic map was provided by the PALEOMAP project (Scotese, 2001). The land area during the Late Jurassic was approximately 219 x 10^6 km^2 (Table 4.5). Predicted coals for the Late Jurassic were based on a minimum precipitation of 250 mm/year. All 5^ox5^o grid cells that contained a 250 mm/year or greater were plotted (Figure 4.17: by the blue squares). A total of 123 x 10^6 km^2 fell within the 250 mm/year annual runoff range. The predicted coals are found in northern North America, northern South America, Central America, Europe, northern Africa, northern Asia, Antarctica, Australia, and the Pacific west coast islands (Figure 4.17).

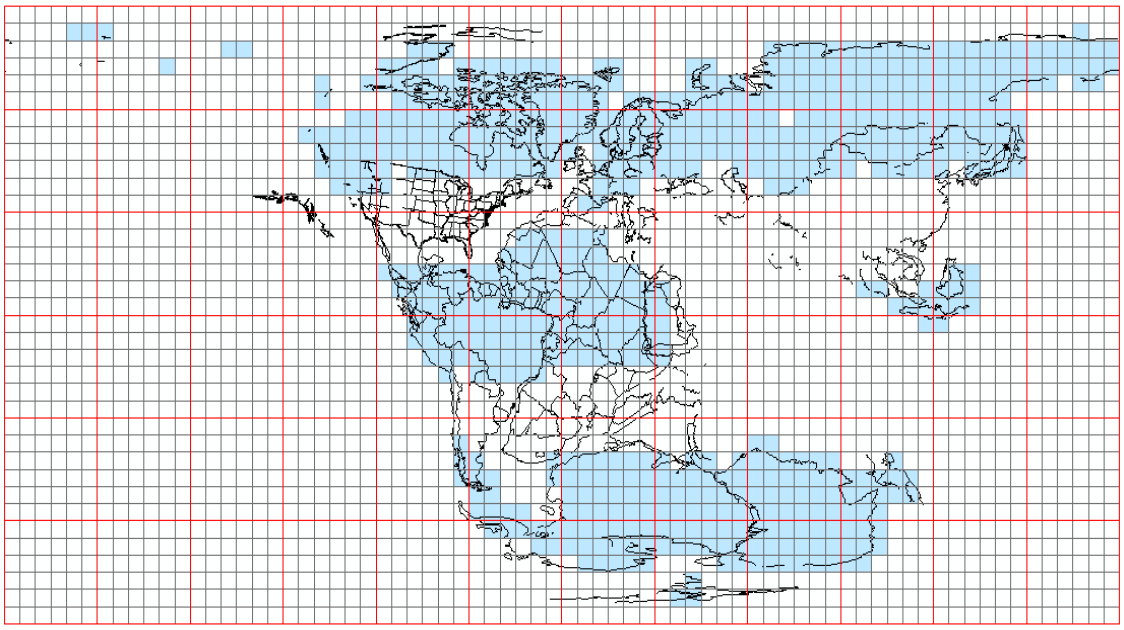

Figure 4.17 Predicted Coal Deposits Area Plotted on 160 Ma Paleogeographic Map

The distribution of observed coal localities was based on the compilation of Boucot et al. (Boucot et al., 2012). Observed coals from Boucot were found in North America, Europe, northern Asia, northern Africa, India, and Australia/Antarctica. A total of 13 x 10^6 km^2 of observed coal area is plotted (Figure 4.18).

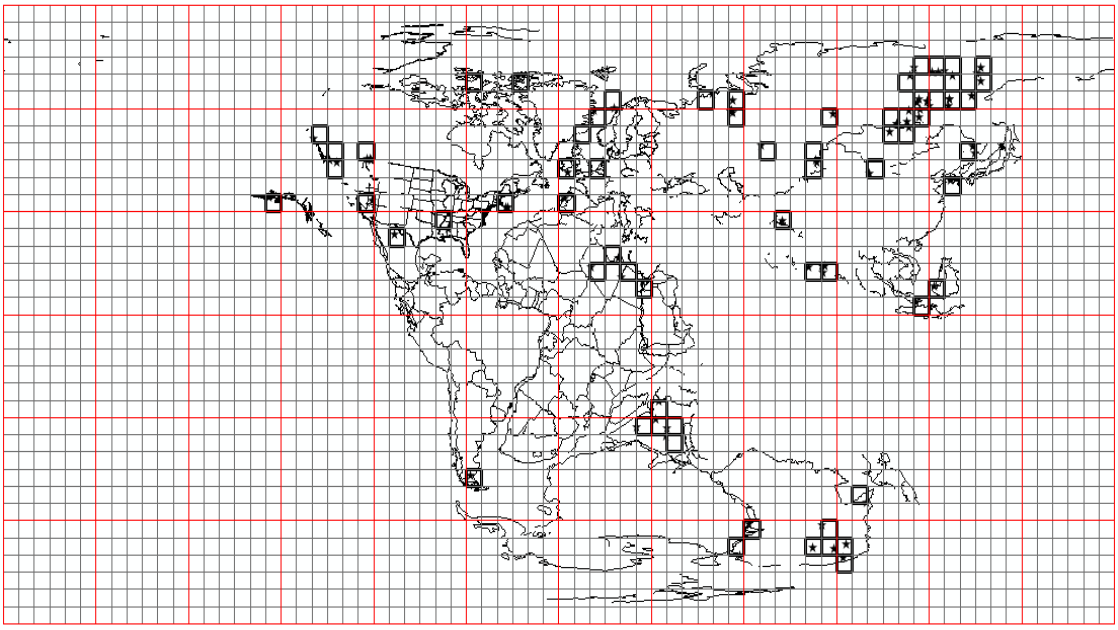

Figure 4.18 Observed Coal Deposits Area Plotted on 160 Ma Paleogeographic Map

Figure 4.19 shows Late Jurassic hits (areas of intersection between observed and predicted coals). All $5^{o}x5^{o}$ grid cells highlighted pink represent areas of "hits." During the Late Jurassic 8 x 10^{6} km^{2} of "hits" were observed. "Hits" can be seen in North America, Europe, northern Asia, Australia, Antarctica, and northern Africa. "Misses" are any observed coal $5^{o}x5^{o}$ grid cells that did not intersect with predicted coal $5^{o}x5^{o}$ grid cells. "Misses" can be seen in India, North America, and southern Asia.

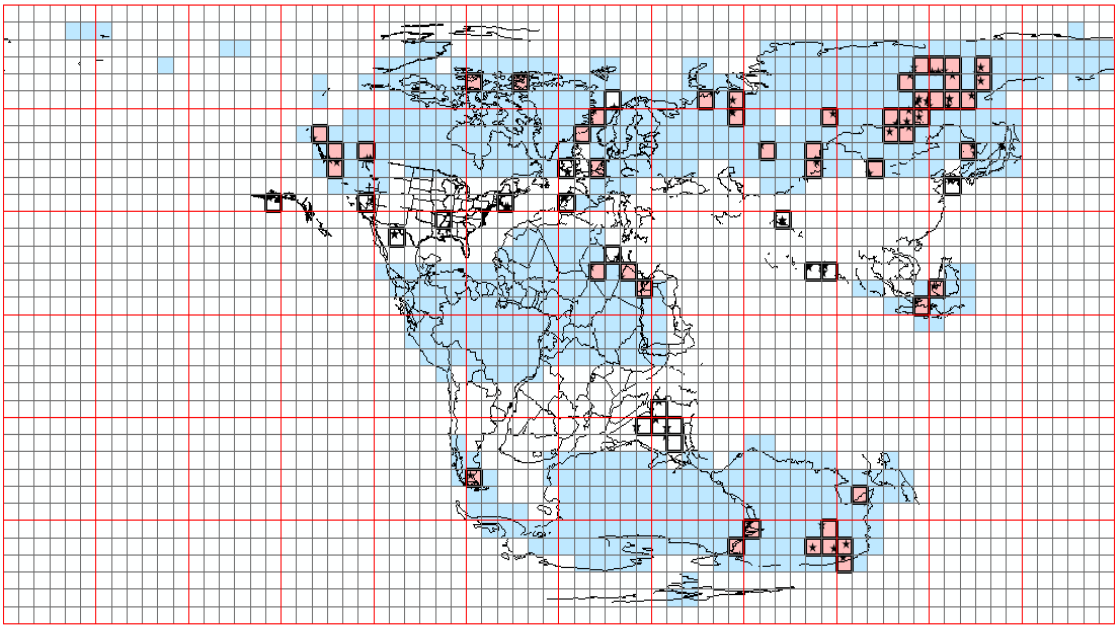

Figure 4.19 Hits Area Plotted on 160 Ma Paleogeographic Map

4.7.1.1 Statistical Analyzes for the Late Jurassic

For the Late Jurassic, there were 219 x 10^6 km^2 of land observed. Of these 219 x 10^6 km^2 of land area, 123 x 10^6 km^2 contained a predicted coal area. This means that 56% of the total land area intersects with a predicted coal 5^ox5^o cell. 13 x 10^6 km^2 contained observed coals. Finally, 8 x 10^6 km^2 containing both observed and predicted coals ("hits") were observed. The results for the entire Late Jurassic can be seen in Table 4.5. Using the statistical analysis outlined in Chapter 2, the expected number of hits was 7 x 10^6 km^2 and the observed number of hits was 8 x 10^6 km^2. This makes the probability of hits due to random process 0.13 which suggests that the observed hits are likely to be insignificant and the null hypothesis stands. Figure 4.20 shows the Poisson distribution for 160 Ma. The red line represents the actual number of hits observed and the dashed black line represents the predicted number of hits during the Late Jurassic. The red box represents area of randomness while the green boxes represent areas of significance. Any point that falls within the green is significant to a degree. During the Late Jurassic, the number of predicted hits area is very similar to the actual hits area. This means it is insignificant and random.

Table 4.5 160 Ma Total Results used during the Statistical Analysis

Total Land	Number of Predicted Coals	% Total Land Occupied by Predicted coals	Number of observed coals	Predicted number of hits	hits	Misses	Probability that Hits are Random
219	123	56	13	7	8	5	0.13

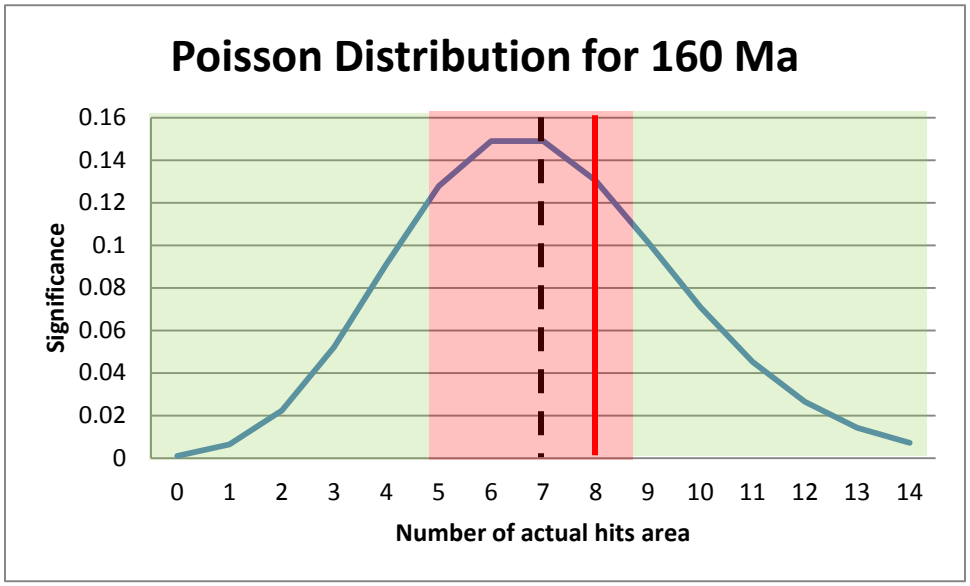

Figure 4.20 Poisson Distribution for 160 Ma

4.8 Early Jurassic (~180 Ma)

The Early Jurassic of the Jurassic period was approximately 180 million years ago. It is defined as a hot house climate with little to no evidence of sea ice at the polar regions (Schlanger, 1976). During the Early Jurassic, Pangea began to breakup with the rifting of Laurasia (North America and Eurasia) from Western Gondwana (South America and Africa) and Western Gondwana from Eastern Gondwana (India, Antarctica, and Australia) (Weissert and Mohr, 1996). This rifting caused an increase in seafloor spreading and volcanism which increased the CO_2 levels in the atmosphere (Weissert and Mohr, 1996). With more CO_2 in the atmosphere, an increase in marine carbonate production occurred (Budyko et al., 1987). This increase in production caused an increase in organic carbon burial and reef growth (Weissert

and Mohr, 1996). These processes are commonly linked with an increase in greenhouse gases which caused an increase in temperature during the Early Jurassic (Budyko et al., 1987). The increased burial was also triggered by mega-monsoonal rainfall patterns created by the breakup of the supercontinent Pangea (Weissert and Mohr, 1996). These mega-monsoons were creating when moisture bearing winds from the Panthalassic Ocean reached the Eurasian continent (Chandler, 1992). The Eurasian continent acted as a barrier for atmospheric winds which then dropped all precipitation it was carrying (Chandler, 1992). As the winds continued across the super continent of Pangea, they lacked moisture and created an arid and hot environment within the interior of the super continent (Chandler, 1992). The following section will discuss the Early Jurassic age observed coal area, predicted coal area, and results of this study for the Early Jurassic.

4.8.1 Early Jurassic Coal Deposits

A paleogeographic map was provided by the PALEOMAP project (Scotese, 2001). The land area during the Early Jurassic was approximately 200 x 10^6 km^2 (Table 4.6). Predicted coals for the Early Jurassic were based on a minimum precipitation value of 250 mm/year. All 5^ox5^o grid cells that contained a 250 mm/year or greater were plotted (Figure 4.21: by the blue squares). A total of 132 x 10^6 km^2 fell within the 250 mm/year annual runoff range. The predicted coals are found in southern North America, Central America, northern South America, Europe, Africa, northern Asia, Antarctica, Australia, and the Pacific west coast islands (Figure 4.21).

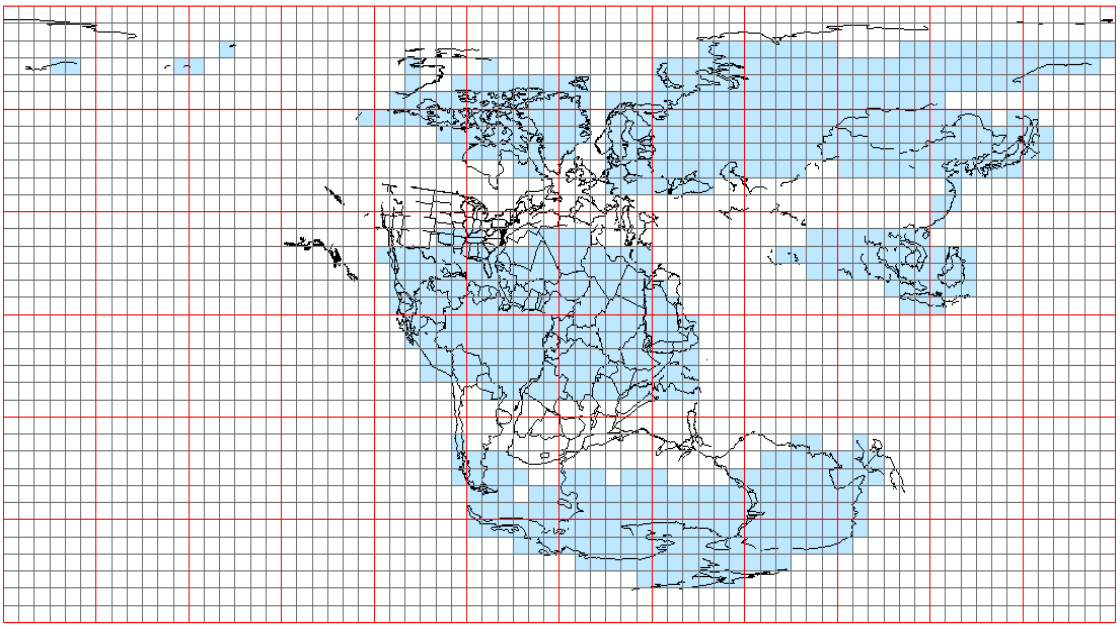

Figure 4.21 Predicted Coal Deposits Area Plotted on 180 Ma Paleogeographic Map

The distribution of observed coal localities was based on the compilation of Boucot et al. (Boucot et al., 2012). Observed coals from Boucot were found in Asia, Europe, North America, Africa, Australia, and Antarctica. A total of 42 x 10^6 km^2 of observed coal area is plotted (Figure 4.22).

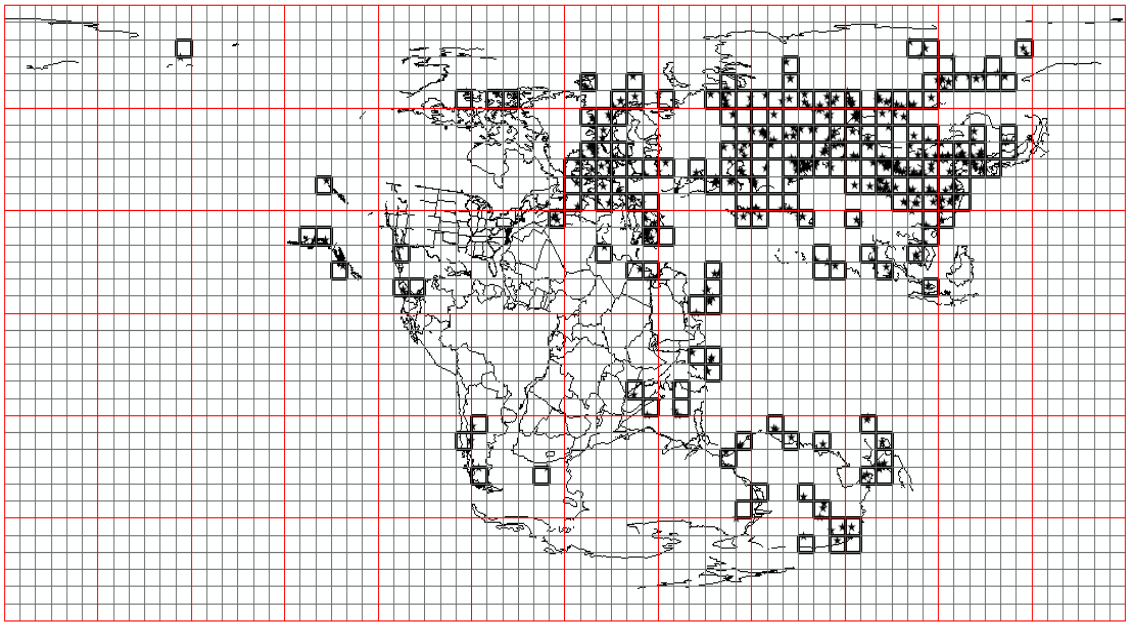

Figure 4.22 Observed Coal Deposits Area Plotted on 180 Ma Paleogeographic Map

Figure 4.23 shows Early Jurassic hits (areas of intersection between observed and predicted coals). All $5^{o}x5^{o}$ grid cells highlighted pink represent areas of "hits." During the Early Jurassic 26 x 10^{6} km^{2} of "hits" were observed. "Hits" can be seen in Asia, Europe, Africa, Australia, and Antarctica. "Misses" are any observed coal $5^{o}x5^{o}$ grid cells that did not intersect with predicted coal $5^{o}x5^{o}$ grid cells. "Misses" can be seen in Europe and southern Asia.

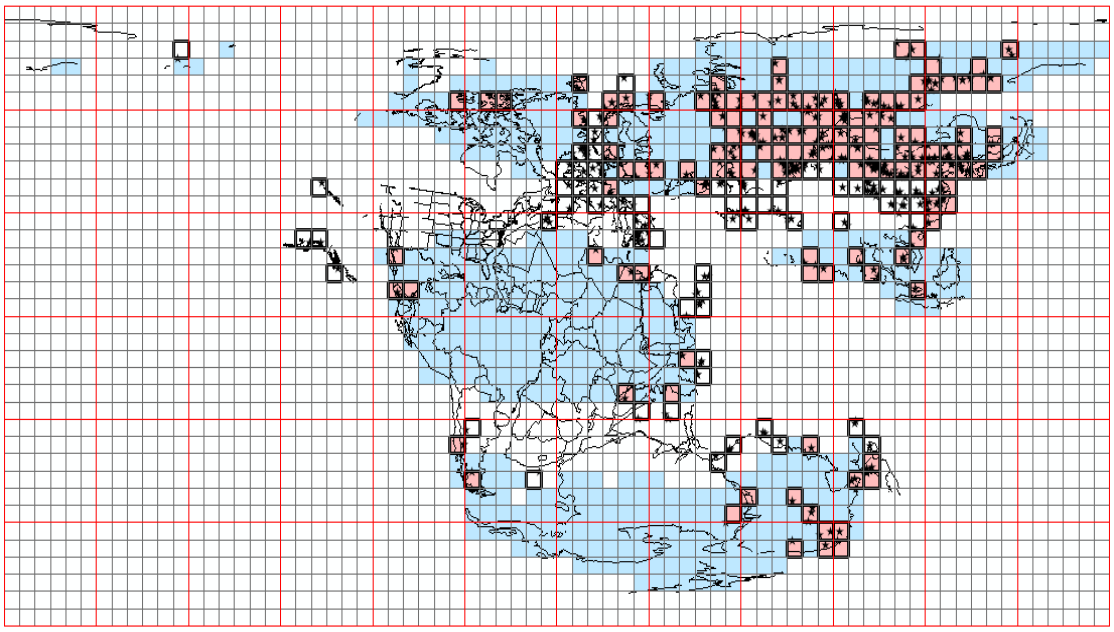

Figure 4.23 Hits Area Plotted on 180 Ma Paleogeographic Map

4.8.1.1 Statistical Analyzes for the Early Jurassic

For the Early Jurassic, there were 200 x 10^6 km^2 of land observed. Of these 200 x 10^6 km^2 of land area, 132 x 10^6 km^2 contained a predicted coal area. This means that 66% of total land area intersects with a predicted coal 5^ox5^o cell. 42 x 10^6 km^2 contained observed coals. Finally, 26 x 10^6 km^2 containing both observed and predicted coals ("hits") were observed. The results for the entire Early Jurassic can be seen in Table 4.6. Using the statistical analysis outlined in Chapter 2, the expected number of hits was 28 x 10^6 km^2 and the observed number of hits was 26 x 10^6 km^2. This makes the probability of hits due to random process 0.07 which suggests that the observed hits are likely to be insignificant and the null hypothesis stands. Figure 4.24 shows the Poisson distribution for 180 Ma. The red line represents the actual number of hits observed and the dashed black line represents the predicted number of hits during the Early Jurassic. The red box represents area of randomness while the green boxes represent areas of significance. Any point that falls within the green is significant to a degree. During the Early Jurassic, the number of predicted hits area is very similar to the actual hits area. This means it is insignificant and random.

Table 4.6 180 Ma Total Results used during the Statistical Analysis

Total Land	Number of Predicted Coals	% Total Land Occupied by Predicted coals	Number of observed coals	Predicted number of hits	hits	Misses	Probability that Hits are Random
200	132	66	42	28	26	16	0.07

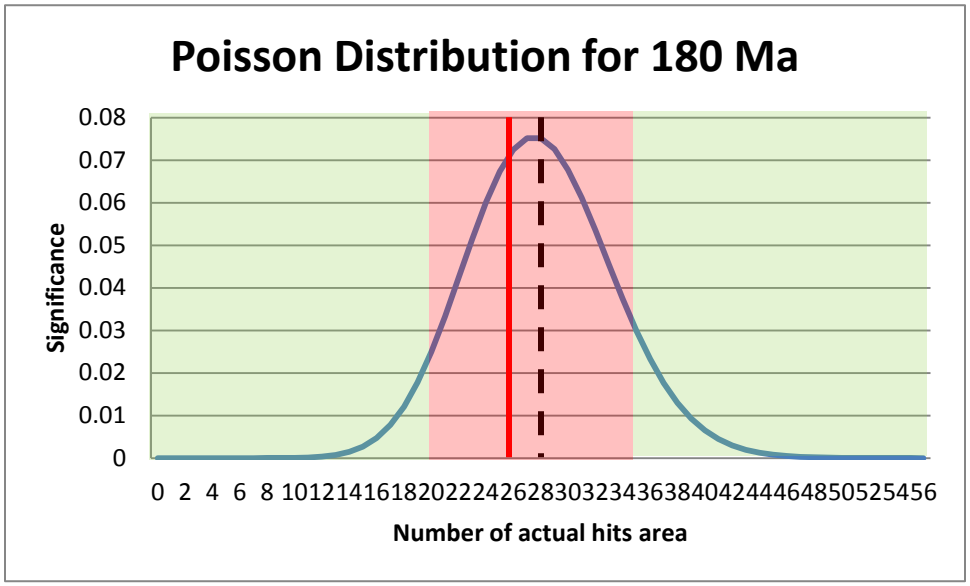

Figure 4.24 Poisson Distribution for 180 Ma

4.9 Middle Triassic (~220 Ma)

The Middle Triassic of the Triassic period was approximately 220 million years ago. Tectonically speaking, the assemblage of the Asia began during this time as the Tethys Ocean began to close. Also, the super-continent of Pangea reached its maximum during this time period. This caused an arid equatorial climatic belt which caused many evaporites to form in the center of the super-continent (Preto et al., 2010). In the Tethys Ocean, the western portion experienced humid conditions which are supported by evidence of palynomorph associations (Preto et al., 2010). In the paleo-Tethys Ocean (the eastern portion of the ocean) a warm and more temperate climate was recorded with the preservation of certain plants such as ferns, conifers, and cycad (Preto et al., 2010). Differing from the Early Triassic, the Middle Triassic did

experience global seasonal changes. These changes were recorded in growth rings, wood in fluvial deposits, and permineralized peats (Preto et al., 2010). The following section will discuss the Middle Triassic age observed coal area, predicted coal area, and results of this study for the Middle Triassic.

4.9.1 Middle Triassic Coal Deposits

A paleogeographic map was provided by the PALEOMAP project (Scotese, 2001). The land area during the Middle Triassic was approximately 209 x 10^6 km^2 (Table 4.7). Predicted coals for the Middle Triassic were based on a minimum precipitation value of 250 mm/year. All 5^ox5^o grid cells that contained a 250 mm/year or greater were plotted (Figure 4.25: by the blue squares). A total of 121 x 10^6 km^2 fell within the 250 mm/year annual runoff range. The predicted coals are found in North America, northern South America, Central America, Europe, northern Africa, northern Asia, Antarctica, and Australia (Figure 4.25).

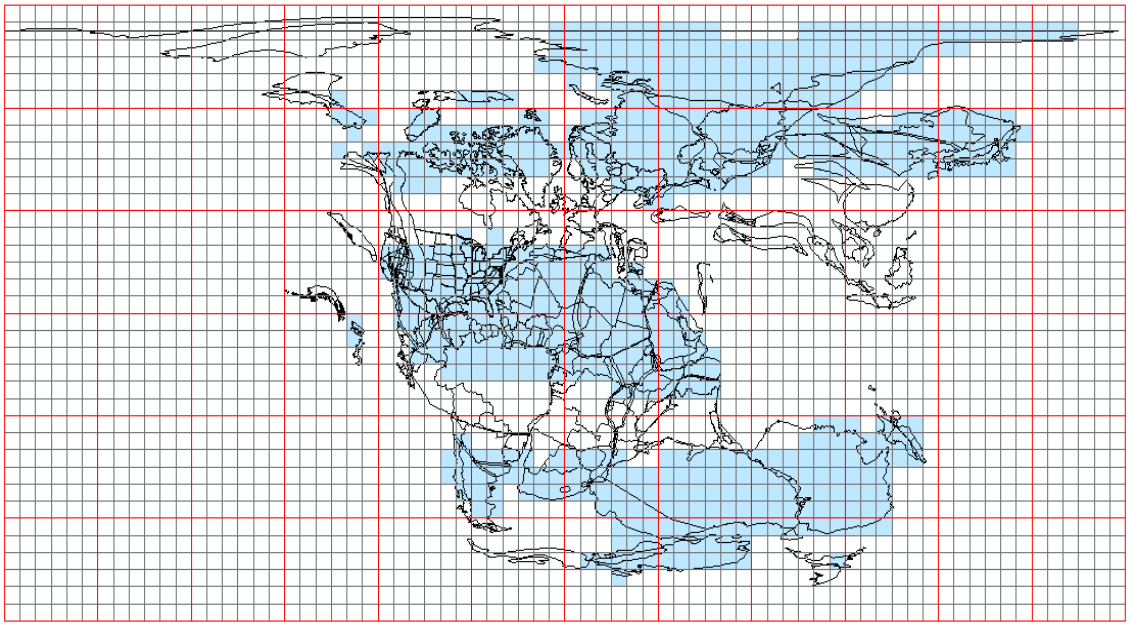

Figure 4.25 Predicted Coal Deposits Area Plotted on 220 Ma Paleogeographic Map

The distribution of observed coal localities was based on the compilation of Boucot et al. (Boucot et al., 2012). Observed coal deposits from Boucot were found in North America,

Europe, Asia, central-western Africa, and Australia/Antarctica. A total of 25 x 10^6 km^2 of observed coal area plotted (Figure 4.26).

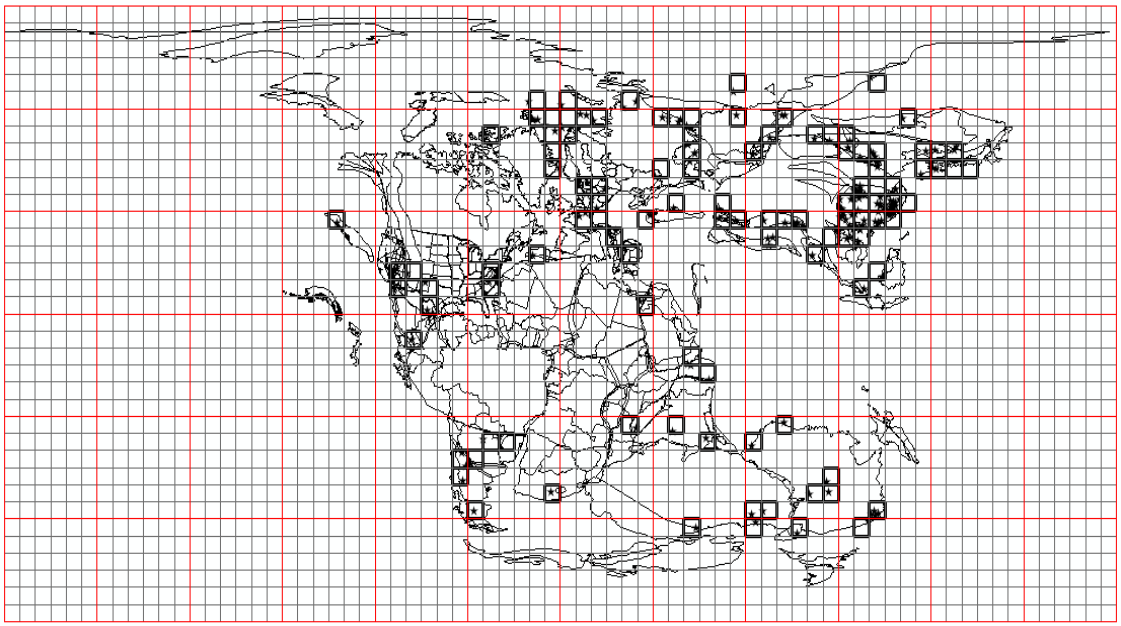

Figure 4.26 Observed Coal Deposits Area Plotted on 220 Ma Paleogeographic Map

Figure 4.27 shows Middle Triassic hits (areas of intersection between observed and predicted coals). All 5^ox5^o grid cells highlighted pink represent areas of "hits." During the Middle Triassic 12 x 10^6 km^2 of "hits" were observed. "Hits" can be seen in North America, Europe, central Africa, northern Asia and, Australia/Antarctica. "Misses" are any observed coal 5^ox5^o grid cells that did not intersect with predicted coal 5^ox5^o grid cells. "Misses" can be seen in the southern Asia, Europe, and western Africa.

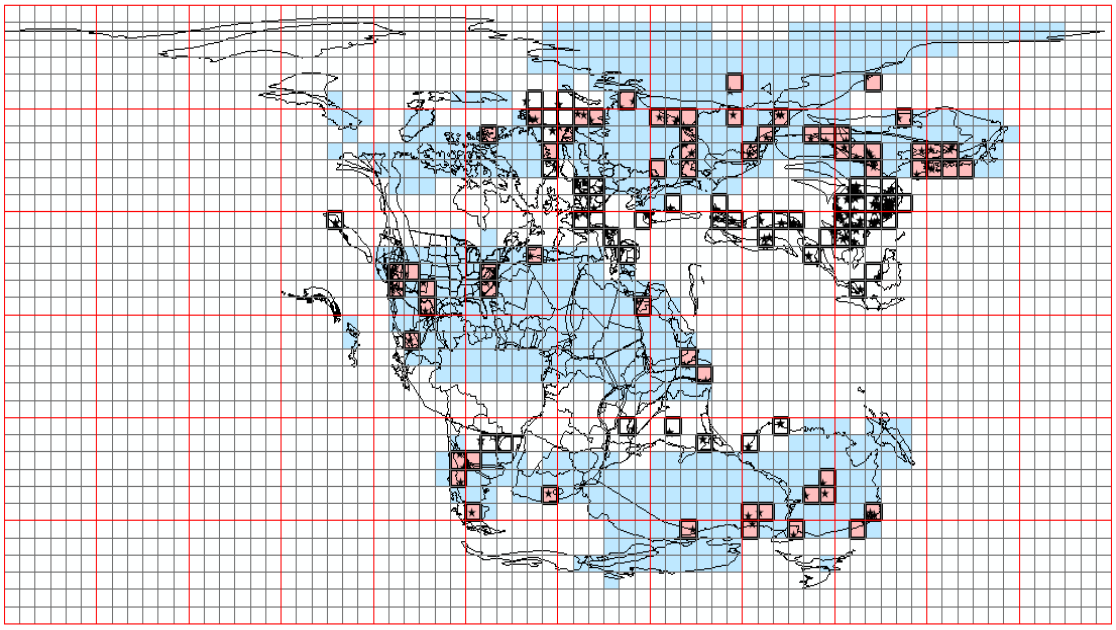

Figure 4.27 Hits Area Plotted on 220 Ma Paleogeographic Map

4.9.1.1 Statistical Analyzes for the Middle Triassic

For the Middle Triassic, there were 209 x 10^6 km^2 of land observed. Of these 209 x 10^6 km^2 of land area, 121 x 10^6 km^2 contained a predicted coal area. This means that 58% of total land area intersects with a predicted coal 5^ox5^o cell. 25 x 10^6 km^2 contained observed coals. Finally, 12 x 10^6 km^2 containing both observed and predicted coals ("hits") were observed. The results for the entire Middle Triassic can be seen in Table 4.7. Using the statistical analysis outlined in Chapter 2, the expected number of hits was 14 x 10^6 km^2 and the observed number of hits was 12 x 10^6 km^2. This makes the probability of hits due to random process 0.09 which suggests that the observed hits are likely to be insignificant and the null hypothesis stands. Figure 4.28 shows the Poisson distribution for 220 Ma. The red line represents the actual number of hits observed and the dashed black line represents the number of predicted hits during the Middle Triassic. The red box represents area of randomness while the green boxes represent areas of significance. Any point that falls within the green is significant to a degree.

During the Early Jurassic, the number of predicted hits area is very similar to the actual hits area. This means it is insignificant and random.

Table 4.7 220 Ma Total Results used during the Statistical Analysis

Total Land	Number of Predicted Coals	% Total Land Occupied by Predicted coals	Number of observed coals	Predicted number of hits	hits	Misses	Probability that Hits are Random
209	121	58	25	14	12	13	0.09

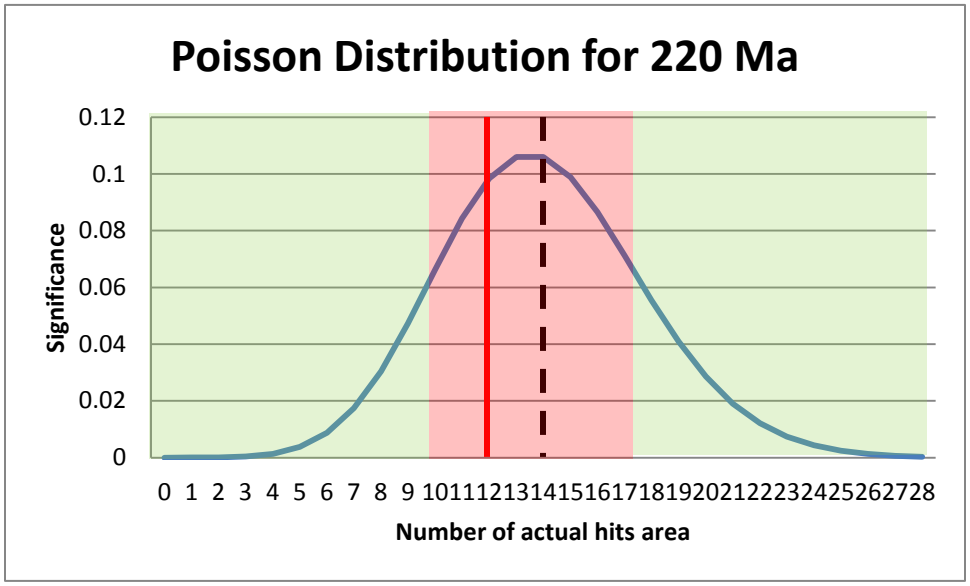

Figure 4.28 Poisson Distribution for 220 Ma

CHAPTER 5

PALEOZOIC COALS

5.1 Introduction

This chapter will discuss in detail the results of Paleozoic Era. In this chapter, the observed coal area will be compared with the predicted coal area for each time interval and the statistical procedures described in Chapter 2 are used to test if the coals pass or fail the null hypothesis.

The Paleozoic Era is broken up into six different time periods: Cambrian (514 Ma), Ordovician (460 Ma), Silurian (425 Ma), Devonian (400 Ma), Carboniferous (Mississippian/Pennsylvanian) (360 Ma-280 Ma), and the Permian (280 Ma). This chapter will discuss the results for the Early Permian (280 Ma), Middle Carboniferous (340 Ma) and, Early Carboniferous (360 Ma). Since organic matter did not exist before the Devonian because of the lack of free oxygen, the Devonian, Silurian, Ordovician, and Cambrian will not be discussed.

5.2 The Paleozoic Era

The Paleozoic Era was highly tectonically active. The formation of Pangea happened during the Paleozoic Era starting in the Cambrian (Shangyou et al., 1990). By the Devonian period, the Paleozoic oceans were closing (Rheic Ocean, Iapetus Ocean, and the Khanty Ocean), and a new Ural Ocean was opening (Shangyou et. al., 1990). Gondwana was near the South Pole and the supercontinent Euramerica (Laurentia and Baltica) was centered along the equator (Shangyou et. al., 1990).

The Paleozoic Era is known for its fluctuation between hot house and ice house climates. At the beginning of the Early Carboniferous, a large sea-level drop happened, creating large epi-continental seas (Bishop et al., 2009). This changed the climate towards a hot house climate (Bishop et al., 2009). These lower sea levels allowed for plant material to develop and thrive (Bishop et al., 2009). The Earth had many swamps and forests which is why many of our

present-day coals come from this period (Bishop et al., 2009). During the Early Carboniferous, terrestrial life had been established and amphibians were the dominant land vertebrate (Bishop et al., 2009). During the Mississippian, the climate was beginning to cool as large ice sheets began to wax and wane from the South Pole (Bishop et al., 2009). Glaciation began in Gondwana as Gondwana moved farther south towards the pole (Bishop et al., 2009). This glaciation continued into the Permian (Bishop et al., 2009). This glaciation caused a decrease in sea levels which caused a mid-Carboniferous major marine extinction in which organisms like crinoids and ammonites began dying rapidly (Bishop et al., 2009). During the Early Permian, the most extensive glaciation (besides from the Pleistocene epoch) occurred (Tabor et al., 2008). Some of the contributing factors to this large-scale glaciation could have been: tectonic drifting, land-sea distribution, supercontinentality, monsoons, and changes in ice sheets (Tabor et al., 2008).

The following sections discuss the results of the Paleozoic time periods used for this study. The amount of land cell area, number of predicted coal area, observed coal area, and hit localities area will be presented in each period.

5.3 Early Permian (~280 Ma)

The Early Permian period was approximately 280 million years ago. By the beginning of the Early Permian, the supercontinent of Pangea was almost complete (Tabor et al., 2008). There were two major oceans surrounding Pangea (the Panthalassa and the paleo-Tethys oceans) Pangea was centered and spanned roughly from pole to pole. With all but a few large islands in the paleo-Tethys ocean, most of the Earth's continents were part of Pangea by this time (Tabor et al., 2008). These large islands during the Early Permian began to close the paleo-Tethys ocean and collided with the northern half of Pangea (Tabor et al., 2008). During the Early Permian, the most extensive glaciation (besides from the Pleistocene epoch) occurred (Tabor et al., 2008). Some of the contributing factors to this large-scale glaciation could have been: tectonic drifting, land-sea distribution, supercontinentality, monsoons, and changes in ice

sheets (Tabor et al., 2008). Tectonic drifting began in the Pennsylvanian and continued through the Early Permian when Pangea began to move northward about 10^{o} to 14^{0} (Tabor et al., 2008). This movement caused changes in the atmospheric circulation which resulted in a decrease in precipitation (Tabor et al., 2008). Land-sea distribution during the Early Permian is very important because during the Early Permian, there was ~22% land and ~78% water covering the Earth (Tabor et al., 2008). This affects the atmospheric circulation as well as oceanic circulation which can cause a decrease in precipitation (Tabor et al., 2008). As Pangea began to assemble during the Early Permian, the concept of supercontinentality begins affect the climatic conditions. Large masses of land centered from pole to pole caused an aridification due to the large amount of land (Tabor et al., 2008). This large landmass also created mega-monsoons in the northern region of Pangea because moisture bearing winds from the Panthalassic Ocean to precipitate out and continued westward, which then dried out the interior of Pangea (Tabor et al., 2008). The atmosphere was also affected by large ice sheets that spanned during this time period (Tabor et al., 2008). These ice sheets acted like areas of uplift, causing the atmospheric winds to move around the ice sheets (Tabor et al., 2008). The following section will discuss the Early Permian observed coal area, predicted coal area, and results of this study for the Early Permian.

5.3.1 Early Permian Coal Deposits

A paleogeographic map was provided by the PALEOMAP project (Scotese, 2001). The land area during the Early Permian was approximately 213 x 10^{6} km^{2} (Table 5.1). Predicted coals for the Early Permian were based on a minimum precipitation value of 250 mm/year. All $5^{o}x5^{o}$ grid cells that contained a 250 mm/year or greater were plotted (Figure 5.1: by the blue squares). A total of 100 x 10^{6} km^{2} fell within the 250 mm/year annual runoff range. The predicted coals are found in North America, northern South America, and southern South American, Central America, Europe, southern Africa, China, and Australia (Figure 5.1).

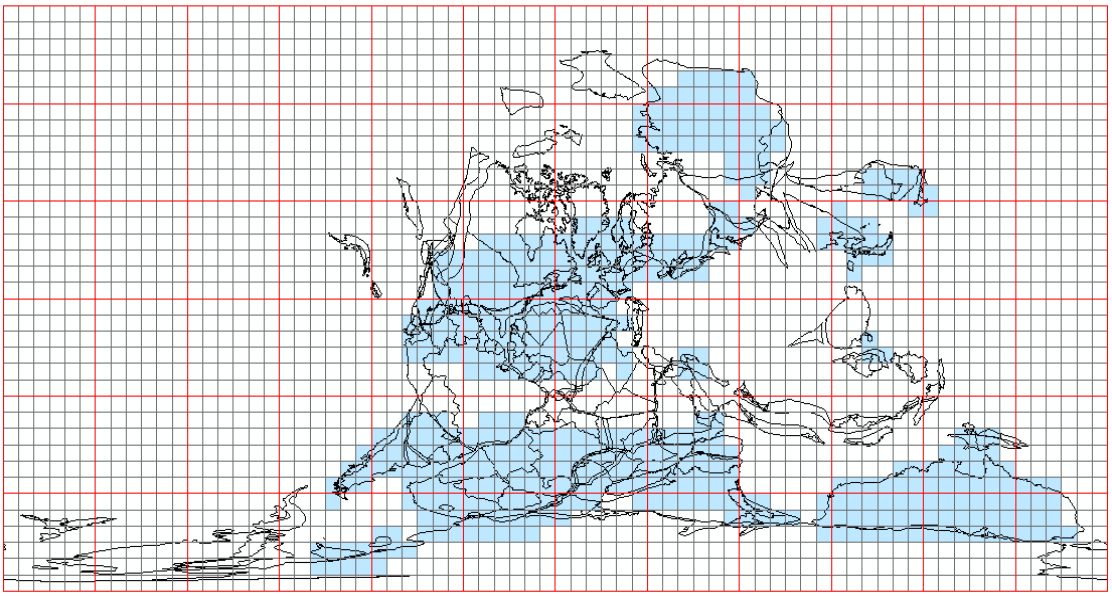

Figure 5.1 Predicted Coal Deposits Area Plotted on 280 Ma Paleogeographic Map

The distribution of observed coal localities was based on the compilation of Boucot et al. (Boucot et al., 2012). Observed coals from Boucot were found in north-western Europe, Asia, Australia, and southern Africa. A total of 23 x 10^6 km^2 of observed coal area is plotted (Figure 5.2).

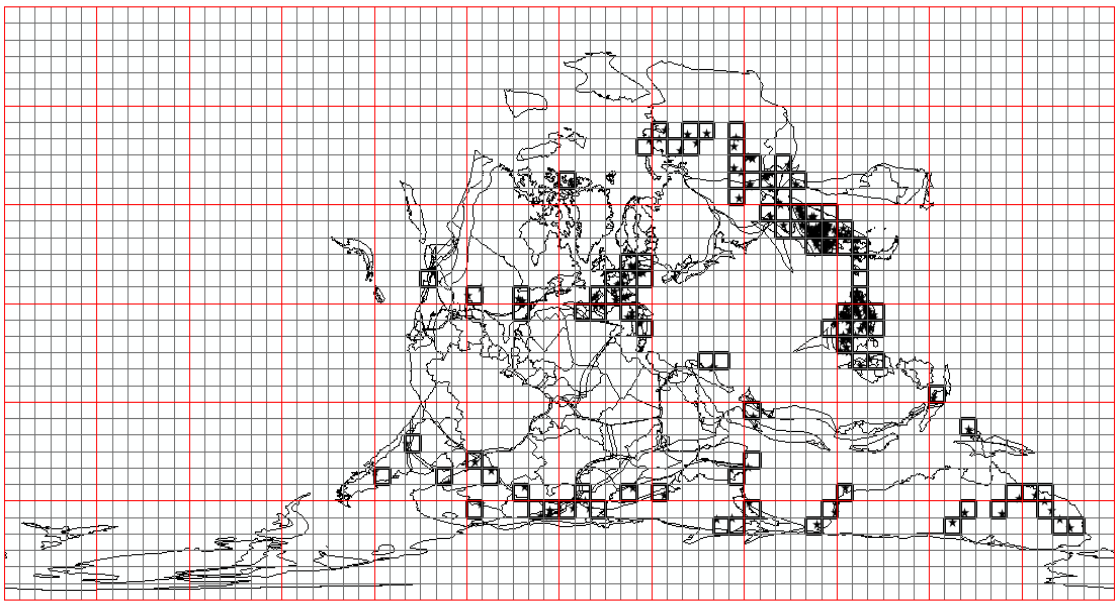

Figure 5.2 Observed Coal Deposits Area Plotted on 280 Ma Paleogeographic Map

Figure 5.3 shows Early Permian hits (areas of intersection between observed and predicted coals). All $5^{o}x5^{o}$ grid cells highlighted pink represent areas of "hits." During the Early Permian 14 x 10^{6} km^{2} of "hits" were observed. "Hits" can be seen in north-western Europe, Asia, southern Africa, and Australia. "Misses" are any observed coal $5^{o}x5^{o}$ grid cells that did not intersect with predicted coal $5^{o}x5^{o}$ grid cells. "Misses" can be seen in Asia and Australia.

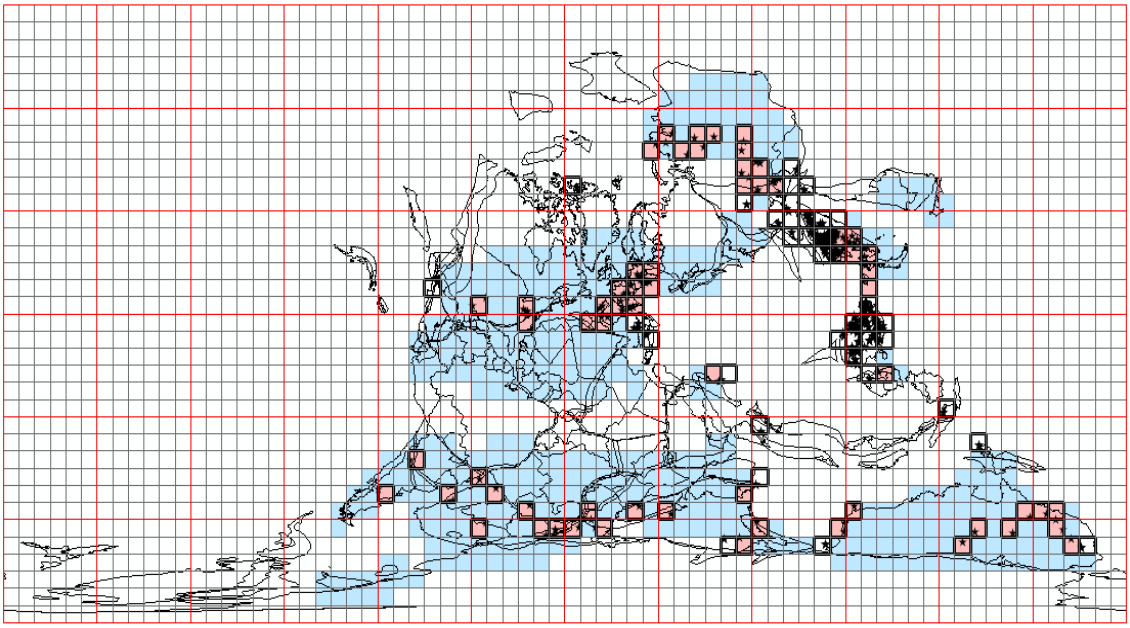

Figure 5.3 Hits Area Plotted on 280 Ma Paleogeographic Map

5.3.1.1 Statistical Analyzes for the Early Permian

For the Early Permian, there were 213 x 10^{6} km^{2} of land observed. Of these 213 x 10^{6} km^{2} of land area, 100 x 10^{6} km^{2} contained a predicted coal area. This means that 47% of total land area intersects with a predicted coal $5^{o}x5^{o}$ cell. 23 x 10^{6} km^{2} contained observed coals. Finally, 14 x 10^{6} km^{2} containing both observed and predicted coals ("hits") were observed. The results for the entire Early Permian can be seen in Table 5.1. Using the statistical analysis outlined in Chapter 2, the expected number of hits was 11 x 10^{6} km^{2} and the observed number of hits was 14 x 10^{6} km^{2}. This makes the probability of hits due to random process 0.07 which suggests that the observed hits are likely to be significant and the null hypothesis fails. Figure 5.4 shows the Poisson distribution for 280 Ma. The red line represents the actual number of hits

observed and the dashed black line represents the predicted number of hits during the Early Permian. The red box represents area of randomness while the green boxes represent areas of significance. Any point that falls within the green is significant to a degree. During the Early Permian, the number of predicted hits area varies from the actual number of hits. This means it is most likely significant and probable.

Table 5.1 280 Ma Total Results used during the Statistical Analysis

Total Land	Number of Predicted Coals	% Total Land Occupied by Predicted coals	Number of observed coals	Predicted number of hits	hits	Misses	Probability that Hits are Random
213	100	47	23	11	14	9	0.07

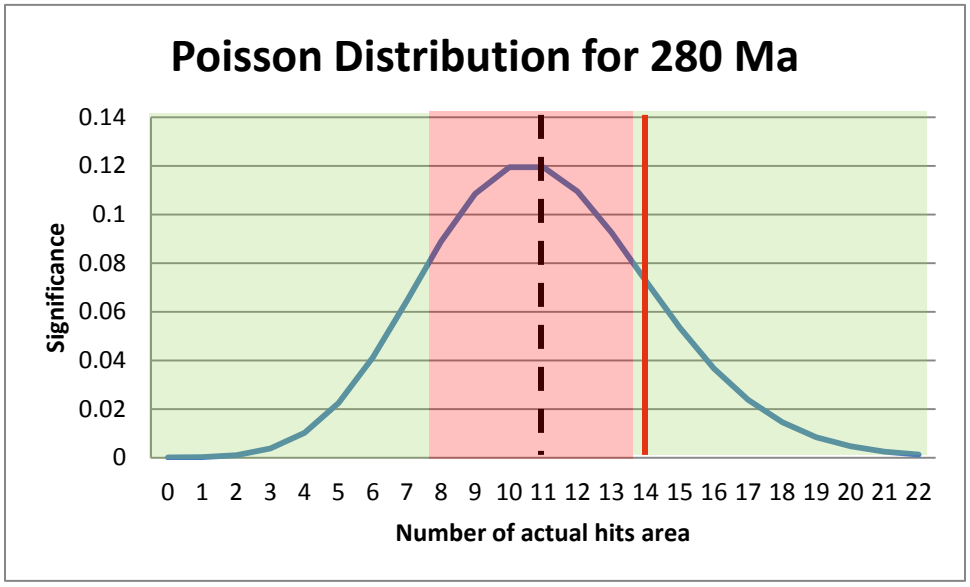

Figure 5.4 Poisson Distribution for 280 Ma

5.4 Middle Carboniferous-Visean age (~340 Ma)

The middle Carboniferous was approximately 340 million years ago. The tectonic plates were in a much different assemblage than today. Most of the continental plates were located in the southern hemisphere near the South Pole, with mostly small islands toward the more northern latitudes (Bishop et al., 2009). This was a time of active plate tectonics as Pangea was

being formed together (Bishop et al., 2009). During middle Carboniferous, the climate was beginning to cool as large ice sheets began to wax and wane from the South Pole (Bishop et al., 2009). Glaciation began in Gondwana as Gondwana moved farther south towards the pole (Bishop et al., 2009). This glaciation continued into the Permian (Bishop et al., 2009). This glaciation caused a decrease in sea levels which caused a mid-Carboniferous major marine extinction in which organisms like crinoids and ammonites began dying rapidly (Bishop et al., 2009). The following section will discuss the Middle Carboniferous observed coal area, predicted coal area, and results of this study for the Middle Carboniferous.

5.4.1 Middle Carboniferous Coal Deposits

A paleogeographic map was provided by the PALEOMAP project (Scotese, 2001). The land area during the Middle Carboniferous was approximately 210 x 10^6 km^2 (Table 5.2). Predicted coals for the Middle Carboniferous were based on a minimum precipitation value of 250 mm/year. All 5^ox5^o grid cells that contained a 250 mm/year or greater were plotted (Figure 5.5: by the blue squares). A total of 113 x 10^6 km^2 fell within the 250 mm/year annual runoff range. The predicted coals are found in North America, Europe, South America, Africa, Antarctica, Australia, and Asia (Figure 5.5).

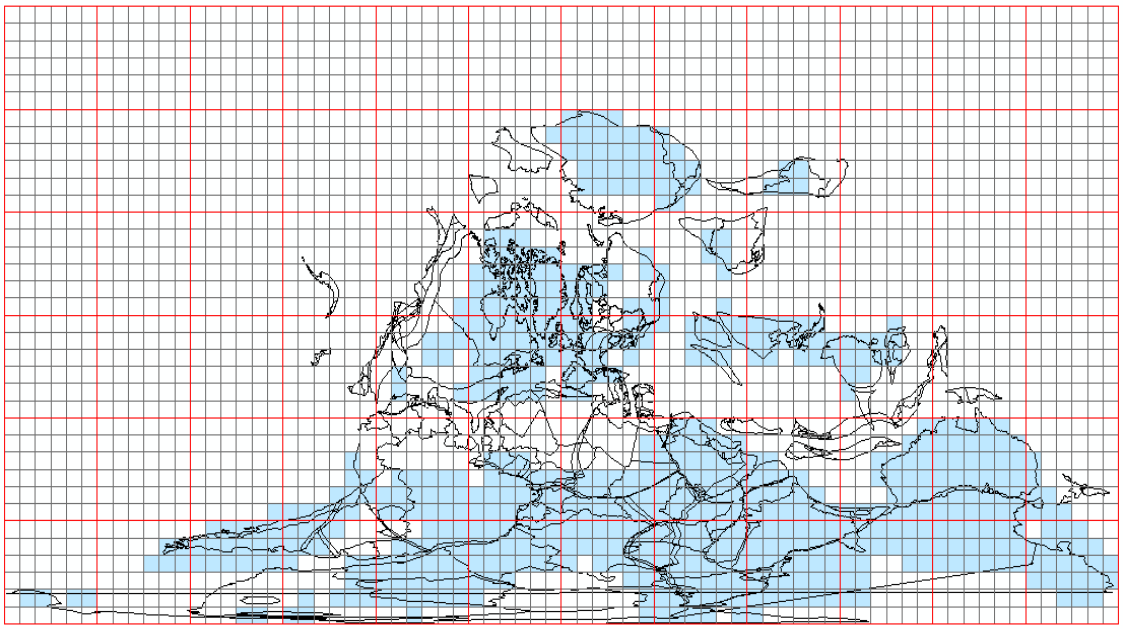

Figure 5.5 Predicted Coal Deposits Area Plotted on 340 Ma Paleogeographic Map

The distribution of observed coal localities was based on the compilation of Boucot et al. (Boucot et al., 2012). Observed coals from Boucot were found in Europe, Asia, Australia, Africa, South America, and northern North America. A total of 24 x 10^6 km^2 of observed coal area is plotted (Figure 5.6).

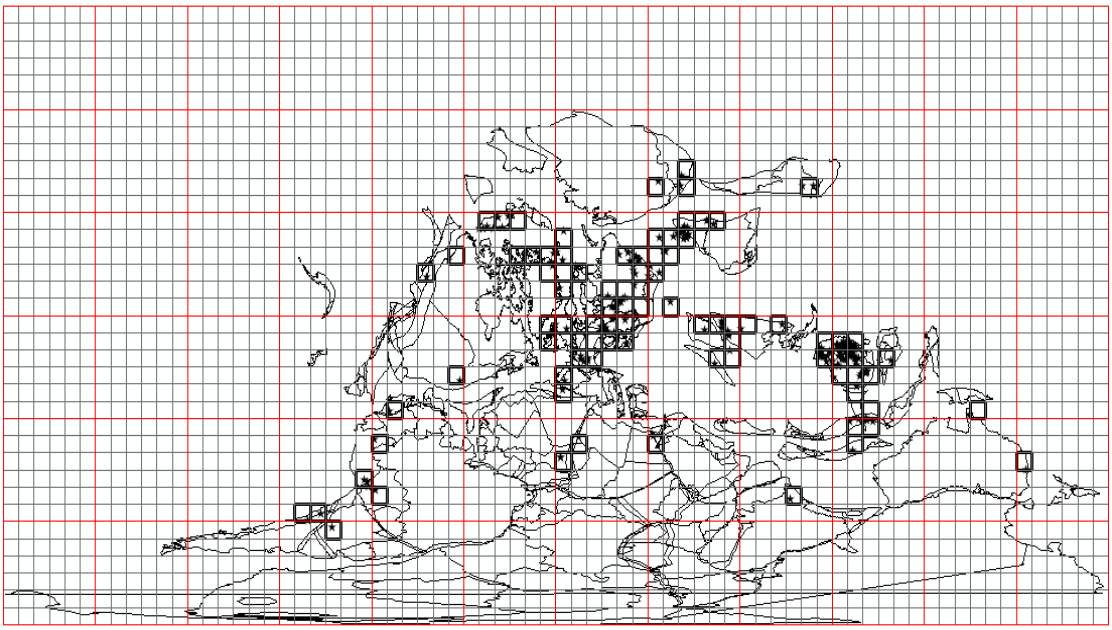

Figure 5.6 Observed Coal Deposits Area Plotted on 340 Ma Paleogeographic Map

Figure 5.7 shows Middle Cretaceous hits (areas of intersection between observed and predicted coals). All $5^{o}x5^{o}$ grid cells highlighted pink represent areas of "hits." During the middle Cretaceous 14 x 10^{6} km^{2} of "hits" were observed. "Hits" can be seen in Europe, South America, northern North America, Asia, Africa, and Australia. "Misses" are any observed coal $5^{o}x5^{o}$ grid cells that did not intersect with predicted coal $5^{o}x5^{o}$ grid cells. "Misses" can be seen in Asia, Europe, North America, and South America.

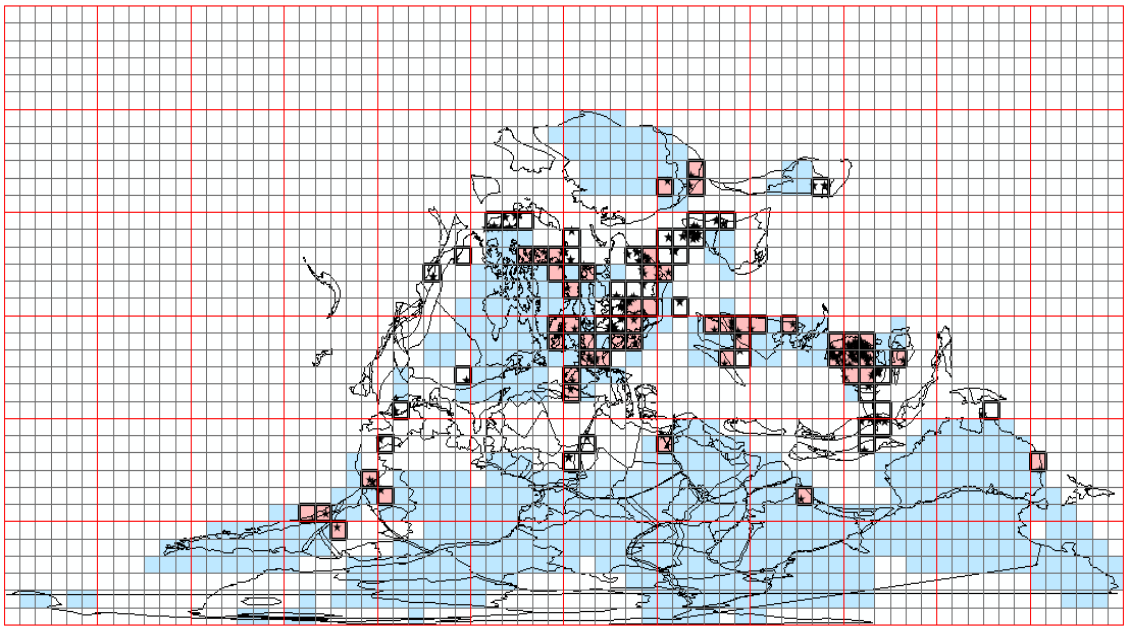

Figure 5.7 Hits Area Plotted on 340 Ma Paleogeographic Map

5.4.1.1 Statistical Analyzes for the Middle Carboniferous

For the Middle Carboniferous, there were 210 x 10^6 km^2 of land observed. Of these 210 x 10^6 km^2 of land area, 113 x 10^6 km^2 contained a predicted coal area. This means that 54% of total land area intersects with a predicted coal 5^ox5^o cell. 24 x 10^6 km^2 contained observed coals. Finally, 14 x 10^6 km^2 containing both observed and predicted coals ("hits") were observed. The results for the entire Middle Carboniferous can be seen in Table 5.2. Using the statistical analysis outlined in Chapter 2, the expected number of hits was 13 x 10^6 km^2 and the observed number of hits was 14 x 10^6 km^2. This makes the probability of hits due to random process 0.10 which suggests that the observed hits are likely to be insignificant and the null hypothesis stands. Figure 5.8 shows the Poisson distribution for 340 Ma. The red line represents the actual number of hits observed and the dashed black line represents the predicted number of hits during the Middle Carboniferous. The red box represents area of randomness while the green boxes represent areas of significance. Any point that falls within the green is significant to a degree. During the Middle Carboniferous, the number of predicted hits area is very similar to the actual hits area. This means it is insignificant and random.

Table 5.2: 340 Ma Total Results used during the Statistical Analysis

Total Land	Number of Predicted Coals	% Total Land Occupied by Predicted coals	Number of observed coals	Predicted number of hits	hits	Misses	Probability that Hits are Random
210	113	54	24	13	14	10	0.10

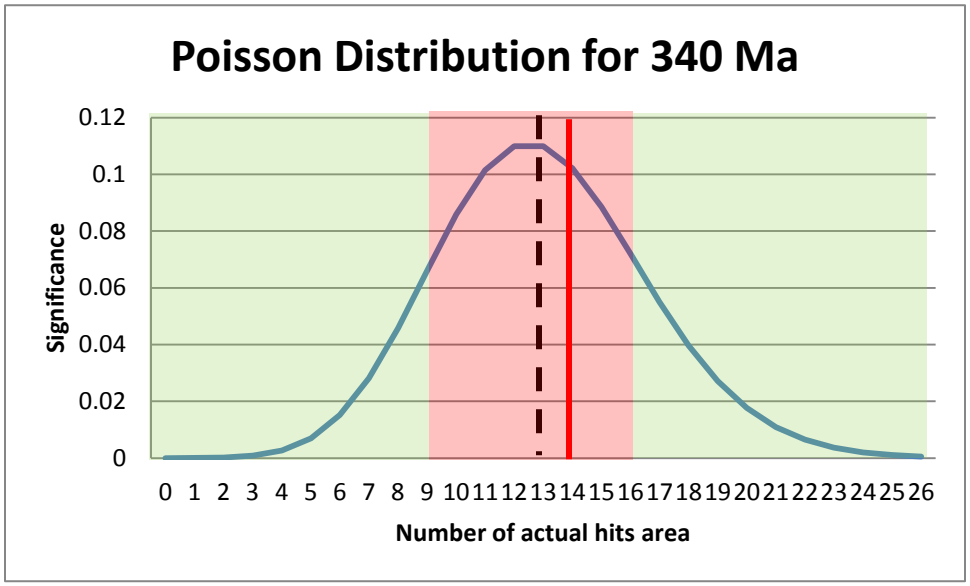

Figure 5.8 Poisson Distribution for 340 Ma

5.5 Early Carboniferous (~360 Ma)

The Early Carboniferous period was approximately 360 million years ago. By the beginning of the Early Carboniferous, the supercontinent of Pangea was almost complete (Bishop et al., 2009). Most of the continental plates were located in the southern hemisphere near the South Pole with mostly small islands toward the more northern latitudes. This was a time of active plate tectonics as Pangea was being formed together (Bishop et al., 2009). At the beginning of the Early Carboniferous, a sea-level increase happened, creating large epi-continental seas (Bishop et al., 2009). This changed the climate towards a hot house climate (Bishop et al., 2009). The Earth had many swamps and forests which is why many of our present-day coals come from this period (Bishop et al., 2009). During the Early Carboniferous,

terrestrial life had been established and amphibians were the dominant land vertebrate (Bishop et al., 2009). The following section will discuss the Early Carboniferous observed coal area, predicted coal area, and results of this study for the Early Carboniferous.

5.5.1 Early Carboniferous Coal Deposits

A paleogeographic map was provided by the PALEOMAP project (Scotese, 2001). The land area during the Early Carboniferous was approximately 206 x 10^6 km^2 (Table 5.3). Predicted coals for the Early Carboniferous were based on a minimum precipitation value of 250 mm/year. All 5^ox5^o grid cells that contained a 250 mm/year or greater were plotted (Figure 3.5: by the blue squares). A total of 106 million km^2 fell within the 250 mm/year annual runoff range. The predicted coals are found in North America, Europe, South America, Africa, Antarctica, Australia, and Asia (Figure 5.9).

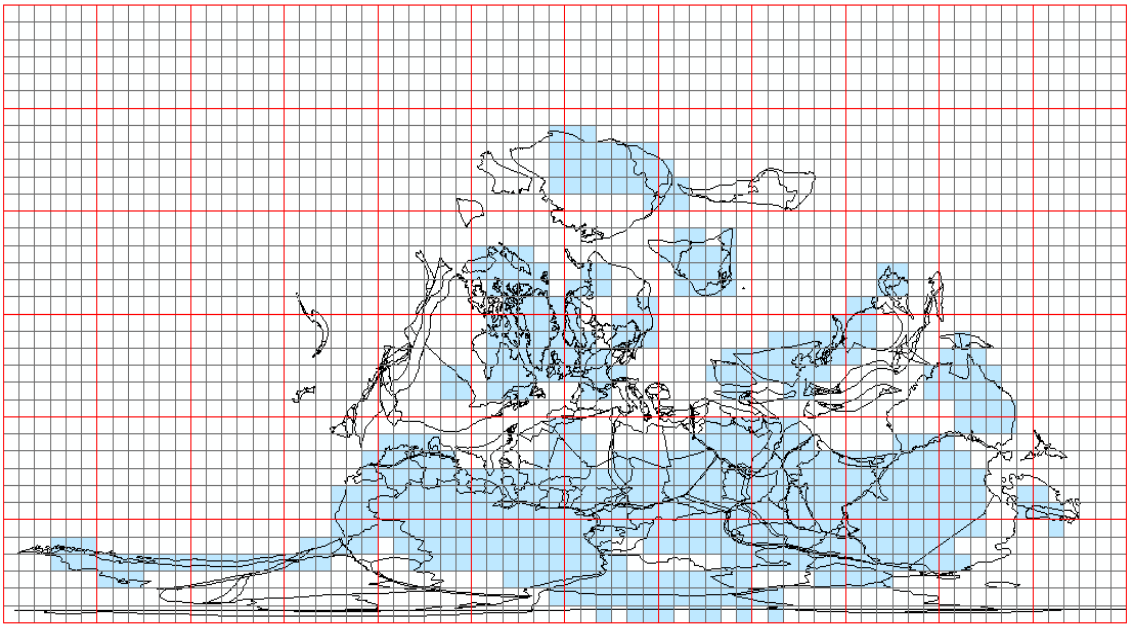

Figure 5.9 Predicted Coal Deposits Area Plotted on 360 Ma Paleogeographic Map

The distribution of observed coal localities was based on the compilation of Boucot et al. (Boucot et al., 2012). Observed coals from Boucot were found in North America, Africa, Asia, Australia, and South America. A total of 4 x 10^6 km^2 of observed coal is plotted (Figure 5.10).

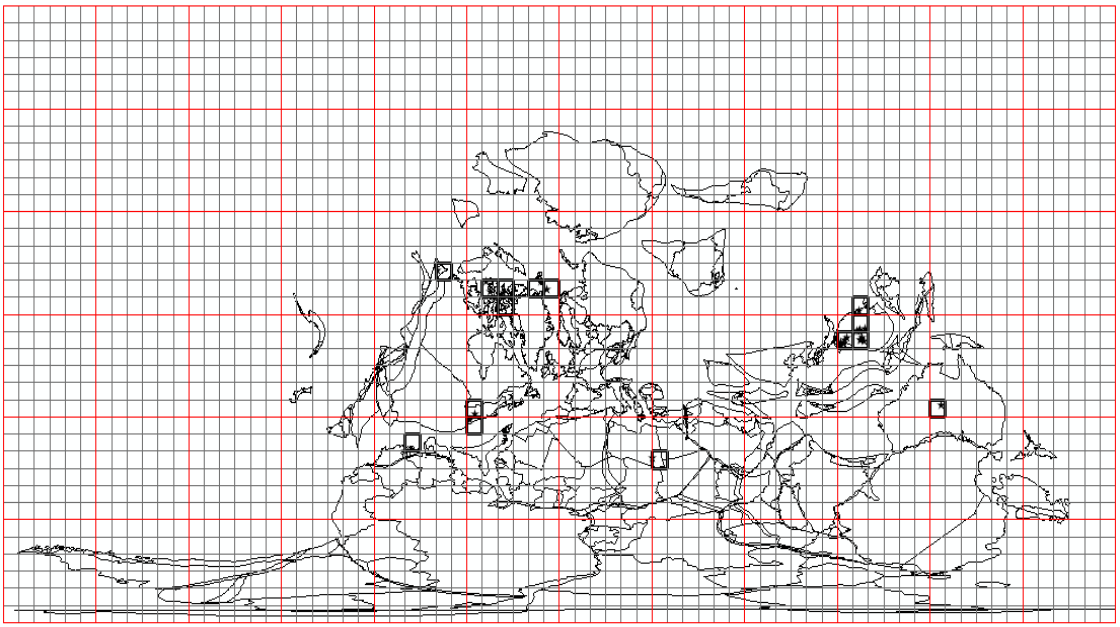

Figure 5.10 Observed Coal Deposits Area Plotted on 360 Ma Paleogeographic Map

Figure 5.11 shows Early Carboniferous hits (areas of intersection between observed and predicted coals). All $5^{o}x5^{o}$ grid cells highlighted red represent areas of "hits." During the Early Carboniferous 3 x 10^{6} km^{2} of "hits" were observed. "Hits" can be seen in North America, South America, Africa, and Asia. "Misses" are any observed coal $5^{o}x5^{o}$ grid cells that did not intersect with predicted coal $5^{o}x5^{o}$ grid cells. "Misses" can be seen in North America and Australia.

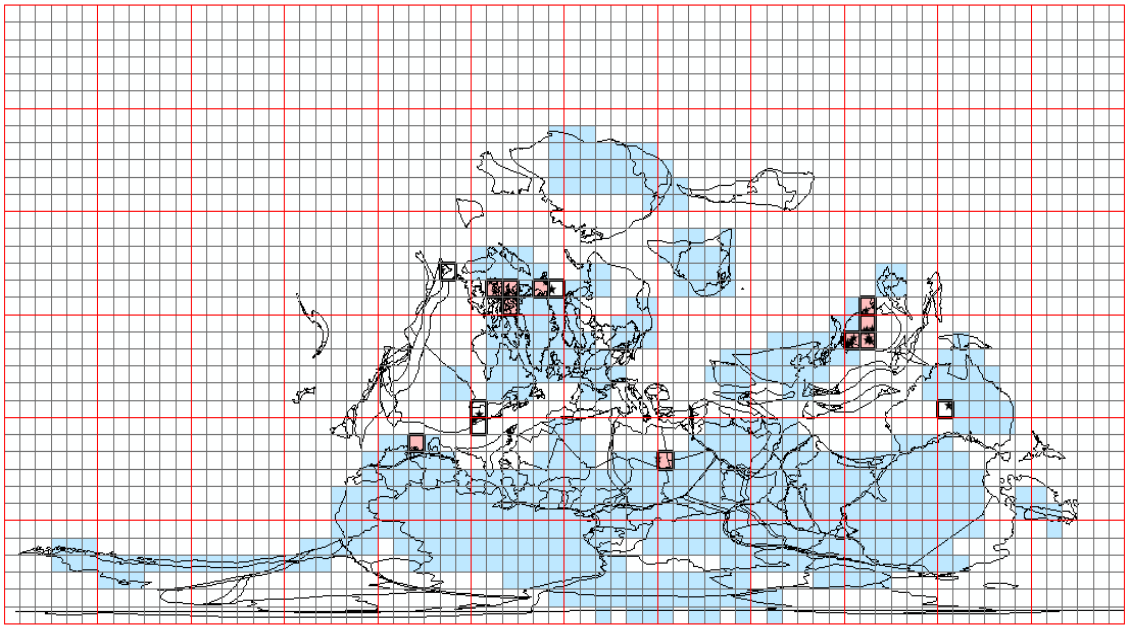

Figure 5.11 Hits Area Plotted on 360 Ma Paleogeographic Map

5.5.1.1 Statistical Analyzes for the Early Carboniferous

For the Early Carboniferous, there were 206 x 10^6 km^2 of land observed. Of these 206 x 10^6 km^2 of land area, 106 x 10^6 km^2 contained a predicted coal area. This means that 51% of total land area intersects with a predicted coal 5^ox5^o cell. 4 x 10^6 km^2 contained observed coals. Finally, 3 x 10^6 km^2 containing both observed and predicted coals ("hits") were observed. The results for the entire Early Carboniferous can be seen in Table 5.3. Using the statistical analysis outlined in Chapter 2, the expected number of hits was 2 x 10^6 km^2 and the observed number of hits was 3 x 10^6 km^2. This makes the probability of hits due to random process 0.18 which suggests that the observed hits are likely to be significant and the null hypothesis fails. Figure 5.12 shows the Poisson distribution for 360 Ma. The red line represents the actual number of hits observed and the dashed black line represents the predicted number of hits during the Early Carboniferous. The red box represents area of randomness while the green boxes represent areas of significance. Any point that falls within the green is significant to a degree. During the Early Carboniferous, the number of predicted hits area varies from the actual number of hits. This means it is most likely significant and probable.

Table 5.3 360 Ma Total Results used during the Statistical Analysis

Total Land	Number of Predicted Coals	% Total Land Occupied by Predicted coals	Number of observed coals	Predicted number of hits	hits	Misses	Probability that Hits are Random
206	106	51	4	2	3	1	0.18

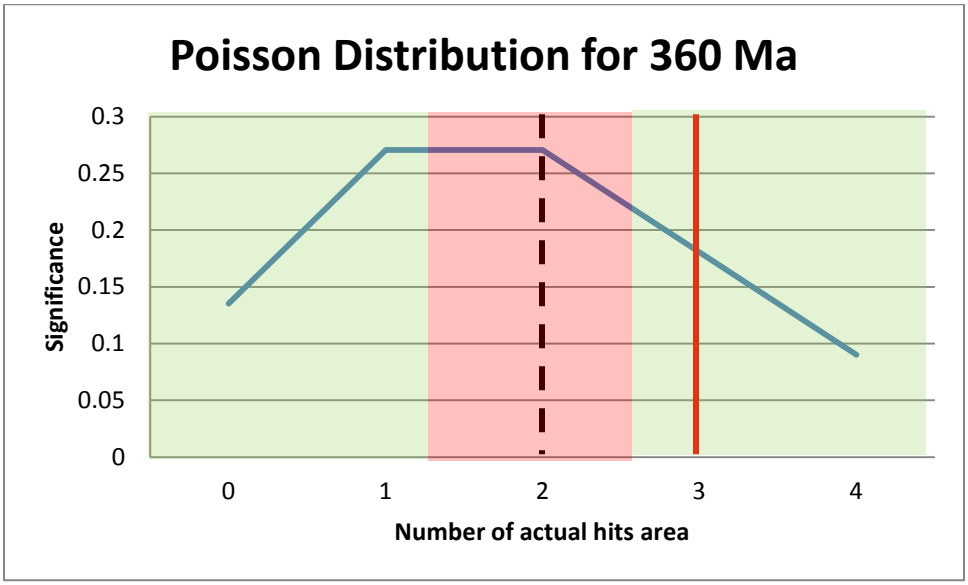

Figure 5.12 Poisson Distribution for 360 Ma

CHAPTER 6

MERIDIONAL DISTRIBUTION OF CENOZOIC, MESOZOIC, AND PALEOZOIC COAL DEPOSITS

6.1 Introduction

This chapter will discuss in detail the meridional distribution Cenozoic, Mesozoic, and Paleozoic coal deposits. Previously, each different time interval was looked at closely, but in this chapter, a study of each Era will be observed. For each Era, the number of predicted coal area, hits area, and misses area will be observed. This will give a better understand of each Era and a more macroscopic look at the data from the previous chapters.

6.2 The Cenozoic Era

All Cenozoic history, paleo-tectonics, and paleo-climate details were discussed in Chapter 3. The Cenozoic is the most recent of the Eras, and thus has the most information about the climate and history than the other two Eras. The following sections will discuss the Cenozoic total land area, predicted coal deposit area, observed coal area, hits area, and misses area.

6.2.1 Cenozoic Total Land

During the Cenozoic Era, most of the land mass has been centered around -15^{o} and 70^{o} latitude with the exception of Antarctica which is at -75^{o} to -90^{o} latitude. Figure 6.1 shows a graphical distribution of the $5^{o}x5^{o}$ grids that contained a land point. A total of 661 x 10^{6} km^{2} of land was observed, which is approximately 220 x 10^{6} km^{2} of land per time interval discussed.

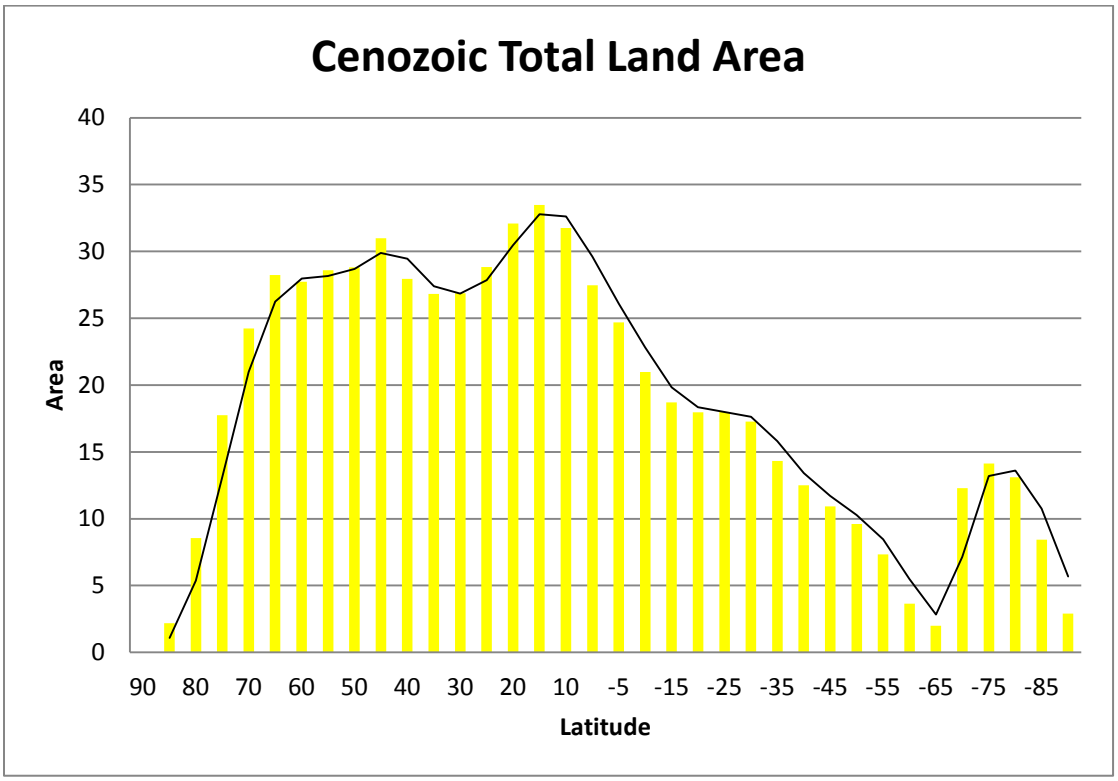

Figure 6.1 Histogram Showing the Area of Total Land within the Cenozoic Era by Latitude

6.2.2 Cenozoic Observed Coal Deposits

During the Cenozoic, three areas of major coal deposits have been observed. The first is between 70^{o} and 40^{o} latitude; the second between 20^{o} and -5^{o} latitude, and the third between -50^{o} and -60^{o} latitude. Typically for observed coals, a bell curve is observed because coals form in low latitude rainy belts and cool mid-latitude rainy belts. The total number of observed coals for the Cenozoic is 165 x 10^{6} km^{2} of observed coals. That is approximately 55 x 10^{6} km^{2} of observed coals per time interval discussed for the Cenozoic.

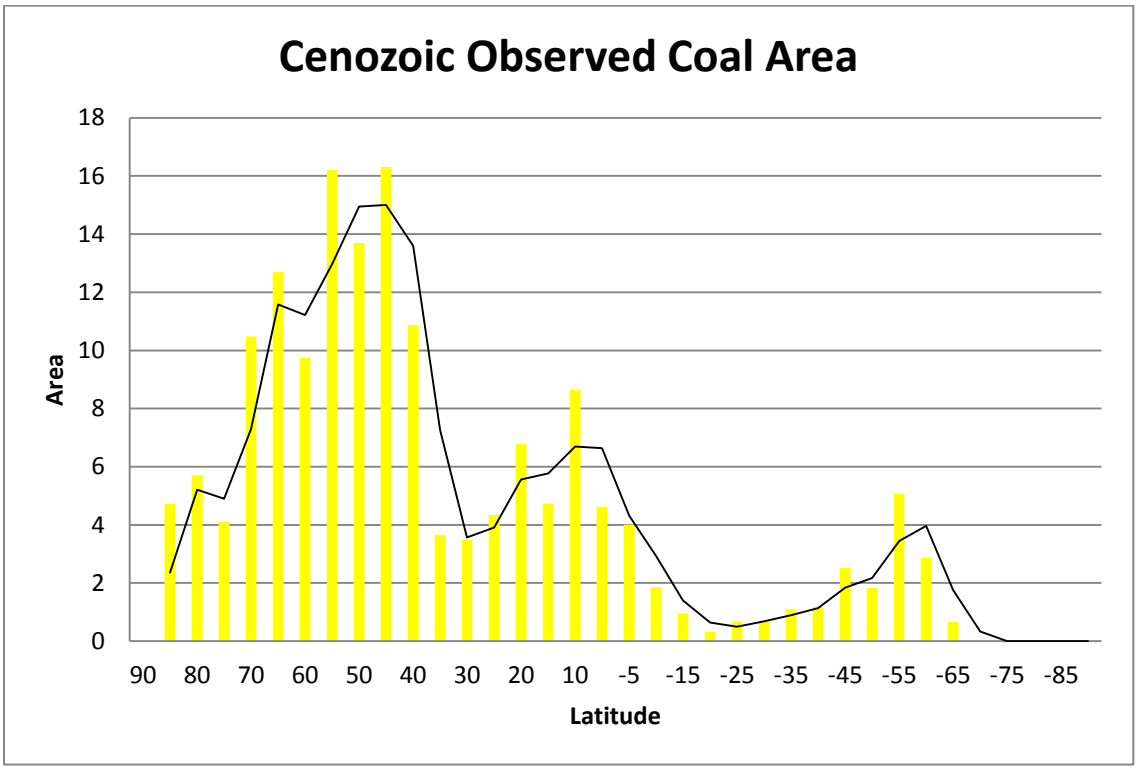

Figure 6.2 Histogram Showing the Area of Observed Coal Deposits within the Cenozoic Era by Latitude

6.2.3 Cenozoic Predicted Coal Deposits

As discussed in Chapter 3, coal deposits were predicted using FOAM simulations. The predicted coals for the Cenozoic Era created three major curves. The first is from 70^{o} to 55^{o} latitude. The second curve is from 20^{o} to -15^{o} latitude. The last curve spans from -70^{o} to -85^{o} latitude. A total of 488 x 10^{6} km^{2} of predicted coals were observed during the Cenozoic Era which is approximately 163 x 10^{6} km^{2} of predicted coals per time period discussed for the Cenozoic.

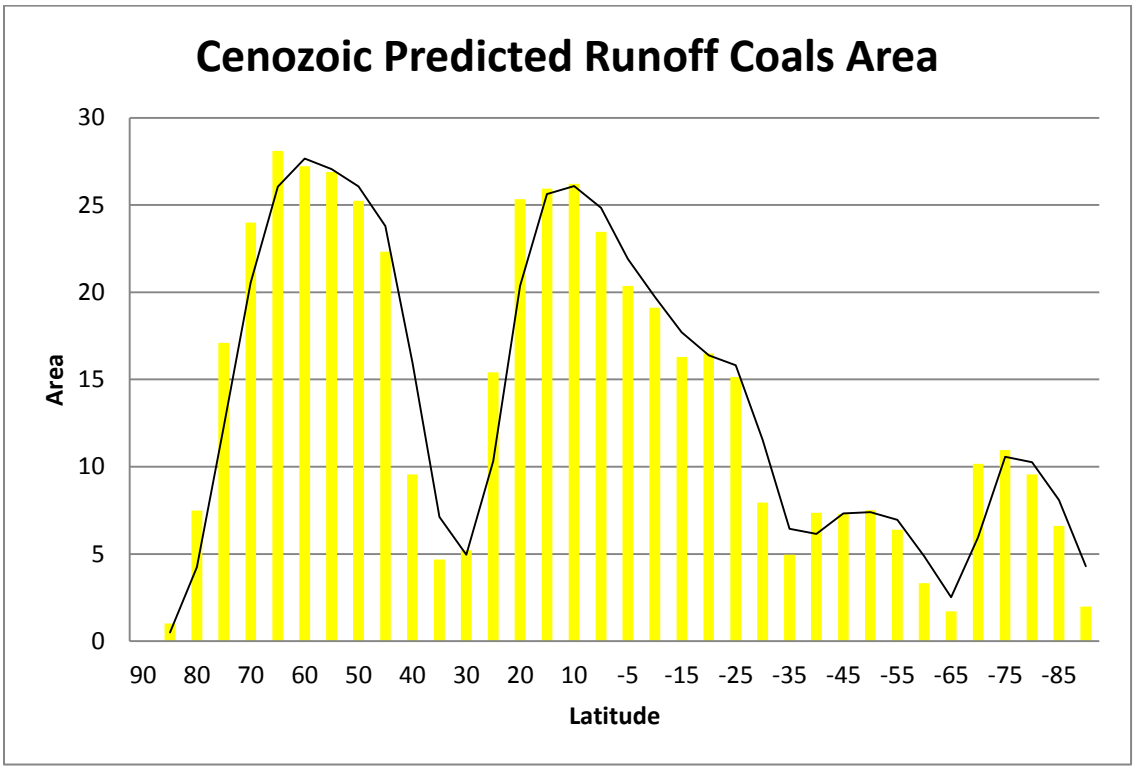

Figure 6.3 Histogram Showing the Area of Predicted Coal Deposits within the Cenozoic Era by Latitude

6.2.4 Cenozoic Hits vs. Misses

As discussed in the previous chapters, "hits" are 5^{o}x5^{o} grid cells that have both an observed coal and a predicted coal. During the Cenozoic a total of 64 x 10^{6} km^{2} of hits were observed. That is approximately 21 x 10^{6} km^{2} of hits per time interval. A "miss" is a 5^{o}x5^{o} grid cell containing an observed coal does not contain a predicted coal. A total of 101 x 10^{6} km^{2} of "misses" were observed during the Cenozoic. That is approximately 34 x 10^{6} km^{2} of misses per time interval discussed for the Cenozoic. Figure 6.4 shows the graphical distribution of hits versus misses. 10 million years has the most hits followed by 30 million years and then followed by 45 million years. Some reasons for this could be lack of data the farther back in time, number of predicted coal area, or number of observed coal area. Likewise, with the number of misses, 10 million years has the most misses, followed by 30 million years and then followed by 45

million years. This could be because of the number of predicted is higher in the 10 million year time interval or because the number of observed coal deposit area could be less during the latter time intervals giving them less opportunity to have misses.

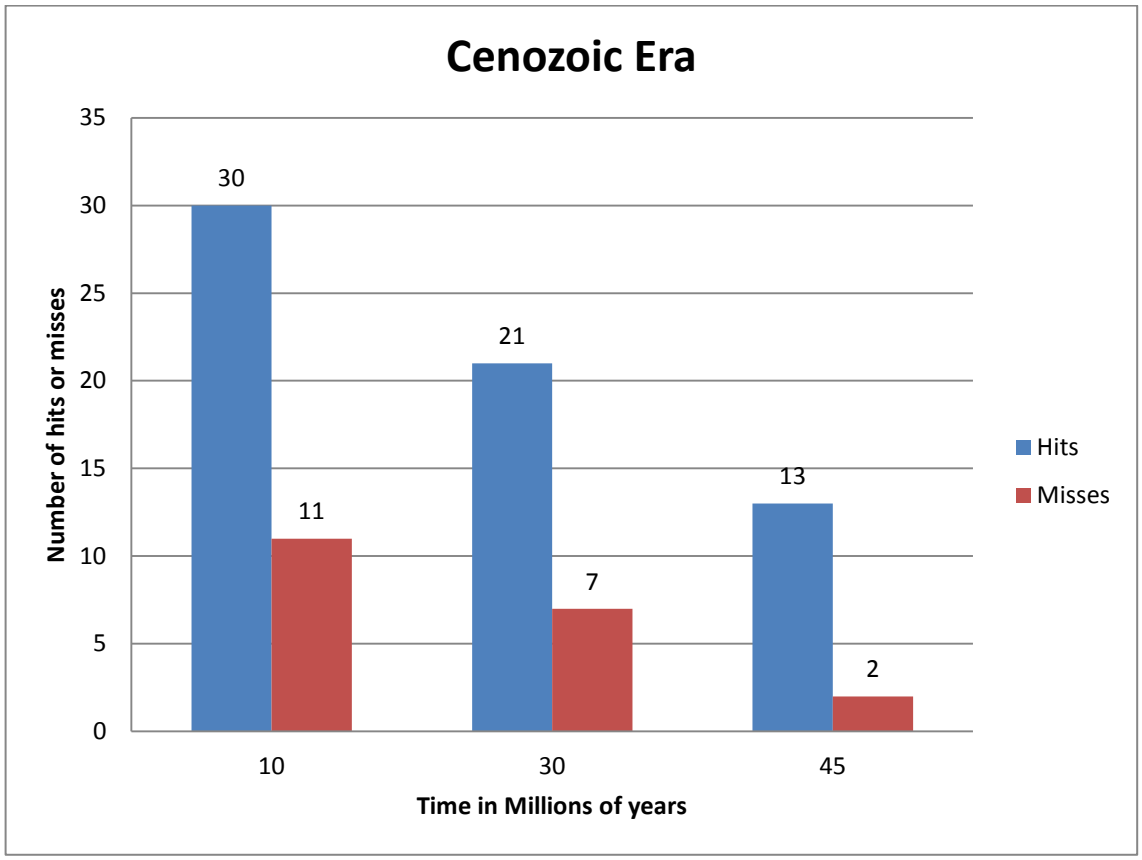

Figure 6.4 Bar Graph Showing Each Time Interval in the Cenozoic Era Number of Hits and Misses

6.3 The Mesozoic Era

All Mesozoic history, paleo-tectonics, and paleo-climate details were discussed in Chapter 4. The Mesozoic is the second most recent Era after the Cenozoic, and thus has more information than the Paleozoic. The following sections will discuss the Mesozoic total land area, predicted coal area, observed coal area, hits area, and misses area.

6.3.1 Mesozoic Total Land

During the Mesozoic Era, most of the land mass has been centered around -70^{o} and -65^{o} latitude. This is the time Pangea was centered from pole to pole so the land distribution is much more even than today. The figure below shows a graphical distribution of the 5^{o}x5^{o} grids that contained a land point. A total of 1473 x 10^{6} km^{2} of land were observed which is approximately 210 x 10^{6} km^{2} of land per time interval discussed for the Mesozoic.

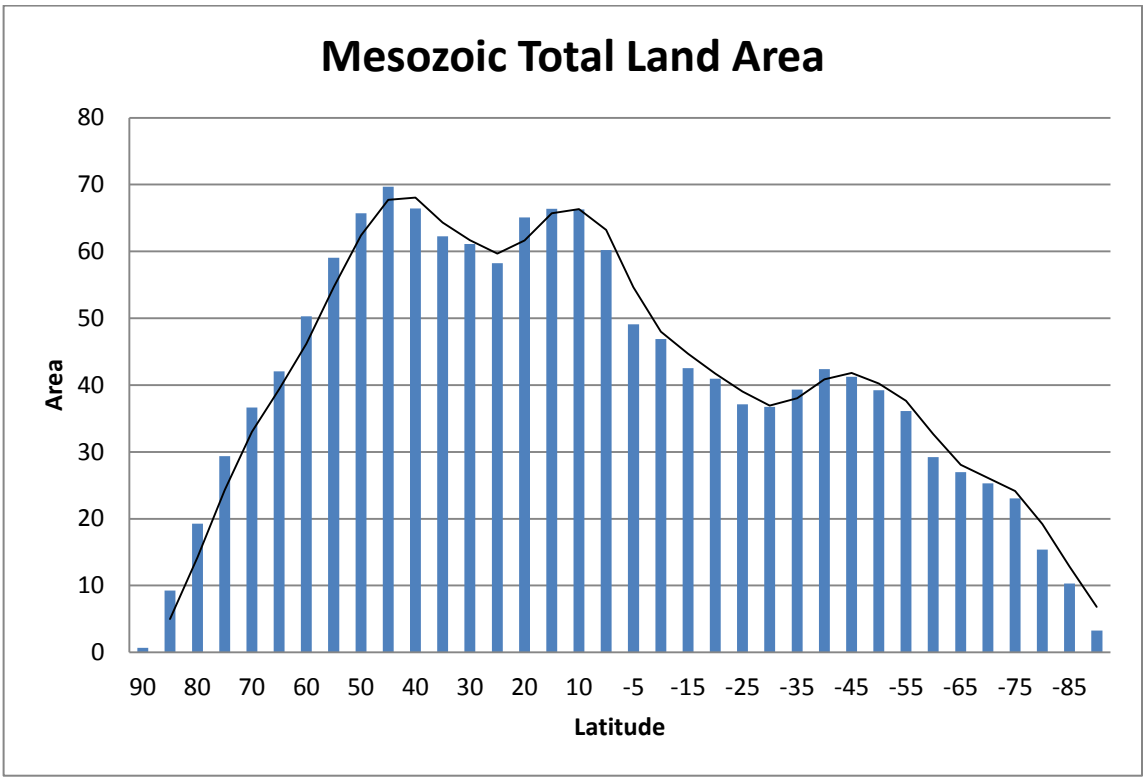

Figure 6.5 Histogram Showing the Area of Total Land within the Mesozoic Era by Latitude

6.3.2 Mesozoic Observed Coal Deposits

During the Mesozoic, there is one large area of observed coal deposits located from 80^{o} to 35^{o}. Typically for observed coals, a 3 curve-bell curve is observed because coals form in low latitude rainy belts and cool mid-latitude environment rainy belts. However, in the Mesozoic, there is not a traditional three curve bell curve. This could be because of lack of data, the continental location, or climate. The total number of observed coals for the Mesozoic is 564 x

10^6 km^2 of observed coals. That is approximately 81 x 10^6 km^2 of observed coals per time interval discussed for the Mesozoic.

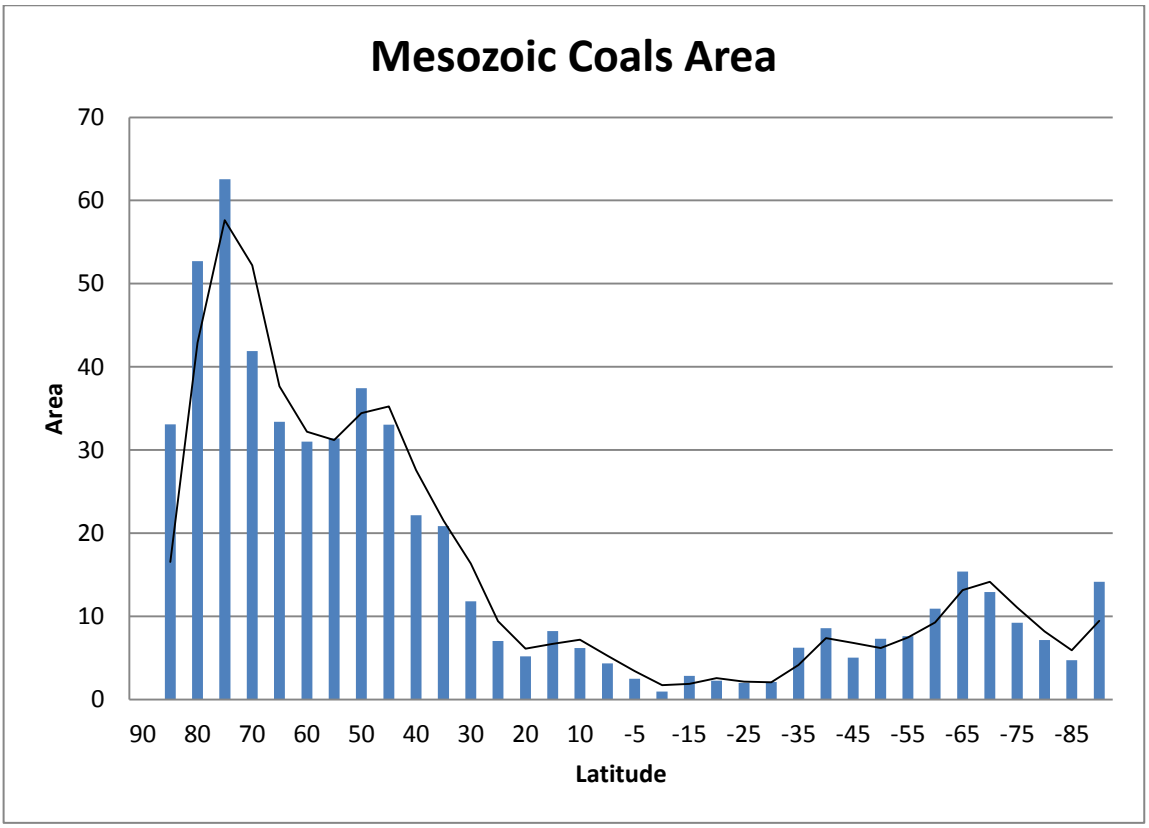

Figure 6.6 Histogram Showing the Area of Observed Coal Deposits within the Mesozoic Era by Latitude

6.3.3 Mesozoic Predicted Coal Deposits

As discussed in Chapter 4, coal deposits were predicted using FOAM simulations. The predicted coal deposits for the Mesozoic Era revealed three major areas of deposits. The first is from 75^o to 40^o latitude. The second curve is from 20^o to -20^o latitude. The last curve spans from -45^o to -75^o latitude. A total of 970 x 10^6 km^2 of predicted coal deposits were observed during the Mesozoic Era which is approximately 139 x 10^6 km^2 of predicted coal per time period for the Mesozoic.

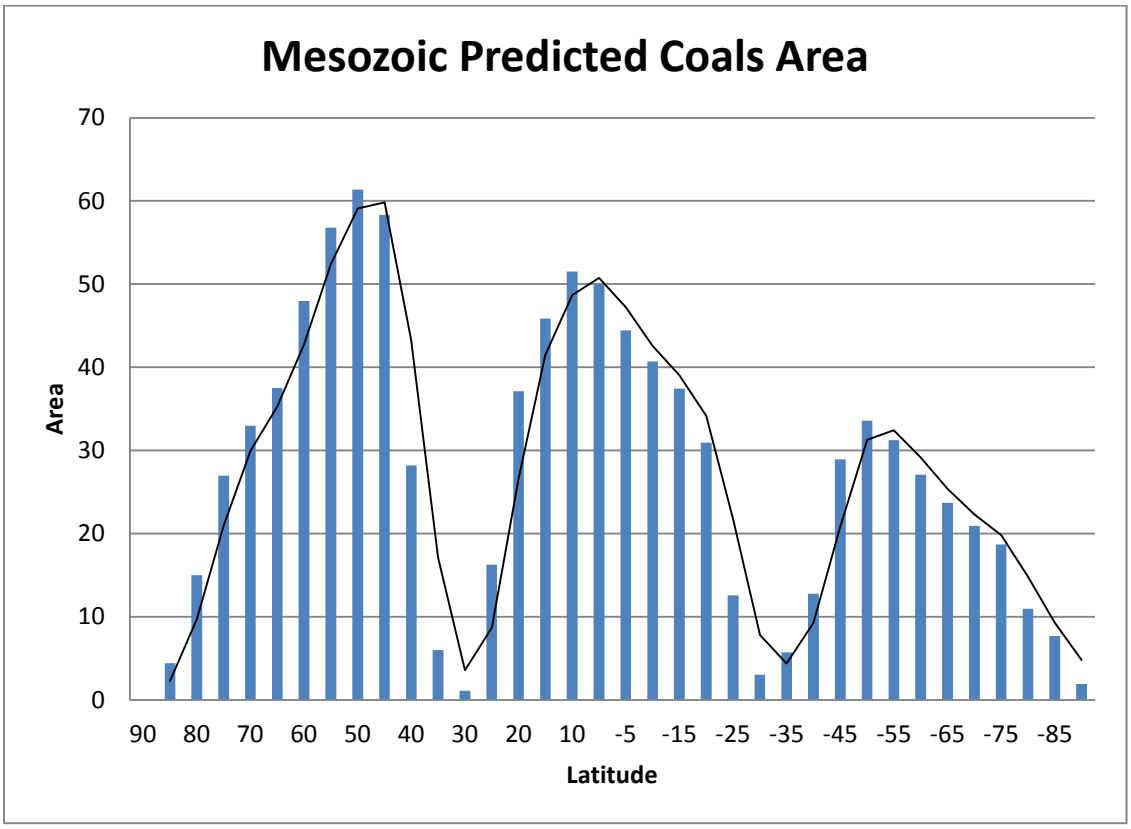

Figure 6.7 Histogram Showing the Area of Predicted Coal Deposits within the Mesozoic Era by Latitude

6.3.4 Mesozoic Hits vs. Misses

As discussed in the previous chapters, "hits" are 5^{o}x5^{o} grids that have both an observed coal and a predicted coal. During the Mesozoic a total of 122 x 10^{6} km^{2} of hits were observed. That is approximately 17 x 10^{6} km^{2} of hits per time interval discussed for the Mesozoic. A "miss" is a 5^{o}x5^{o} grid containing an observed coal does not contain a predicted coal. A total of 442 x 10^{6} km^{2} of "misses" were observed during the Mesozoic. That is approximately 63 x 10^{6} km^{2} of misses per time interval discussed for the Mesozoic. Figure 6.8 shows the graphical distribution of hits versus misses. 180 million years has the most hits followed by 120 million years and then followed by 140, 90, 70 and 220 million years, respectively. Some reasons for this could be lack of data the farther back in time, number of predicted coal area, or number of observed coal

area. Likewise, with the number of misses, 180 million years has the most misses, followed by 220 million years and then followed by 140, 70, 90, 120 and 160 million years, respectively. This could be because of the number of predicted area is higher in the 180 million year time interval or because the number of observed coal area could be less during the latter time intervals giving them less opportunity to have misses.

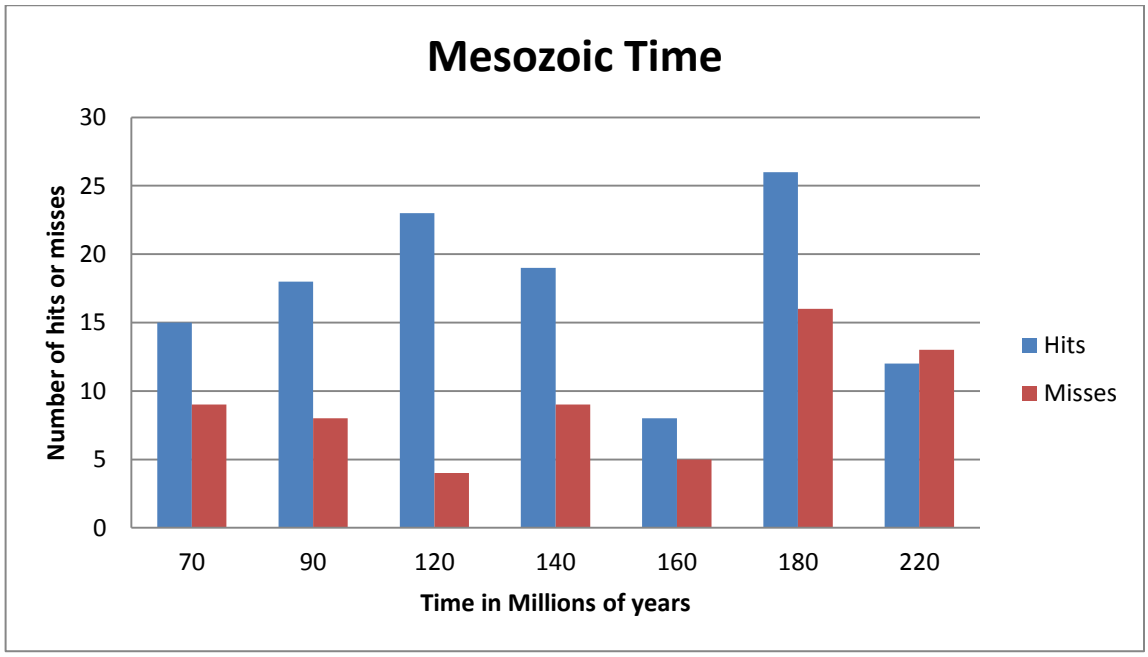

Figure 6.8 Bar Graph Showing Each Time Interval in the Mesozoic Era Number of Hits and Misses

6.4 The Paleozoic Era

All Paleozoic history, paleo-tectonics, and paleo-climate details were discussed in Chapter 5. The Paleozoic is the least recent of the Eras, and thus has less information has been preserved during that Era. The following sections will discuss the Paleozoic total land area, predicted coal area, observed coal area, hits area, and misses area.

6.4.1 Paleozoic Total Land

During the Paleozoic Era, most of the landmass has been centered around 55^{o} and -80^{o} latitude. This is the time that most of the land mass was around the South Pole. Gondwana and

Laurentia were both below the equator and most land mass that was above were island arcs. The figure below shows a graphical distribution of the 5^{o}x5^{o} grids that contained a land point. A total of 628 x 10^{6} km^{2} of land was observed, which is approximately 209 x 10^{6} km^{2} of land per time interval discussed.

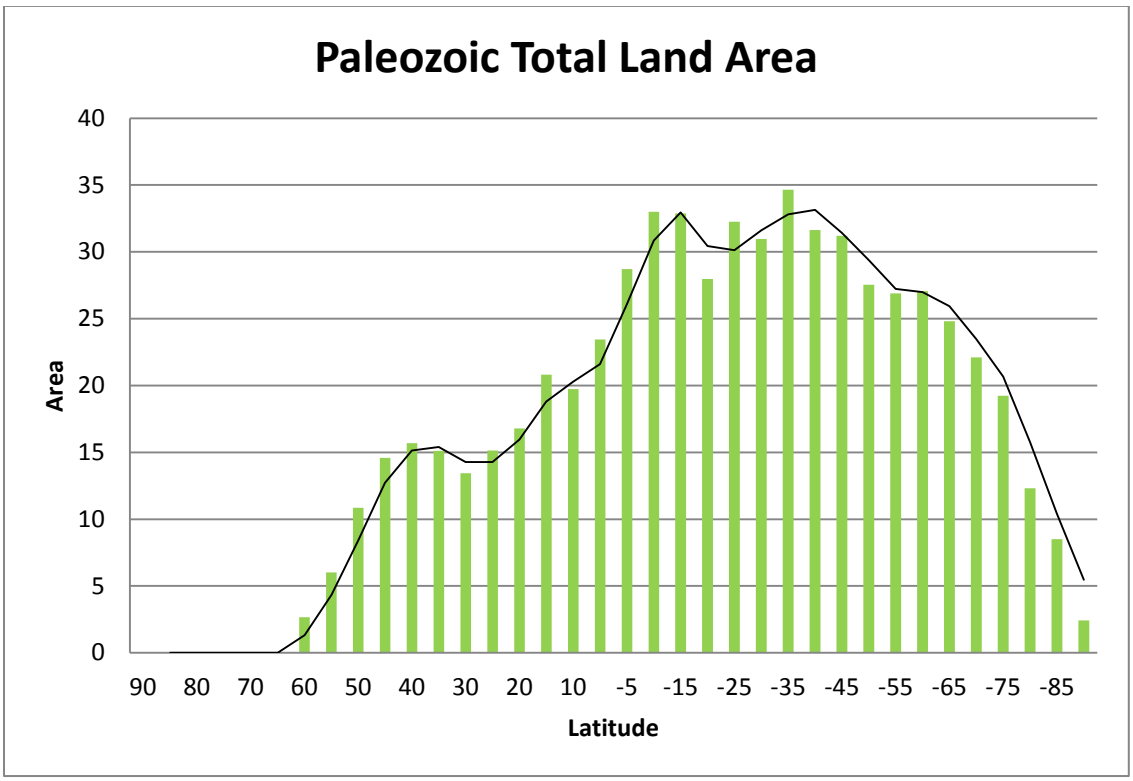

Figure 6.9 Histogram Showing the Area of Total Land within the Paleozoic Era by Latitude

6.4.2 Paleozoic Observed Coal Deposits

During the Paleozoic, there is one distinct curve and two smaller curves of observed coals. The major curve is located from -55^{o} to -75^{o} latitude. Typically for observed coals, a three curve graph is observed because coals form in low latitude rainy belts and cool mid-latitude environment rainy belts. However, in the Paleozoic, there is not a traditional three curve graph. This could be because of lack of data, the continental location, or climate. The total number of observed coals for the Paleozoic is 47 x 10^{6} km^{2} of observed coals. That is approximately 16 x 10^{6} km^{2} of observed coals per time interval discussed.

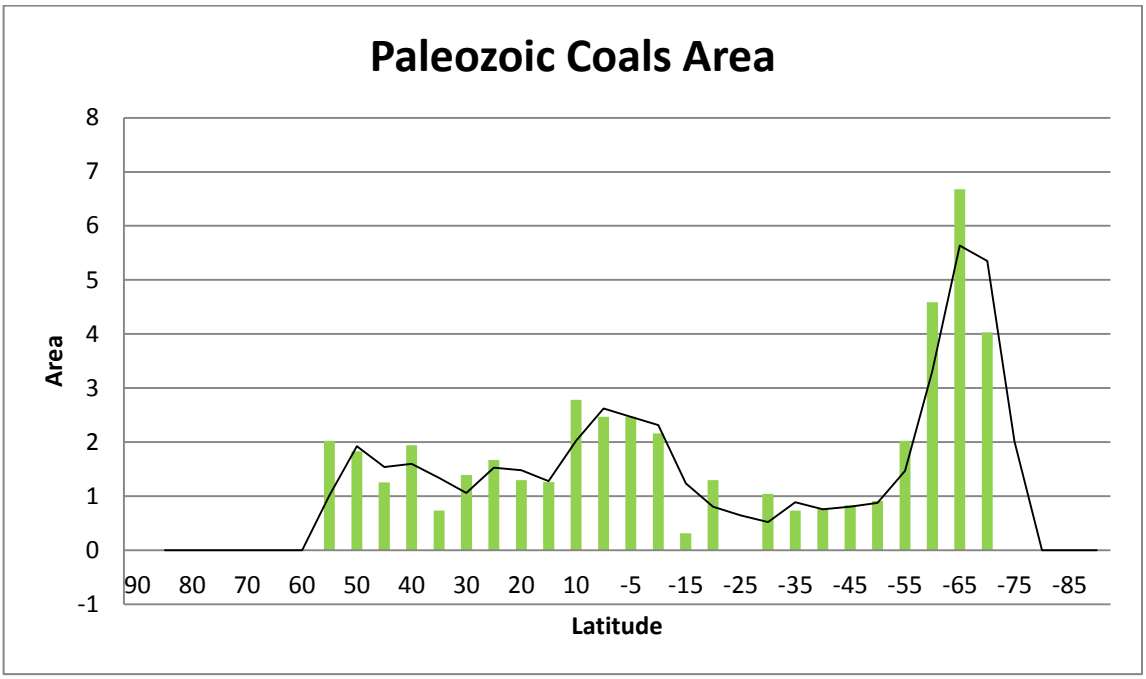

Figure 6.10 Histogram Showing the Area of Observed Coal Deposits within the Paleozoic Era by Latitude

6.4.3 Paleozoic Predicted Coal Deposits

As discussed in Chapter 5, coal deposits were predicted using FOAM simulations. The predicted coals for the Paleozoic Era created three major curves. The first is from 60^{o} to 35^{o} latitude. The second curve is from 20^{o} to -25^{o} latitude. The last curve spans from -45^{o} to -75^{o} latitude. A total of 319 x 10^{6} km^{2} of predicted coal area was observed during the Cenozoic Era which is approximately 106 x 10^{6} km^{2} of predicted coal area per time period.

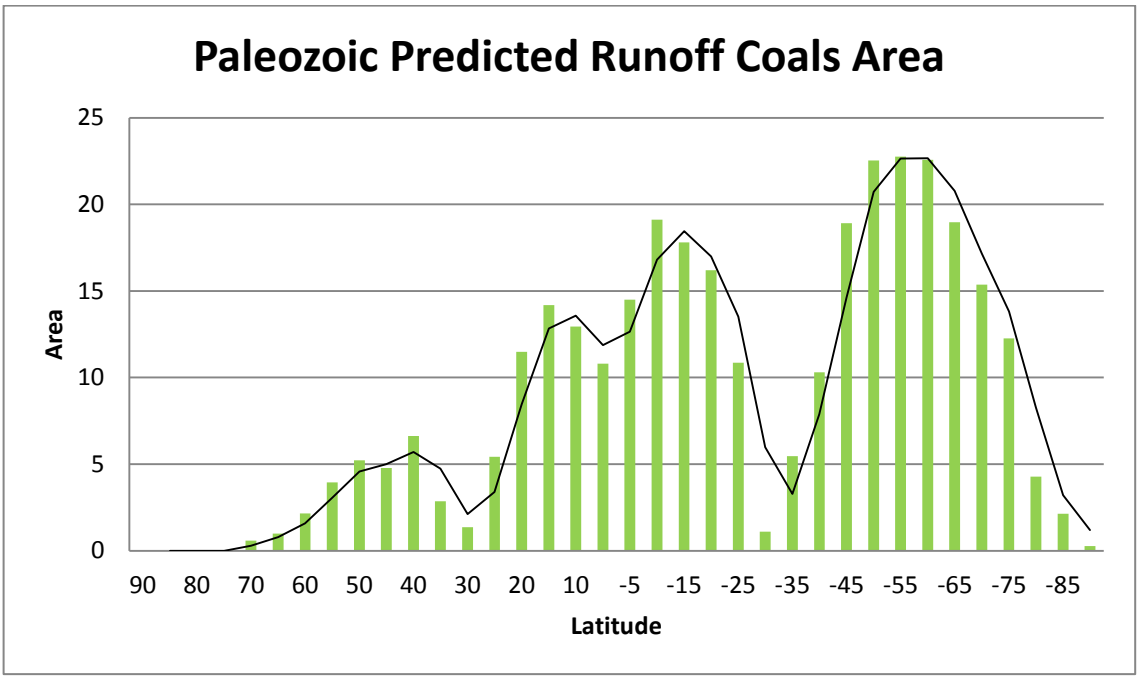

Figure 6.11 Histogram Showing the Area of Predicted Coal Deposits within the Paleozoic Era by Latitude

6.4.4 Paleozoic Hits vs. Misses

As discussed in the previous chapters, "hits" are $5^{o}x5^{o}$ grids that have both an observed coal and a predicted coal. During the Paleozoic a total of 30 x 10^{6} km^{2} of hits were observed. That is approximately 10 x 10^{6} km^{2} of hits per time interval. A "miss" is a $5^{o}x5^{o}$ grid containing an observed coal does not contain a predicted coal. A total of 17 x 10^{6} km^{2} of "misses" were observed during the Paleozoic. That is approximately 6 x 10^{6} km^{2} of misses per time interval. Figure 6.12 shows the graphical distribution of hits versus misses. 340 million years has the most hits followed by 280 million years and then followed by 360, respectively. Some reasons for this could be lack of data the farther back in time, number of predicted coals, or number of observed coals. Likewise, with the number of misses, 340 million years has the most misses, followed by 280 million years and then followed by 360, respectively. This could be because of the number of predicted is higher in the 340 million year time interval or because the number of

observed coals could be less during the latter time intervals giving them less opportunity to have misses.

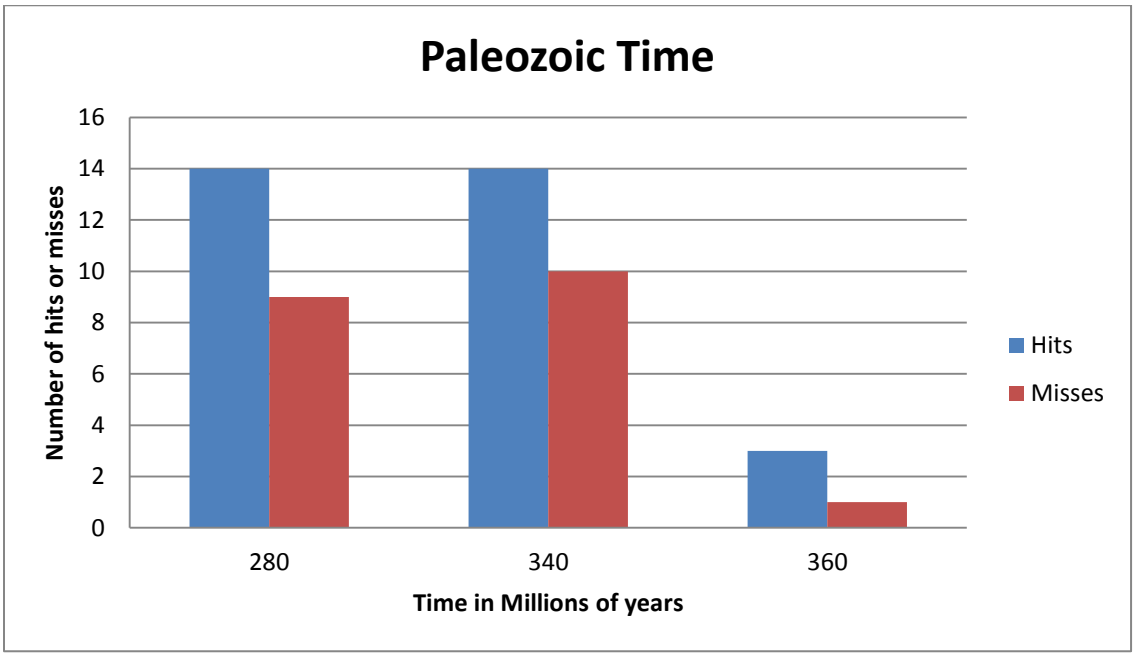

Figure 6.12 Bar Graph Showing Each Time Interval in the Paleozoic Era Number of Hits and Misses

6.5 Time Intervals Data Summary

It can be seen that throughout most of the time intervals, the FOAM simulation model seems to predict randomly. In this section, we will look at all the time intervals and see if there are any correlations between the data and the time intervals that passed or failed the null hypothesis. Figure 6.13 shows the data summary chart for all thirteen time intervals and the areas for total land, predicted coals, observed coals, and hits. The two time intervals highlighted in yellow are the only two time intervals to fail the null hypothesis. Figure 6.14 show the data percentage summary chart. It shows the percentage of land occupied by predicted coal area, percentage of land occupied by observed coal area, and percentage of land occupied by hits area. As with Figure 6.13, the two time intervals highlighted in yellow are the only two time intervals to fail the null hypothesis. It can be seen that the total area of land stays relatively the

same (around 200-230 x 10^6 km^2). The amount of predicted coal area, however; changes quite a bit between 10 Ma and 360 Ma. 360 Ma most likely failed the null hypothesis because there is lack of data during this time interval. 280 Ma is harder to explain why it failed the null hypothesis. Many factors could be contributing to this time interval failing the null hypothesis. First, it can be observed that any time interval that has predicted coals in higher latitudes is more likely to pass the null hypothesis. 280 Ma did not have as much predicted coal area in higher latitudes. This could explain why it is failing the null hypothesis. It can also be seen in Figure 6.13 that there is less predicted coal deposit areas for 280 Ma and 360 Ma. With less prediction you have less opportunity to have hits. The failing of the hypothesis could also be explained by poor data or even lack of data. Finally, climate patterns may have been different during the older time intervals. We do not fully understand the climates during the older time intervals and prediction models use modern climate patterns to model past climates.

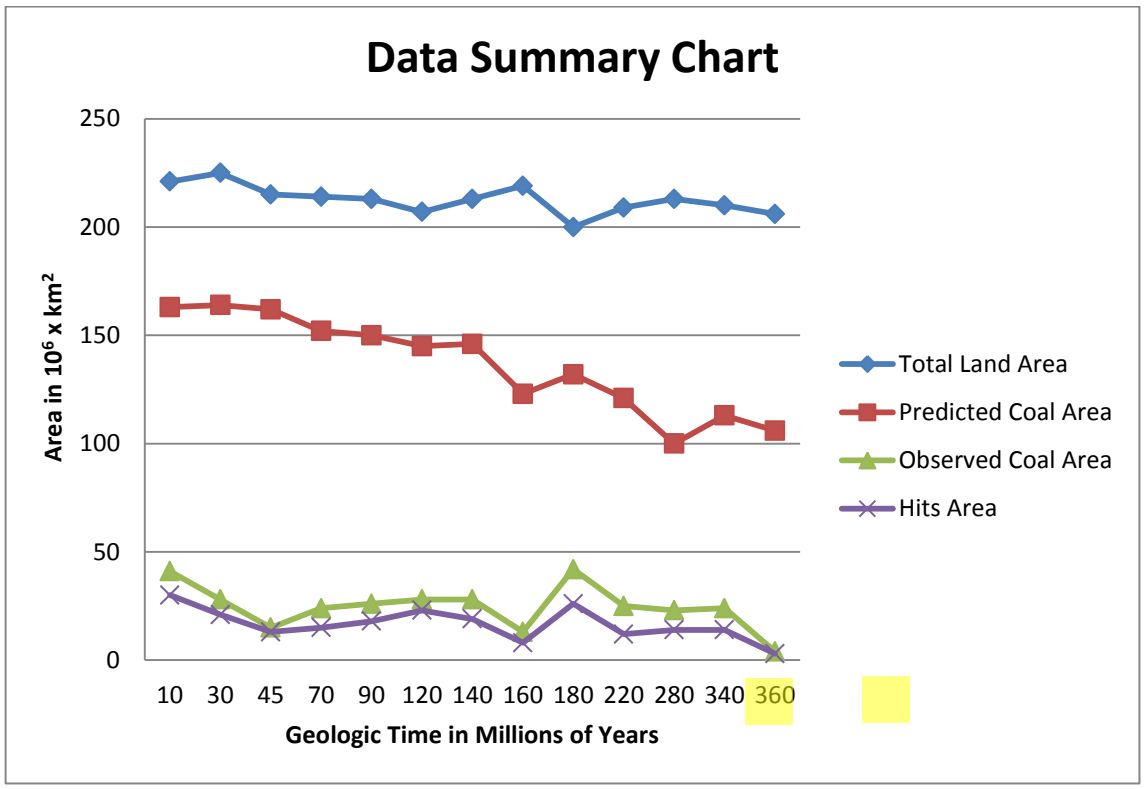

Figure 6.13 Graph Showing the Data Summary for All Thirteen Time Intervals

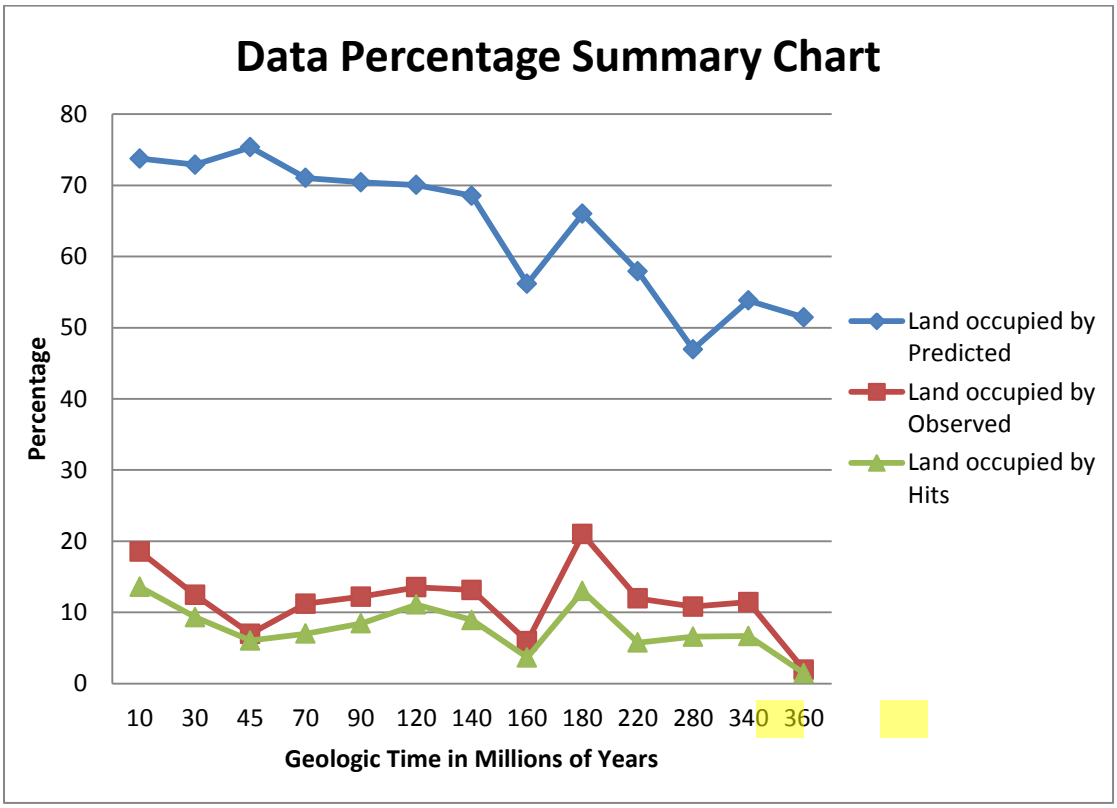

Figure 6.14 Graph Showing the Data Percentage Summary for All Thirteen Time Intervals

6.6 Hits Versus Misses Throughout Time

As discussed in the previous chapters, "hits" are $5^{o}x5^{o}$ grids that have both an observed coal and a predicted coal. Throughout all thirteen time intervals a total of 216 x 10^{6} km^{2} of hits were observed. That is approximately 17 x 10^{6} km^{2} of hits per time interval. A "miss" is a $5^{o}x5^{o}$ grid cell containing an observed coal that does not contain a predicted coal. A total of 104 x 10^{6} km^{2} "misses" were observed throughout all thirteen time intervals. That is approximately 8 x 10^{6} km^{2} of misses per time interval. Figure 6.15 shows the graphical distribution of hits versus misses. It can be seen throughout time that on average more hits were observed during the Cenozoic and Mesozoic than in the Paleozoic. More misses were observed during the Paleozoic and Mesozoic than the Cenozoic. The question to be asked then is why? Many factors could have contributed to distribution of hits and misses. Landmass location, data supply, climate, or error in prediction models are all factors that could explain this distribution.

However, it can be said that for most time intervals more hits than misses were observed.

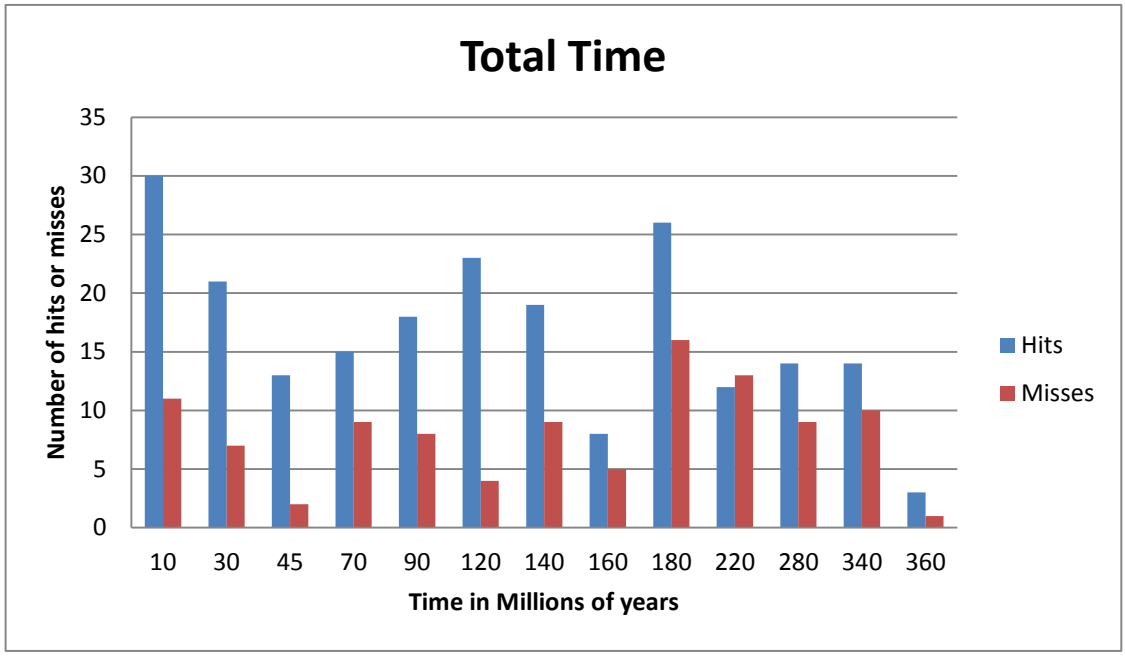

Figure 6.15 Bar Graph Showing All Thirteen Time Intervals' Number of Hits and Misses

6.7 Conclusion

Climate can greatly change and influence coal distribution and extent. It can be observed that the statistical method using Poisson's distribution to evaluate the fit is useful in the Paleozoic but not in the Cenozoic or Mesozoic. All time intervals but the Early Permian and Early Carboniferous passed the null hypothesis. This means that the FOAM model is predicting coals randomly and not in any type of significant order. There seems to be a significant model-data bias for the Paleozoic because of uncertainties in the model boundary conditions.

Eleven out of thirteen time intervals did not fail the null hypothesis. This means that two did fail the null hypothesis. Thus it can be said that 86% of the time intervals were due to random process and this prediction method is a not good prediction tool for climatic indicators. Looking at hits versus misses throughout time shows that the farther back in time, the less data there is available to work with. By using prediction methods, such as ones like this thesis, we can better understand past climate based on the information we have.

This research could be better developed by using a more valid climate model, and improvement of the model resolution and reconstruction of model boundary conditions. Further research on coal deposits using other climate parameters would help to better tell the story of past climates. Using other climate indicators such as bauxites, laterites, calcrete, tillites, glendonites, etc. with the same prediction method will lead to a better understanding of what the Earth's climate was during the past.

REFERENCES

American Coal Foundation, 2011. *Coal's Past, Present, and Future*. Washington D.C: American Coal Foundation. <http://teachcoal.org/coals-past-present-and-future>.

Bishop, J.W., Montanez, I.P., Gulbranson, E.L., and Brenckle, P. L., 2009. The onset of mid-Carboniferous glacio-eustasy: Sedimentologic and diagenetic constraints, Arrow Canyon, Nevada. *Palaeogeography, Palaeoclimatology, Palaeoecology*, 276, 217-243.

Boucot, A., Chev, X., & Scotese, C., 2012. Phanerozoic Atlas of Climate Indicators. *SEPM.*

Budyko, M.I., Ronov, A.B., and Yanshin, A.L., 1987. History of the Earth's Atmosphere. Springer: Heidelberg, 139 pp.

Chandler, M.A., 1992. The Early Jurassic climate: General circulation model simulations and the paleoclimate record. University of Columbia, 1-314.

Clack, J., 2007. Devonian climate change, breathing, and the origin of the tetrapod stem group. *Integrative and Comparative Biology*, 47: number 4, 510-523.

"Coal Over Geologic Time - Eocene." *Wyoming State Geological Survey*. 2002. Web. 22 Mar. 2011. <http://www.wsgs.uwyo.edu/coalweb/library/coaltime/EOCENE.ASPX>.

Considine, G.D., Kulik, P.H., 2008. Van Nostrands's Scientific Encylopedia. New Jersey: John Wiley&Sons, Inc. 1176-1188.

Dietrich, Richard and Skinner, B. Rocks and Rock Minerals. New York: John Wiley and Sons, Inc., 1979.

Downing, D., & Clark, J. (1989). Statisitcs the easy way. Barron's educational series.

Fluteau F, Ramstein G, Besse J, 1999. Simulating the evolution of the Asian and African monsoons during the past 30 Myr using an atmospheric general circulation model. *Journal of Geophysical Research and Atmospheres.* 104:11,995–12,018.

Föllmi, K.B., 2012. Early Cretaceous life, climate and anoxia. *Cretaceous Research*, 35, 230-257.

Hallam, A., 1985. A review of Mesozoic climates. *Journal of Geologic Society of London*, 142, 433-445.

Joachimski, M.M., Breisig, S., Buggisch, W., Talent, J.A., Mawson, R., Gereke, M., Morrow, J.R., Day, J., Weddige, K., 2009. Devonian climate and reef evolution: Insights from oxygen isotopes in apatite. *Earth and Planetary Science Letters*, 284, 599-609.

Katz, M.E., Miller, K.G., Wright, J.D., Wade, B.S., Browning, J.V., Cramer, B.S., Rosenthal, Y., 2008. Stepwise transition from the Eocene greenhouse to the Oligocene icehouse. *Nature Geoscience*, 1, 329-334.

Keating-Bitonti C.R., Ivany, L.C., Affek, H.P., Douglas, P., and Samson, S.D., 2011. Warm, not super-hot, temperatures in the early Eocene subtropics. *Geology*, August 2011; v. 39, no. 8, p 771-774.

Keller, C.E., Hochuli, P.A., Weissert, H., Bernasconi, S.M., Giorgioni, M., Garcia, T.I., 2011. A volcanically induced climate warming and floral change preceded the onset of OAE1A (Early Cretaceous). *Palaeogeography, Palaeoclimatology, Palaeoecology,* 305, 43-49.

Kutzbach JE, Behling P, 2004. Comparison of simulated changes of climate in Asia for two scenarios: early Miocene to present, and present to future enhanced greenhouse. *Global Planet Change*. 41:157–165.

Legates, D., & Willmott, C. (1990a). Mean seasonal and spatial variability in gauge corrected, and global precipitation. *International Journal of Climatology, 10*, 111-127.

Micheels A, Bruch AA, Uhl D, Utescher T, Mosbrugger V., 2007. A Late Miocene climate model simulation with ECHAM4/ML and its quantitative validation with terrestrial proxy data. *Palaeogeography, Palaeoclimatology, Palaeoecology* 253:267–286.

Morley, R.J., 2000. *Origin and Evolution of Tropical Rainforests*. Wiley, New York, 362 pp.

Negrelle, R.R.B., 2002: The Atlantic forest in the Volta Velha Reserve: a tropical rainforest site outside the tropics. *Biodiversity and Conservation* 11, 887-919.

Ocampo, A., Vajda, V., Buffetaut, E., 2006. Unravelling the Cretaceous-Paleogene (KT) turnover, evidence from flora, fauna and geology. Biological processes associated with impact events, 197-219.

Otto-Bliesner, B. L., and Upchurch G.R., 1997. Vegetation-unduced warming of high-latitude regions during the Late Cretaceous period. *Nature*. 385, 804-807.

Otto-Bliesner, B., Brady, E. C., Shin, S., Liu, Z., & Shields, C., 2003. Modeling el nino and its tropical teleconnections during the last glacial-interglacial cycle. *Geophysical Research Letters, 30*(23), 4-4.

Otto-Bliesner, B., Brady, E., & Kothavala, Z., 2004. Climate sensitivity of the last glacial maximum from paleoclimate simulations and observations. *EOS, Transactions, American Geophysical Union, 85*(47). (Cenozoic)

Parrish, J.T., 1998. *Interpreting Pre-Quaternary Climate from the Geologic Record*, 338 pp. Columbia University Press, New York.

Peppe, D.J., Royer, D.L., Cariglino, B., Oliver, S.Y., Newman, S., Leight, E., Enikolopov, G., Fernandez-Burgos, M., Herrera, F., Adams, J.M., Correa, E., Currano, E.D., ERICKSON, J.M., Hinojosa, L.F., Hoganson, J.W., Iglesia, A., Jaramillo, C.A., Johnson, K.R., Jordan, G. J., Kraft, N.J.B., Lovelock, E.C., Lusk, C. H., Niinemets, U., Penuelas, J., Rapson, G., Wing, S. L., Wright, I. J., 2011. Sensitivity of leaf size and shape to climate: global patterns and paleoclimatic applications. *New Phytologist*, 1-16.

Poulsen, C. J., Pollard, D., Montanez, I. P., & Rowley, D., 2007. Late paleozoic tropical climate response to gondwanan deglaciation. *Geology (Boulder),* 35(9), 771-774.

Preto, N., Kustatscher, E., Wignall, P.B., 2010. Triassic climates- State of the art and perspectives. *Palaeogeography, Palaeoclimatology, Palaeoecology*, 290, 1-10.

Ramstein G, Fluteau F, Besse J, Joussaume S , 1997. Effect of orogeny, plate motion and land-sea distribution on Eurasian climate change over past 30 million years. *Nature* 386:788–795.

Raymo M.E., Ruddiman, W.F., 1992. Tectonic forcing of late Cenozoic climate. *Nature*. 359, 117.

Royer, Dana L. and Robert A. Berner, Isabel P. Montañez, Neil J. Tabor, David J. Beerling (2004) CO_2 as a primary driver of Phanerozoic climate *GSA Today* July 2004, volume 14, number 3, pages 4-10

Ruddiman, W.F., 2008. Earth's Climate: Past and Future. 2nd edition.

Ruddiman WF, Kutzbach JE, Prentice IC, 1997. Testing the climatic effects of orography and CO2 with general circulation and biome models. *Tectonic uplift and climate change*. Plenum Press, New York, pp 203–235.

Schlanger, S.O., and Jenkyns, H.C., 1976. Cretaceous Oceanic Anoxic events: Causes and Consequences. Geologie en Mijnbouw, 55, 179-184.

Schneck, R., Micheels, A., Mosbrugger, V., 2012. Climate impact of high northern vegetation: Late Miocene and present. *International Journal of Earth and Science*. 101, 323-338.

Scotese, C. (2001). Atlas of Earth History. In *Paleogeography, PALEOMAP project* (Vol. 1, p. 52).

Arlington.

Scotese, C.R., Illich, H., Zumberge, J, and Brown, S., and Moore, T., S., 2007. The GANDOLPH Project: Year One Report: Paleogeographic and Paleoclimatic Controls on Hydrocarbon Source Rock Deposition, A Report on the Methods Employed, the Results of the Paleoclimate Simulations (FOAM), and Oils/Source Rock Compilation for the Cenomanian/aTuronian (93.5 Ma), Kimmeridgian/Tithonian (151 Ma),

Sakmarian/Artinskian (284 Ma), and Frasnian/Famennian (375 Ma), Conclusions at the End of Year One, February, 2007. GeoMark Research Ltd, Houston, Texas, 142 pp.

Scotese, C.R., Illich, H., Zumberge, J, Brown, S., and Moore, T., 2008. The GANDOLPH Project: Year Two Report: Paleogeographic and Paleoclimatic Controls on Hydrocarbon Source Rock Deposition, A Report on the Methods Employed, the Results of the Paleoclimate Simulations (FOAM), and Oils/Source Rock Compilation for the Miocene (10 Ma), Aptian/Albian (120 Ma), Berriasian/Barremian (140 Ma), Late Triasssic (220 Ma), Early Silurian (430 Ma), Conclusions at the End of Year Two, July, 2008. GeoMark Research Ltd, Houston, Texas, 177 pp.

Scotese, C.R., Illich, H., Zumberge, J, Brown, S., and Moore, T.,2009. The GANDOLPH Project: Year Three Report: Paleogeographic and Paleoclimatic Controls on Hydrocarbon Source Rock Deposition, A Report on the Methods Employed, the Results of the Paleoclimate Simulations (FOAM), and Oils/Source Rock Compilation for the Eocene (45 Ma), Early/Middle Jurassic (180 Ma), Mississippian (340 Ma), and Neoproterozoic (600 Ma), Conclusions at the End of Year Three, August, 2009. GeoMark Research Ltd, Houston, Texas, 154 pp.

Scotese, C.R., Illich, H., Zumberge, J, Brown, S., and Moore, T.,2011. The GANDOLPH Project: Year Four Report: Paleogeographic and Paleoclimatic Controls on Hydrocarbon Source Rock Deposition, A Report on the Methods Employed, the Results of the Paleoclimate Simulations (FOAM), and Oils/Source Rock Compilation for the Oligocene (30 Ma), Cretaceous/Tertiary (70 Ma), Permian/Triassic (250 Ma), Silurian/Devonian (400 Ma), and Cambrian/Ordovician (480 Ma), Conclusions at the End of Year Four, April 2011. GeoMark Research Ltd, Houston, Texas, 219 pp.

Shangyou, N., Rowley, D.B., Ziegler, A.M., 1990. Constraints on the location of Asian microcontinents in Palaeo-Tethys during the Late. *Paleozoic. Paleozoic, Palaeogeography, and Biogeography*, 12, 397-409.

Tabor, N.J., Poulsen, C. J., 2008. Palaeoclimate across the Late Pennsylvanian-Early Permian tropical palaeolatitudes: A review of climate indicators, their distribution, and relation to palaeophysiographic climate factors. *Palaeogeography, Palaeoclimatology, Palaeoecology*, 268, 293-310.

Walter, H, 1985. *Vegetation of the Earth and Ecological Systems of the Geo-biospere*, 3rd edn, 318 pp. Springer-Verlag, New York.

Weissert, H and Mohr, H., 1996. Late Jurassic climate and its impact on carbon cycling. *Palaeogeography, Palaeoclimatology, Palaeoecology*, 122, 27-43.

Wolfe, JA, 1985. Distribution of major vegetational types during the Tertiary. *Geophysical Monograph* 32, 357-375.

World Coal Institute, 2005. *The Coal Resource: A Comprehensive Overview of Coal*. London: Cambridge House. 1-44.

Zanazzi, A., Kohn, M. J., MacFadden, B. J. & Terry, J., O., 2007. Large temperature drop across the Eocene–Oligocene transition in central North America. Nature. 445, 639–642.

Ziegler, A.M. Eshel, G., Rees, P. M, Rothfus, T., Rowley, D., and Sunderlin, D., 2003. Tracing the tropics across land and sea: Permian to present. Lethaia, Vol. 36, pp. 227-254.

BIOGRAPHICAL INFORMATION

Mandi Beck is a graduate student at the University of Texas at Arlington in the College of Science. She received her Bachelors of Science from Stephen F. Austin State University in 2009. There she was a member of AAPG student chapter and SGE student chapter. Currently, Mandi works for Petro-Hunt L.L.C., a privately owned oil and gas company in Dallas, TX. In the future, she plans to explore more heavily in petroleum geology and one day pursue her doctoral degree..